SERIAL AND PARALLEL PROCESSING IN PRIMATE AUDITORY CORTEX: A COMPARISON OF RESPONSE PROPERTIES IN THE CORE, BELT, AND PARABELT

By

Corrie Randolph Camalier

Dissertation

Submitted to the Faculty of the

Graduate School of Vanderbilt University

in partial fulfillment of the requirements

for the degree of

DOCTOR OF PHILOSOPHY

in

Neuroscience

December, 2010

Nashville, Tennessee

Approved:

Professor Troy Hackett

Professor Jon Kaas

Professor Ford Ebner

Professor Mark Wallace

ACKNOWLEDGEMENTS

To grossly paraphrase the words of Jacques Derrida, I dedicate this series of studies to the people who gave them to me. To properly acknowledge the unique contributions of the many people who have helped make this process go would take almost as many pages as the dissertation itself, so it is with reluctance that I will be brief.

First and foremost, to the 'audlab', particularly to Troy Hackett and Lisa de la Mothe. It has been a privilege to move in the intellectual pull of this syzygy for the last four years. Troy has been a model of a careful and passionate scientist, an exacting scholar, and above all, a generous mentor, whose perspective and example I will continue to rely on (probably more than he wants). Lisa's many thoughtful conversations have pushed and honed these ideas, and the laughter has smoothed the journey. More than a labmate, it has been like having an intellectual sister. To Bill D'Angelo and Susanne Sterbing-D'Angelo who pioneered the awake macaque preparation in the lab, provided careful training, and continue to be enthusiastic collaborators. To Yoshi Kajikawa who was more of a collaborator than he needed to be, and additionally trained Troy to expect characters in his physiologists. To the students who I have been fortunate to advise: Alok Saini, Sean Toomey, Shuey Lim, Mike Garcia, Angie Voyles, Jakai Nolan, and David Lee. Lastly, to Jon Kaas for his open door, his advice and encouragement, and especially his example.

To the members who have graciously served on my committee, Mark Wallace (chair), Ford Ebner, and Andrew Rossi (former chair and member). Their insight and guidance

both in and outside our formal meetings has been invaluable - they have been true advocates for these ideas, and are inspiring scientists in their own right.

To Shigeyuki Kuwada (University of Connecticut) and Mitchell Steinschneider (Albert Einstein College of Medicine) who provided expert advice in the experimental design and analysis. To the mentors of my early training, Jeff Schall, Gordon Logan. Tom Palmeri, René Marois, Leanne Boucher, and Stephanie Shorter. To Elaine Saunders-Bush for inspiration and encouragement during the critical early years. And to Wes Grantham for letting me be a psychophysicist in my off hours. Their influence and example have profoundly affected my thinking about brain and behavior. I am a composite of what was given to me, and am more grateful than I can say.

To the incredible animal care of Wilson Hall, particularly the care of our veterinarians and technicians Maggie McTighe, Troy Apple, Paula Austin, and Mary Feurtado, and to PJ, Spike, and Daisy for letting this be possible.

To the fabulous labmates, officemates, and other individuals with whom I have had fruitful conversations, Kim Curby, Alan Wong, Erik Emeric, Pierre Pouget, Jeremiah Cohen, Rich Heitz, Matt Nelson, Min-Suk Kang, Jay Todd, Phil Branning, Daryl Fougnie, Paul Dux, Mike Remple, Omar Ghabarwie, Peiyan Wong, Mark Burish, Christina Cerkevitch, Nicole Young, Jascha Swisher, Vivek Khatri, Ayan Ghoshal, Roan Marion, Paul Marasco, Trent Kriete, Julia High, Hui-Xin Qi, Geoff Woodman, Dan Polley, A.B. Bonds, Anna Roe, Poppy Crum (Johns Hopkins University), Pawel

Kusmierek (Georgetown University), Dennis Barbour (Washington University of St Louis), and Brian Malone (NIH). They have been intellectually generous and fearless in discussion, as well as really fun people to be around. Jamie Reed particularly should be highlighted for many productive discussions (especially on the use of the JPSTH) and her hawkish editorial eye on these chapters.

To my friends, whose friendship I don't deserve and am too fortunate to have.

To Jana and Louise, my mother and sister, who are studies on determination, perseverance, and grace, and to the memory of Cam, my father.

This work was supported by NIH\NIDCD RO1 DC04318 to T. Hackett, a grant from the McDonnell foundation to J. Kaas, and T32 MH075883 to Vanderbilt Kennedy Center for statistical consulting.

TABLE OF CONTENTS

LIST OF TABLES

LIST OF FIGURES

CHAPTER I

INTRODUCTION TO THE PRIMATE AUDITORY PATHWAYS AND NECESSARY BACKGROUND CONSIDERATIONS

Excerpts of this chapter were submitted in: C.R. Camalier and J. Kaas. Functional organization of primate auditory pathway and interactions with pathways of reward. In: Sensation and Reward, ed. Jay A. Gottfried.

1.1 Introduction

From the wail of an ambulance to the soothing melody of a Mozart sonata, it is clear that sound in our environment carries enormous meaning. We are able to process sounds rapidly and accurately in daily life, yet the mechanisms that underlie the ability to do this remain largely mysterious. In mammals, one logical place to investigate the mechanisms of sound processing is in the auditory cortex. The basic organization and function of the areas contained in auditory cortex, an organization sometimes referred to as the 'primate model', is still under active investigation. The studies contained in this dissertation aim to test and refine current hypotheses about processing flow. To give some necessary background for this, this chapter will start with some perspective on the evolution of primate auditory cortex, review basic properties of sound that we will concern ourselves with, and also cover some ethological considerations in sound processing. The auditory cortex evolved to process sound within the constraints of the surrounding environment; an understanding of this background is useful to provide context for hypotheses about sound processing in cortex. Later this chapter introduces the

general organization and major pathways of the auditory system, with a particular focus on primates. Due to the incomplete nature of primate literature, conclusions based on data from other species will be discussed. Insights from other mammalian species (i.e., cats, ferrets, rats) can be used to shape hypotheses, but it is worth noting that important species differences may exist, even within primates. Lastly, this chapter discusses objectives and aims of this dissertation that relate to better understanding of the functional organization of primate auditory cortex.

1.2 Origins of Auditory Cortex: A Comparative Perspective

Sound has a necessarily complex role in guiding behavior, and the systems that subserve auditory processing have had a long time to develop. To give some context for understanding the function of the auditory system, we will first briefly cover the evolutionary development of this system in mammals, particularly primates. The part of the auditory system that is most varied in mammals is the auditory cortex (for review, see: Hackett, 2008). While reptiles have a dorsal cortex that is homologous to neocortex, this dorsal cortex does not have auditory inputs. Instead, the projections of the auditory thalamus are subcortical. Yet, all studied mammals have a region of temporal cortex that gets inputs from the auditory thalamus and is responsive to auditory stimuli. Thus, early mammals or the ancestors of mammals somehow acquired direct thalamic auditory projection to cortex. Most studied mammals have several areas of auditory cortex, including two or three primary or primary-like areas that are characterized by direct inputs from the tonotopically organized ventral nucleus of the medial geniculate complex,

MGv, and are in turn also tonotopically organized. In addition, these primary fields are surrounded by a belt of secondary auditory areas, and additional, higher-level areas of auditory or multisensory processing may be present. For now, conclusions about how auditory cortex varies in organization across mammals need to be limited, as species in some of the major branches of mammalian evolution have not been studied, and studies have been few and incomplete for species in other major branches.

More progress has been made in studies of carnivores (cats, dogs, ferrets) where at least two primary areas exist, an anterior auditory field (AAF) and the classical primary field (A1). A posterior field (P or PAF) has some of the characteristics of a primary field, and seven or eight secondary fields have been described. With more than one field having primary area features, identifying the same (homologous) areas across members of different orders of mammals has been challenging. Primates also have at least two primary fields, a posterior A1 and an anterior "rostral" area, R. The more anterior rostrotemporal area, RT, has some of the characteristics of a primary area. Given these uncertainties about the identities of primary areas and the limited comparative evidence, there is little understanding of what secondary areas may be homologous, if any, across mammalian taxa. For now, we can surmise that early mammals had at least one primary area and a bordering secondary area or areas, and this organization has been partly retained, but variously elaborated in the major lines leading to extent mammals.

1.3 Properties of Sound

To define some basic properties of sound that we will refer to, consider a marmoset monkey twittering a "love song" to its mate in the dense tree cover of a

Brazilian rain forest. It is plausible to suggest that this call is a meaningful stimulus worth processing, and it serves as a useful example. The first important question one has to ask (if one is a marmoset): Who is she? Identity cues can include frequency structure (i.e., which frequencies are in the call) and temporal modulation rates (i.e., how the strength of the frequencies change in time). These frequency and temporal modulation cues end up giving rise to complex percepts such as rhythm, pitch, and harmonicity. These percepts, combined with other systems such as emotion and memory systems, in turn can give rise to meaning and speaker identity (Moore, 1997).

The second important question is: Where is she? Location cues can include loudness (is she getting louder?), frequency structure (the outer ear, or pinna, filters sound in particular ways depending on the vertical location of the source), and differences between the two ears in intensity (interaural intensity differences: IID) and time (interaural time differences: ITD). These properties give rise to cues about the direction of motion, and vertical and horizontal location, respectively. Spatial percepts about the location of the sound source, combined with other systems that subserve interpersonal space can help guide action, such as the marmoset properly orienting to its mate. Note that both object identity and location rely on partially overlapping sets of acoustic cues.

1.4 Ethological Considerations in Sound Transmission and Implications for Perception

No animal processes sound outside of the confines of the environment it is surrounded by. Any forest, grassland, or classroom is like an auditory hall of mirrors,

absorbing, reflecting, and distorting sound in characteristic ways (reviewed in: Hauser, 1996; Fitch, 2002). The acoustic environment presents numerous challenges to the detection and discrimination of sounds. First is the degradation of sounds as they propagate through space – sounds will be subject to frequency dependent attenuation, reverberation, and irregular amplitude fluctuations due to inhomogeneities in the air temperature or velocity (i.e. atmospheric effects). Also affecting sound detection and discrimination are the levels and quality of ambient noise in the surroundings.

These transmission hurdles affect sound in different environments differently. For example in forest biome, reverberation off of objects such as trees is more severe than in an open habitat, and this reverberation is worse for higher modulation frequencies. Thus the higher frequencies of amplitude modulated sounds and rapid repetitive frequency modulation will be masked in a closed environment. In contrast, in open environments amplitude fluctuations from atmospheric inhomogeneities are more likely to be a factor. These inhomogeneities are generally less than 50 Hz, and so will affect low frequencies of modulation of the sound (reviewed in: Wiley and Richards, 1978; Brown and Handford, 2000). In both environments, frequency dependent degradation gets worse with increasing frequency, but for the forest environments, there appears to be a low frequency window (200 Hz in Brown 1986, 700-1200 Hz in Morton 1975). This may be due to lower frequency sound bouncing off of the canopy or the thermal gradient that the canopy creates during certain times of day. Thus, open environments propagate sound best with relative low spectral frequencies and high frequency modulation and closed environmennts propagate sound best that contain low spectral frequencies (especially in the window) with slower rates of modulation. Ground attenuation is also a factor, and is

similar for both environments. At 1 M above the earth, sounds in the range of 300-3000 Hx are attenuated the greatest, and the higher the transmitter is, the less attenuation occurs, especially at higher frequencies (Wiley and Richards, 1978). Lastly the source and frequency content of background noise is different for different habitats (Brown and Waser, 1988).

It has been pointed out that not all degradation is necessarily harmful, and that sound transmission is more than just long distance propagation. Since different cues (i.e. spectral frequency, modulation frequency) degrade at different rates and in different ways, weighing the relative degradation of a signal may tell a receiving organism something about the transmitter's location or environment (Wiley and Richards 1978}. This hypothesis necessarily relies on a transmitter signaling a highly stereotyped call.

To what extent can ethological considerations bear on constraints of the vocal behavior (and auditory perception) of primates? An influential hypothesis is that animals that are communicating over long distances and do not have a complex social structure will communicate in a nongraded system, one with a large feature distance between exemplars which makes it easier to distinguish between calls, even degraded ones (Marler, 1975). In contrast, animals that have close contact and easy visual access, such as in a grassland, will develop graded vocalizations schema, where the calls have variability in a given exemplar and there may be little difference between different calls. This hypothesis also makes a second prediction that most long-range communication calls should exhibit a graded structure due to transmission difficulties.

Certain species of primate such as macaques have what are termed graded vocalizations, where there are only graded distinctions between individuals and call

types. Even long range calls, such as shrill barks, are graded when they should be nongraded (Fischer et al., 2001). However, macaques live in highly variable habitat, from forest to semidesert, and many live in villages and towns. Clearly a communication system highly adapted to a particular ecology would be maladaptive for such a diversified animal. We can conclude that ecological acoustics are not a primary factor in the evolution of acoustical processing to production of the macaque vocal repertoire. However, just because macaque calls do not follow Marler's predictions does not mean there is at least one example where macaque calls to appear to be optimized for long range communication. 'Lost' calls in toque macaques come in two basic types one that is long duration (0.3-0.7 sec) and low frequency (500-1800 Hz), better for long distance propagation, and the other that is higher frequency (3.5-5Khz), with shorter with repetitions, better to transmit location cues based on differences between the two ears (Dittus, 1988). Also, studies have shown that calls from forest primates are more robust when played in an arboreal environment as compares to savanna dwelling calls in their native habitat, suggesting that these forest vocalizations have been subject to greater acoustic selection pressure for preservation of long distance communication (Brown et al., 1995).

Given the difficulties in ambiguous transmission in a graded repertoire, why the shift to such a system? Graded repertoires may instead be able to carry more information (Hauser, 1996). It appears that graded differences between similar calls are often the mark of individual voices (Hammerschmidt and Todt, 1995). For example, spectral peak patterns or differences in spectral composition in certain vocalizations (coos) help identify individual voices (Hauser and Fowler, 1992; Rendall et al., 1996; Rendall et al.,

1998) (but not screams). These are likened to human vocal tract resonances and are supposed to cue individual identity and morphology (i.e. size, gender) (Ghazanfar et al., 2007).

In contrast, marmosets do have a set ecology. Due in part to extremely high predation pressures, they are primarily arboreal in nature. As per the laws described above, a prediction would be made that their vocal communication would be lower frequency with low modulation frequencies. Indeed this is the case for modulation frequency – most of the modulations in a marmoset vocalization are in the range of 7-15 Hz (Epple, 1968). However it does not appear to be the case for frequencies – most spectra energy is concentrated in the range of 5-15 kHz (Epple, 1968). Perhaps due to the high predation pressures it is instead adaptive to communicate in frequency ranges that quickly degrade over space. Also counter to Marler's hypothesis, it has been shown that some marmoset vocalizations are graded (Schrader and Todt, 1993).

Thus for primates with and without a set biome, it appear that Marler's predictions are of limited usefulness for prediction. This is true for other species of primates, both old word monkeys such as alarm calls in baboons (Fischer et al., 2001), and for other new world arboreal species such as squirrel moneys and tamarins (Hauser, 1996).

If one ascribes to the school of thought developed by Barlow (Barlow, 1961) the auditory system evolved to process behaviorally relevant sound, and limiting factors in the auditory environment would serve to limit the kinds of sounds that an organism would need to process. Thus, these ethological considerations have strong implications for the cortical coding of auditory signals. Consider the coding of temporal modulation

frequencies. It is interesting that though subcortical temporal tuning of these stimuli is up to hundreds of Hz (reviewed in: Langner, 1992), tuning in cortical structures of marmoset, such as A1, is concentrated in the lower modulation frequencies (Lu et al., 2001; Liang et al., 2002; Kajikawa et al., 2005; Bendor and Wang, 2008). It could be argued that the shift in cortical tuning to low frequencies is to reflect these lower frequencies that transmit better in the arboreal environment (X. Wang, personal communication). However, the similarities emerging between macaque and marmoset tuning seem to suggest that this tuning is not driven by a specific ecological niche, but instead reflects encoding common to primates, possibly as a result of timing and integration constraints placed on it by cortical processing (this is discussed in more detail in Chapter III). Low modulation frequencies predominate in both macaque and marmoset vocalizations so the shift towards low frequencies in cortex may also be due to selection pressure to be able to efficiently process conspecific vocalizations.

To understand the mechanisms by which we process complex sounds to guide optimal behavior, a natural place to start is by understanding the neural mechanisms of sound processing. From the earlier marmoset example we can see that both auditory object identity and location rely on partially overlapping sets of cues. The frequency structure of the sound is important for both, and the changes of amplitude and frequency content over time are important for both. Because auditory cues are so time dependent, a strong characteristic of the auditory system is its highly parallel nature. Auditory processing is characterized by multiple interacting streams even at its earliest levels. Also, context plays a large role in the relative importance of processing identity or space. Sometimes you need to know if it is your mate. At other times it is more important to

know that an object is on a collision path with you than to specifically identify what it is you are dodging!

In the next two sections, the main features and pathways of the auditory cortical system are reviewed in order to provide a foundation for the other chapters. It describes auditory processing as sound waves hit the cochlea, travels up through the nuclei of the brainstem, further disseminates in multiple cortical streams, and finally arrives at associative areas such as the prefrontal and orbitofrontal cortices. Processing streams that have been identified anatomically are described, and physiological properties and possible functions are described where data are available.

.

1.5 Early Auditory Processing Streams and Pathways: The Path to Cortex

Cochlea to the Inferior Colliculus

The most obvious and possibly most fundamental organizing principle of the auditory system is tonotopy, an orderly representation of sound frequency across a one-dimensional space. Tonotopy is first established at the level of the sensory epithelium (the cochlea). When sound waves hit the spiraled structure of the cochlea, the nature of the basilar membrane in the cochlea splits up the sound into its frequency components. The basilar membrane has graded stiffness along its length, so wave amplitude changes in a frequency-dependent manner as it is propagated along the basilar membrane. Higher frequencies stimulate inner hair cells at the closest portion of the membrane (the base),

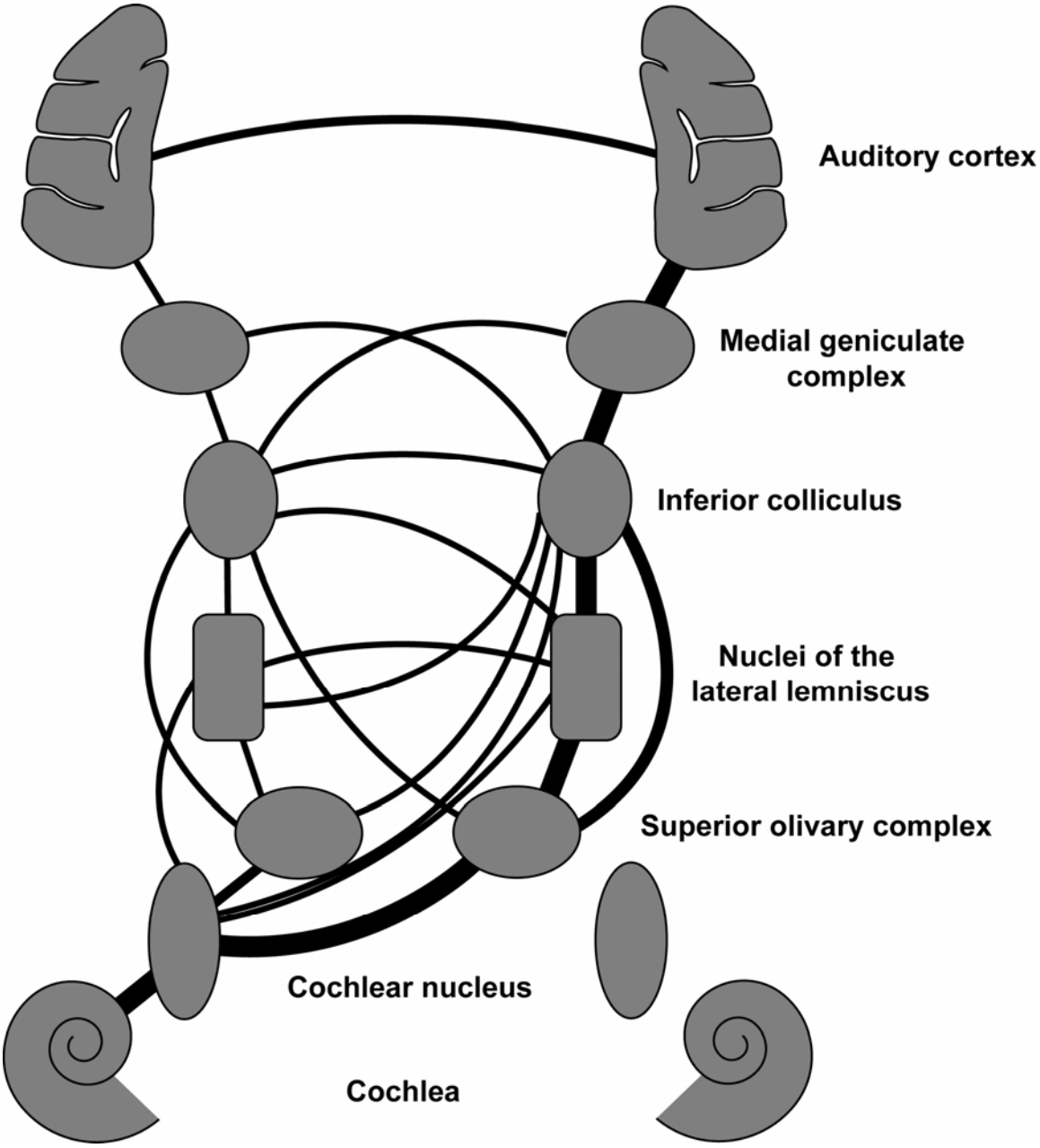

Figure 1-1. Major ascending connections of the subcortical auditory system
Selected ascending pathways from the cochlea to auditory cortex, major pathways are shown in thick lines. Divisions of subcortical nuclei are indicated in text.

and lower frequencies stimulate inner hair cells at the farthest portion (the apex). In mammals, the length of the basilar membrane is related to the length of the range of frequencies an animal can hear (West, 1985). Thus, the cochlea establishes tonotopy; an organizational principle preserved though the levels of auditory processing through auditory cortex.

Responses from the cochlea project via the eighth nerve to the cochlear nucleus. The cochlear nucleus projects to structures in the superior olivary complex (SOC) such as the medial superior olive (MSO), the lateral superior olive (LSO) and the medial nucleus of the trapezoid body (MNTB) (figure 1-1) (reviewed in: Pickles, 1988; Rouiller, 1997). It also projects to the nuclei of the lateral lemniscus. Again, each of these structures maintains a basic tonotopy established by the cochlea.

Response properties of these structures show that neurons still faithfully represent sound by encoding spatial frequency at very high resolution. Neurons in these structures also demonstrate temporal tuning (or how fast the neuron can synchronize with the temporal structure of the sound) at high rates (see Langner, 1992). Nuclei of the superior olivary complex are especially important for the encoding of sound location, as they are the first place where ascending information from the two ears is combined (for review, see: Kelly et al., 2002). From these structures and nuclei of the lateral lemniscus, responses reach the inferior colliculus of the midbrain. The inferior colliculus can be divided into two major portions, the central and external nuclei. Investigators also commonly distinguish the dorsal cortex, the dorsoventral nucleus, and the pericentral nucleus of the inferior colliculus.

The central nucleus (ICc) is considered to be the main relay nucleus of the inferior colliculus. It is tonotopically organized and receives a direct projection from the lateral lemniscus. Responses are tightly tuned to tones, modulation rate encoding shows synchronization up up to 120 Hz and response latencies are generally short (Ryan and Miller, 1978; Langner and Schreiner, 1988; Schreiner and Langner, 1988). In contrast, the external nucleus (ICx) is not tonotopically organized, neurons have longer latencies, and they receive most of inputs from sources other than the lateral lemniscus. Thus begins two pathways: a fast, direct, tonotopically organized pathway (lemniscal pathway through the ICc) and a slower, indirect, nontonotopically organized pathway (nonlemniscal pathways through the ICx).

When compared to other sensory systems, the proliferation of brainstem nuclei in the auditory system is striking. The exact meaning of this is not well understood, but it may allow for greater and faster stimulus processing early in the stream to transform a simple one-dimensional representation of tone frequency in time into complex percepts in space and time. This element of parallel processing is one of the highlights of the auditory system, and is best suited to processing stimuli that occur on a very fast timescale, as in audition.

The Auditory Thalamus

Lying just medial and posterior to the lateral geniculate of the visual system, the medial geniculate complex (MGC) is a small and heterogeneous thalamic structure. There are other auditory-responsive nuclei in the thalamus (see below), but the MGC is characterized as the primary feedforward auditory division because its inputs are

dominated by the inferior colliculus (Winer et al., 1992; Jones, 2003). There is a multiplicity of pathways from the cochlea to the thalamus, but the MGC is an obligatory relay of auditory information into auditory cortex. Thus, it is useful to spend some time describing the organization and response properties of neurons in the MGC, since cortical responses can best be understood in the light of their thalamic inputs.

While the functional organization of the MGC has not been extensively explored, especially in primates, a general picture based on connectivity and microelectrode studies is emerging (reviewed in: de Ribaupierre, 1997). The MGC of primates consists of at least three main divisions: ventral (MGv), dorsal (MGd), and medial (MGm). Based partly on the paucity of data, the nature and specialization of these divisions has been a matter of speculation for some time. For example Poljak (Poljak, 1926) posited that the ventral division pathway aided in localization, and the MGd division was involved in the discrimination of sounds. Later, Evans (Evans, 1974) put forth a similar idea, that the MGv was involved in localization and the MGd was involved in pattern recognition. The current understanding of the MGC is that the divisions perhaps do not divide function so cleanly. What has become clear is that these divisions have different input connections and internal architecture, leading to neurons with different frequency tuning properties, modulation rate tuning, response latencies, and sometimes multisensory properties.

One division of the MGB, the MGv, receives tonotopically organized projections from both the ipsi- and contralateral ICc, but ipsilateral input is stronger. This leads to a structure that is itself tonotopically organized. Neurons respond well to pure tones, and are generally narrowly tuned to tone frequency - they respond best to a small range of frequencies even at high intensities, perhaps only a quarter of an octave (Allon et al.,

1981; Calford, 1983). Response latencies are quite short. In addition, temporal envelope tuning indicates that the responses of these neurons can follow and distinguish very rapid rates of stimulation (Allon et al., 1981; Wang et al., 2008). In terms of selectivity to sound identity or location, the majority are primarily excited by sound coming from the contralateral ear, and sensitive to difference cues such as interaural intensity and time differences (Starr and Don, 1972; Calford, 1983; Barone et al., 1996). These MGv neurons are not selective for particular vocal stimuli either (Symmes et al., 1980), evidence that complex sound identity cues, such as call type, are not distinguished at this level.

A second division of the auditory thalamus is the MGd. It receives most of its input from noncentral portions of the inferior colliculus. There is no evidence of tonotopy in MGd and its neurons are generally poorly responsive to pure tones, with broad or multi-peaked frequency tuning. These neurons have long response latencies, consistent with their inputs from noncentral collicular nuclei. However, MGd neurons exhibit robust responses to complex sounds (Allon et al., 1981; Calford, 1983; He and Hu, 2002). An important caveat is that MGd can be further subdivided. It has been suggested that this region has two divisions in primates, an anterior (MGad) and a posterior (MGpd) division (reviewed in: Jones, 2003). It is possible that the response properties differ between the two subdivisions, and it is suspected that the anterior portion of the dorsal division (MGad) may in fact be tonotopically organized and have neurons with short latencies, thus resembling MGv neurons (Imig and Morel, 1984, 1985a, b).

A third division of the auditory thalamus is the MGm. This nucleus receives inputs from both the central and external divisions of the inferior colliculus. MGm also

receives significant projections from vestibular nuclei, spinal cord, and superior colliculus (SC) (Calford and Aitkin, 1983; Rouiller et al., 1991; Winer et al., 1992; Rouiller, 1997). Connectivity of neurons within this nucleus may be highly variable, as MGm neurons project to all three core belt and parabelt regions of auditory cortex (see below), as well as other regions. MGm has not been extensively studied but there is evidence that different cell classes within MGm project to different cortical layers (Hashikawa et al., 1995). There may be tonotopy in the rostral division of the MGm (Rouiller et al., 1989), but for the most part tonotopy through the entire structure is lacking. Much like the MGd, neurons are broadly tuned and are often multi-peaked to tone stimuli. Response latencies are also variable (Allon et al., 1981; Calford and Aitkin, 1983), and consistent with its heterogeneous inputs, there is evidence for neurons with multisensory responses in at least some nonprimate species (e.g. Calford and Aitkin, 1983; LeDoux et al., 1987; Rouiller et al., 1989).

There are other auditory related areas in the primate thalamus, but their primary inputs are from structures such as cortical and nonprimary subcortical auditory structures, and cortical multisensory and brainstem nuclei. These include the posterior nuclear group (PO), the medial pulvinar (PM), suprageniculate (SG), and limitans (Lim) (de Ribaupierre, 1997; Rouiller and Durif, 2004; de la Mothe et al., 2006a). The posterolateral section of the thalamic reticular nucleus is heavily implicated in mediating feedback cortical efferents. The posterior nuclear group lies dorsal and medial to the MGC. The medial pulvinar is the auditory-responsive region of the pulvinar and receives inputs from the superior coliculus, but whether it receives inputs from the inferior colliculus is not known. The medial pulvinar projects broadly to temporal, frontal, and

cingulate cortex (Gutierrez et al., 2000). The thalamic reticular nucleus can be broken down into three parts, an anterior division that responds primarily to somatosensory inputs, a dorsal part that responds primarily to visual inputs, and a ventral part that responds primarily to auditory inputs. Neurons in the auditory sector are broadly tuned to tones, but can act in a frequency-specific manner mediated by connections with the MGC (Crabtree, 1998).

The importance of the MGC cannot be overestimated in understanding auditory cortical processing: it is an obligatory relay to the cortex. In primates the 3-4 divisions of the MGC each transform and modulate auditory neural responses in different ways. These divisions project to different parts of auditory cortex in different degrees (see figure 1-4), creating the firmament of the organization and response properties seen there.

Auditory Cortex

Auditory cortex includes cortex that gets preferential projections from the MGC and is responsive to auditory stimuli. In humans, auditory cortex corresponds to Brodmann's areas 41 and 42 located in the vicinity of Heschl's gyrus on the superior temporal plane (Hackett et al., 2001; Hackett, 2008). In macaques, auditory cortex is located on caudal portion of the lower bank of the lateral sulcus and the superior temporal gyrus (see figure 1-2). Since only a small portion is visible on the surface of this macaque brain (upper brain), the parietal cortex has been 'cut' away to reveal the areas of auditory cortex hidden deep in the lateral and circular sulcus (lower brain). From the figure, it is easy to appreciate one difficulty of studying auditory cortex: it is almost completely

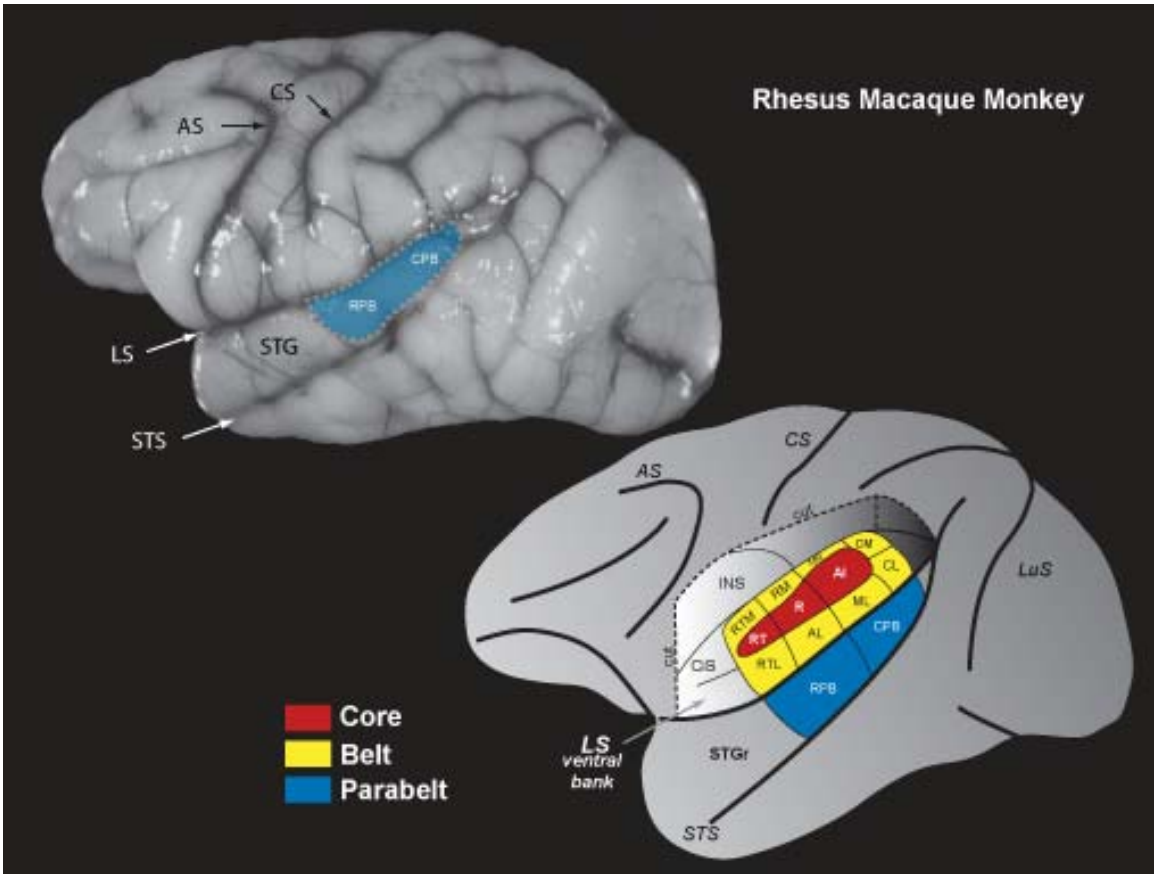

Figure 1-2. Location of primate auditory cortex (macaque).
Upper figure: location of auditory cortex in macaque. Note that only the parabelt (blue: RPB, CPB) is exposed on the surface of the brain. Lower figure: the parietal and frontal cortices have been graphically cut away to reveal approximate location of core and belt (red and yellow). Abbreviations: LS lateral sulcus, STS superior temporal sulcus, AS arcuate sulcus, CS central sulcus, STG superior temporal gyrus, STS superior temporal sulcus, CIS circular sulcus, INS insula, LuS lunate sulcus.

covered by the parietal lobe in Old World primates such as macaques, chimpanzees, and humans.

In this chapter, we emphasize a model of auditory cortical organization that is based on decades of anatomical and physiological research (Kaas and Hackett, 1998, 2000; Hackett, 2010). According to this working model, auditory cortex is first divided

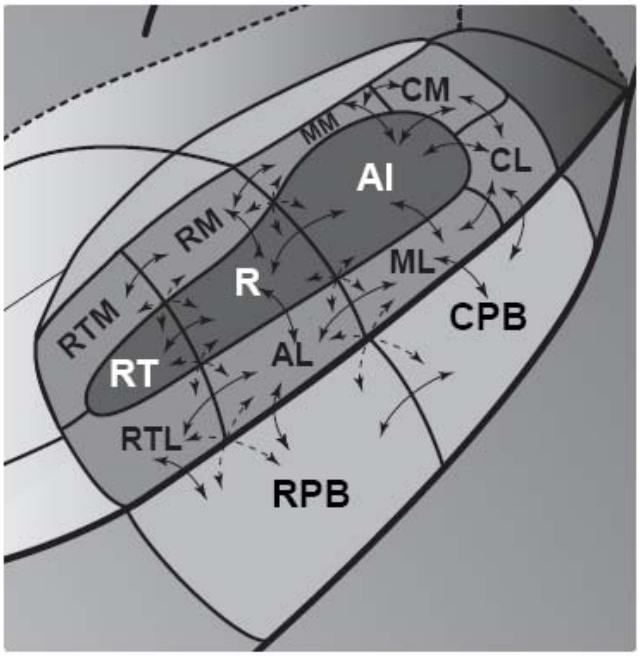

Figure 1-3. Organization of primate auditory cortex.
A schematic of primate auditory cortex showing core, belt, and parabelt regions with areal subdivisions, and some short range connections. For clarity, medial belt projections to parabelt are not pictured.

into three **regions**, which can be thought of as levels of processing (see figure 1-3). These regions are further subdivided into twelve **areas**. In short, regions are subdivisions of auditory cortex, and areas are subdivisions of regions. Subdivisions are distinguished based on three things: *connections* (i.e., from thalamus and to other cortical areas), the cellular and histochemical *architecture* of cortical tissue, and *functional organization*, presumably reflected by specificity of neural response properties (such as patterns of tonotopic organization and the differences in response properties). The anatomical differences in connections and architecture are thought to subserve the differences in

function between regions and between areas. In the following section, we will first describe general regional characteristics, and then fill in the details, where known, of areal characteristics.

In auditory cortex, three major regions are defined: *core*, a *belt* that wraps around this, and a *parabelt* region lying lateral to the belt. Distinguishing architectonic features of auditory cortex can include markers for differences in cellular and molecular features such as cytochrome oxidase (CO), acetylcholinesterase (AChE), parvalbumin, the vesicular glutamate transporter 2 (vGluT2), and density of myelination. These markers change roughly stepwise as one progresses from medial to lateral according regional distinctions (de la Mothe et al., 2006b; Hackett and de la Mothe, 2009).

The core region receives its primary input from the MGv, and also receives a projection from the MGm (figure 1-4). The core has a broad layer IV that is densely myelinated and exhibits a high expression of CO, AChE, parvalbumin and vGluT2, all consistent with receiving a dense and rapidly conducting projection from the thalamus (de la Mothe et al., 2006a, b). This core region is densely connected within and across divisions of the core region, and with the divisions in the adjoining belt region, but not to the parabelt (we will come back to this later). Compared to other regions, neurons in the core tend to have short response latencies (though this varies across areas, see below), with narrow tone frequency tuning functions, and relatively fast modulation frequency tuning (e.g. Merzenich and Brugge, 1973; Vaadia et al., 1982; Steinschneider et al., 1992; Bieser and Muller-Preuss, 1996; Bieser, 1998; Recanzone, 2000a; Cheung et al., 2001; Kajikawa et al., 2005; Lakatos et al., 2005; Philibert et al., 2005; Bendor and Wang,

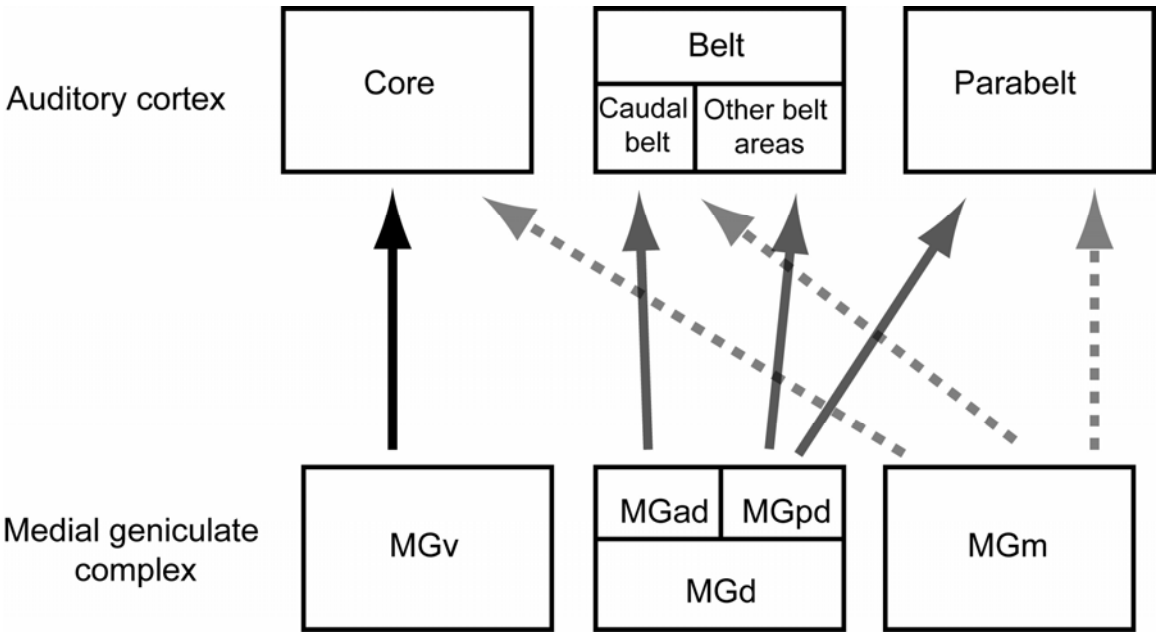

Figure 1-4. Connections of the medial geniculate complex with regions of auditory cortex A schematic of connections of the three subdivisions of the MGC (MGv, MGd, MGm) with the three regions of auditory cortex (core, belt, parabelt). For simplicity, only major connections are shown. Arrow type denotes different thalamic sources, not quantity of projections.

2008; Kajikawa et al., 2008; Oshurkova et al., 2008; Kusmierek and Rauschecker, 2009; Crum et al., submitted).

The belt region receives thalamic projections from the MGd and MGm, but not MGv (figure 1-4). The belt has a less pronounced layer IV than core, and it is also less myelinated and exhibits reduced expressions of the markers described above, consistent with a less robust projection from the MGC. The belt is divided into a medial and a lateral region, relative to its position to the core. The medial belt region is most connected within itself and the adjoining core regions (figure 1-3). The lateral belt is most

connected within itself, adjoining core and adjoining parabelt. The belt has been less well studied electrophysiologically than core because most of the region responds poorly under anesthesia. Compared to core, belt neurons appear to have wider tuning functions, often with broad or multipeaked frequency tuning, and respond well to complex sounds(Vaadia et al., 1982; Rauschecker and Tian, 2004; Tian and Rauschecker, 2004; Kajikawa et al., 2008; Recanzone, 2008; Kusmierek and Rauschecker, 2009; Crum et al., submitted). Belt neurons also exhibit longer latencies and do not entrain as well to temporal stimuli (Bieser, 1995; Crum et al., submitted) stimuli may be encoded by firing rate (see: Wang et al., 2008).

The third region, the parabelt, also receives thalamic projections from the MGd and MGm (figure 1-4). The parabelt has a less pronounced layer IV than core or belt, which is also less myelinated and exhibits further reduced expression of the markers described above, consistent with an even less robust projection from the MGC (Hackett et al., 1998b; de la Mothe et al., 2006b; Hackett and de la Mothe, 2009). The parabelt region is most connected within itself and with the adjoining lateral belt region (figure 1-3). It may have a weak feedback projection to core (de la Mothe et al., 2006b), but no direct projection from it. The response properties of parabelt neurons have not been well studied (but see: Crum et al., submitted), but based on patterns of connections and responses known thus far, parabelt neurons are expected to exhibit long latencies and respond extremely poorly to tones, with wide and probably complex frequency tuning functions. This region will probably be more responsive to sounds that are both spectrally and temporally complex, such as vocalizations over pure tones or even wideband noise.

While the distinctions between regions is roughly stepwise in a medial to lateral direction, it is also important to note that superimposed on these regions is a rostral to caudal gradient of the same molecular markers described above (i.e markers for differences in cellular and molecular features such as cytochrome oxidase (CO), acetylcholinesterase (AChE), parvalbumin, the vesicular glutamate transporter 2 (vGluT2), and density of myelination). In general, these features change gradually, but the strongest expression of these markers in a given region is caudally and the weakest expression is rostrally (de la Mothe et al., 2006a, b; Hackett and de la Mothe, 2009)

Upon this regional organization, these regions are divided into areas (see figure 1-3 and 4) (Kaas and Hackett, 1998, 2000). The core region contains three areas (from caudal to rostral): the 'primary' area A1, the rostral area R, and the rostral temporal area RT. The medial belt contains four areas, also named by location: the caudal medial area CM, the middle medial area MM, the rostral medial area RM, and the rostrotemporal medial area RTM. The lateral belt also has four areas: the caudal lateral area CL, the medial lateral ML, the anterolateral area AL, and the rostrotemporal lateral area RTL. Lastly, the parabelt has at least two areas: the caudal parabelt area CPB and the rostral parabelt area RPB. At least most of these areas have its own, often crude, tonotopic map which flips representational order along caudorostral borders (for most complete map, see Petkov et al., 2006). Distinctions of connections, architecture and functional characteristics between areas within a region are less pronounced than distinctions between regions, but these weaker differences allow us to further subdivide regions into areas. The function of any of these areas has not been fully elucidated, partly because they must be interpreted in the context of the functions of the others. However, we do

know something about specificities of neural responses in some areas, and can make educated predictions about the rest.

Given these subdivisions of regions and areas, how does auditory information flow between and across regions and areas? A picture of graded hierarchy of informational flow between regions is emerging from both connectional anatomy and physiology. Given that only the MGv has demonstrated strong tonotopy, the tonotopy exhibited in the belt and parabelt (which do not receive projections from the MGv) is considered to be inherited from the core (Rauschecker et al., 1997; Kaas and Hackett, 2000). Additionally, there is no direct projection from core to parabelt, further suggesting a degree of serial, hierarchical processing from core to belt to parabelt. There is a convergence of inputs from each region to the next, which presumably leads to the wider frequency tuning and altered response specificity as one progresses across levels.

In further support of this direction of flow, latencies increase from core to lateral belt at the same rostrocaudal level (Vaadia et al., 1982; Bieser and Muller-Preuss, 1996; Recanzone, 2000a; Crum et al., submitted). For example, latencies in A1 are shorter than those in ML. Other support comes from rate level functions. At lower levels, loudness is encoded as a monotonic function: as sound level rises, so does neural firing rate. As one ascends the hierarchy of sound processing, one sees more complex, non-monotonic cells, where cells reach peak firing at a certain sound level, and then have less robust firing rates at higher sound levels. As one progresses from core to belt, neural response thresholds for lowest amplitude to elicit a response get higher. Tuning widths for tone frequencies also become wider for neurons from core to belt, presumably reflecting convergence of more tightly tuned inputs originating at earlier levels (i.e. core) (Bieser

and Muller-Preuss, 1996; Recanzone, 2000a; Rauschecker and Tian, 2004; Kusmierek and Rauschecker, 2009; Crum et al., submitted). Peak temporal modulation tuning also progressively decreases, thought to be due to imprecisions in timing of activations introduced by successive synaptic delays (Crum et al., submitted). A nonsynchronized firing rate code for modulation rate also emerges at the level of auditory cortex (reviewed in Wang et al., 2008). It is worth distinguishing that while information flow may be roughly serial, informational processing is not thought to occur in a strictly staged process. Instead, many perceptual processes are occurring in parallel with each other.

Bear in mind that informational flow across regions is not strictly serial, or strictly in parallel within a region. As mentioned before, the regions express dramatic medial to lateral stepwise changes in architecture and connectivity described above. Within each region, the architecture and response properties follow a less dramatic, but distinct caudal to rostral decrease in molecular marker expression and MGC connectivity. Also, connectivity within a region seems to have a preferential caudal to rostral feedforward characteristics (Fitzpatrick and Imig, 1980; Galaburda and Pandya, 1983; de la Mothe et al., 2006b). In support of this, latencies have also been seen to increase in a caudorostral direction (Bieser and Muller-Preuss, 1996; Bendor and Wang, 2008; Kusmierek and Rauschecker, 2009).

Caudorostral changes in architecture and differences in connectivity indicate that each area within a region has a unique profile of architecture and connectivity, presumably subserving differences in functions between areas. For example, the caudal most core area (A1) is more myelinated than the most rostral portion of the core (i.e. de la Mothe et al., 2006b) and demonstrates faster latencies (Bendor and Wang, 2008). Current

evidence suggests that most of the belt areas exhibit slower latencies than the core area corresponding to that caudorostral level (i.e. A1 slower than ML). However, due to this caudorostral gradient it is not as easy to make predictions of response latencies between regions that do not correspond to the same caudorostral level. There is growing evidence that the most caudal belt region, CM, has many neurons with response latencies that are as fast or faster than those in the most caudal core region, A1 (Rauschecker and Tian, 2004; Kajikawa et al., 2005; Lakatos et al., 2005; Oshurkova et al., 2008). However, CM (and caudal belt in general) receives its MGd inputs from the MGad nucleus, which as discussed earlier may exhibit tonotopy and fast latencies. Yet, physiological and lesion evidence seems to suggest that CM appears to depend completely on A1 inputs for its tone responses (Rauschecker et al., 1997). Clearly these and other findings are presenting challenges to the present model in terms of information flow within auditory cortex.

As discussed previously, auditory object location and identity share partially overlapping cues, the coding of which are described above. To date, there has been little evidence of strong feature identity selectivity (e.g. for different calls) for neurons in core and belt areas of auditory cortex (Wang et al., 1995; Recanzone, 2008; Kusmierek and Rauschecker, 2009). Currently there is a bias for recording in the larger and more accessible caudal core and belt areas, so the lack of selectivity found thus far may be simply due to this. One aspect of object identity is the subjective perception of pitch (irrespective if whether the frequency is actually present). A module of neurons that appears to be selective for pitch has been described on the lateral low frequency border of A1 with RT (Bendor and Wang, 2005, 2010), and there seems to be converging evidence for a similar processing zone in core auditory cortex from fMRI evidence in humans,

thought it is often not as tightly localized (reviewed by: Bendor and Wang, 2006; but see: Hall and Plack, 2009).

The coding of object location in auditory cortex has been an area of intense interest. Many neurons appear to be spatially selective for free-field sounds as well as interaural intensity and time differences (IID and ITD) have been demonstrated, especially in the caudal belt fields (Ahissar et al., 1992; Recanzone, 2000b; Woods et al., 2006; Scott et al., 2007; Miller and Recanzone, 2009). How this spatial selectivity is propagated has still not been well elucidated, as spatial selectivity in the MCG is virtually unknown. There has been little evidence for an ordered spatiotopic map in auditory cortex - instead, location in space is represented across a distributed population of neurons (Miller and Recanzone, 2009). A co-registration of auditory information within an ordered spatiotopic map could occur in lower layers of the superior colliculus (SC), which have significant inputs from auditory and multisensory areas of neocortex (Huerta and Harting, 1984; Morel and Kaas, 1992; Collins et al., 2005). Higher order spatial perception such as the perception of auditory motion is also poorly understood, but belt areas have been shown to be sensitive to the presentation of approaching 'looming' stimuli (Maier and Ghazanfar, 2007).

1.6 Auditory-Responsive Cortex Beyond Classical Auditory Cortex: Superior Temporal Gyrus, Prefrontal and Insular Cortices, and Corticofugal Pathways

Superior Temporal Gyrus

Areas of the superior temporal sulcus (STS) include Ts1, Ts2, the superior temporal polysensory region (STP) and Tpt. These areas have been shown to have dense

reciprocal connections with belt and parabelt (figure 1-5), as well some exhibit weaker auditory thalamic inputs from the MGC and multisensory nuclei of he posterior thalamus (PO, SG, etc.) (Trojanowski and Jacobson, 1975; Galaburda and Pandya, 1983; Markowitsch et al., 1985; Pandya and Rosene, 1993; Pandya et al., 1994; Kosmal et al., 1997; Hackett et al., 1998a, b; Hackett et al., 2007). These regions have not been well explored electrophysiologically, but evidence from fMRI and PET studies in primates responsiveness to auditory stimuli, as well as other modalities (Poremba et al., 2003; Poremba et al., 2004; Gil-da-Costa et al., 2006; Petkov et al., 2008). Rostral STS has been shown to be responsive to vocalizations, and there is growing evidence for a voice identity processing area in the superior temporal region – one that responds preferentially to the vocal identity of particular callers (Poremba et al., 2004; Petkov et al., 2008; see also review of human literature by Belin, 2006).

Prefrontal Cortex

Auditory cortical belt and parabelt project to areas in the prefrontal cortex, orbitofrontal cortex and cingulate cortices in a topographic manner, in that the caudal parabelt primarily projects to dorsal prefrontal cortex and ventral parabelt primarily projects to ventral prefrontal cortex (fgure 1-5). Auditory-related areas on the STG described above project in a similar topographic manner (Pandya et al., 1969; Hackett et al., 1999; Romanski et al., 1999a; Romanski et al., 1999b; Cavada et al., 2000; Petrides and Pandya, 2002; Morecraft et al., 2004; Barbas et al., 2005; Barbas, 2007; Kayser et al., 2007; Petrides and Pandya, 2007; Roberts et al., 2007; Saleem et al., 2008; Gerbella et al., 2010). These areas can show auditory responsiveness to complex stimuli such as

vocalizations or in a task specific manner (Ito, 1982; Azuma and Suzuki, 1984; Bodner et al., 1996; Fuster et al., 2000; Kikuchi-Yorioka and Sawaguchi, 2000; Romanski and

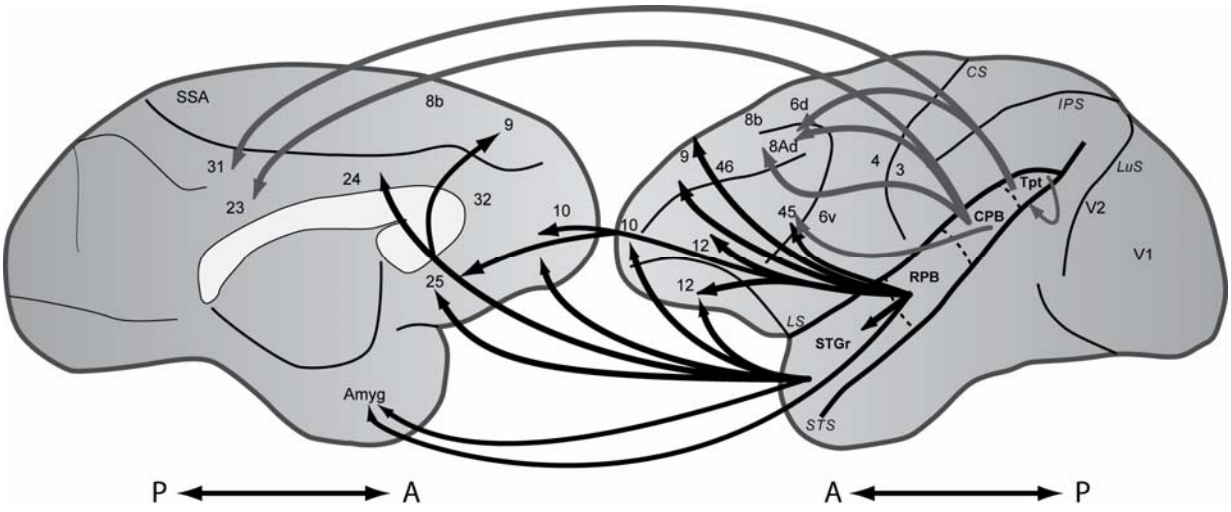

Figure 1-5. Auditory cortical projections to prefrontal, limbic structures
Long-range connections of auditory and auditory-related cortical fields to prefrontal and limbic structures projected on a macaque brain. Note the dorsoventral topography. For clarity, projections from core and belt of auditory cortex, insular cortex, basal ganglia, and basal nuclei projections are not shown.

Goldman-Rakic, 2002; Gifford et al., 2005; Romanski et al., 2005; Cohen et al., 2006; Sugihara et al., 2006; Artchakov et al., 2007; Cohen et al., 2007; Romanski, 2007; Lemus et al., 2009). For example, the dorsal most portion of the frontal eye field responds to auditory stimuli, and it is thought to mediate auditory-guided saccades. This is consistent with projection patterns described above showing a caudal projection from the caudal belt and adjoining association cortices to the portion of the frontal cortex containing the frontal eye fields. Auditory responsiveness has also been explored in the ventrolateral prefrontal cortex. Neurons in this part of cortex are responsive to vocalizations, but not responsive to tones or noise, and have been shown to discriminate between different

vocalizations (Romanski and Goldman-Rakic, 2002; Romanski et al., 2005; Cohen et al., 2006; Cohen et al., 2007; Russ et al., 2008; Lemus et al., 2009; reviewed in Romanski and Averbeck, 2009).

This dorsoventral topography of auditory belt and parabelt projections to frontal cortex has led to the proposal that there exists a domain specificity of auditory processing in auditory cortex (Romanski et al., 1999a; Romanski et al., 1999b; but see: Recanzone and Cohen, 2009), much like the domain specificity described in the visual or somatosensory cortices (Mishkin, 1979; Ungerleider and Mishkin, 1982; Disbrow et al., 2003). It is hypothesized that the dorsal prefrontal cortex receive projections from the dorsocaudal 'where' stream of auditory processing and the ventral prefrontal cortex receives projections from the ventrocaudal 'what' stream of auditory processing along the temporal lobe (Romanski et al., 1999b), which translates to functional specialization prefrontal and auditory cortices (e.g. Rauschecker and Tian, 2000; Tian et al., 2001; Romanski and Goldman-Rakic, 2002).

Insular Cortex

Another auditory-responsive region is insular cortex, lying just medial to the medial belt of auditory cortex. This area is connected to the auditory areas of the medial belt, and to a lesser extent lateral belt and parabelt, as well as areas of the superior temporal gyrus and prefrontal cortex (de la Mothe et al., 2006b; Smiley et al., 2007). Early studies indicated its responsiveness to both simple auditory stimuli, such as tones and clicks, and more complex stimuli such as vocalizations in single unit studies (Sudakov et al., 1971; Bieser and Muller-Preuss, 1996; Bieser, 1998; see also Remedios

et al., 2009). Insular cortex has also been implicated in auditory functions in both human and primate imaging studies (Zatorre et al., 1994; Griffiths et al., 1997), lending further support to the idea that it is another region of auditory cortical processing. In a recent study, insular neurons responded preferentially to conspecific vocalizations over sounds with similar spectral or envelope structure, indicating that they are responding preferentially to the vocalization (Remedios et al., 2009). Their vocalization selectivity was not more than neurons in the ventrolateral prefrontal cortex, discussed above. How insular cortex fits into the 'what versus where' stream hypothesis has yet to be determined.

Corticofugal Projections

There are extensive corticalfugal projections from auditory and auditory related cortex (reviewed in Winer, 2005), presumed to play a major role in top down modulatory effects as well as possibly learning effects. These connections have been most extensively demonstrated in cats, but have been demonstrated in primates as well (FitzPatrick and Imig, 1978; Luethke et al., 1989; Morel and Kaas, 1992; de la Mothe et al., 2006a). These projections target primarily ipsilateral nuclei and structures. There are massive projections to the MGC (Winer et al., 2002; de la Mothe et al., 2006a), inferior colliculus (mostly outside of the central nucleus) (Winer et al., 1998), superior olivary complex (SOC), cochlear nucleus (CoN), pons (Brodal, 1972) and basal ganglia (Reale and Imig, 1983). Input to claustrum and entopeduncular nucleus also arises from areas of auditory cortex (Beneyto and Prieto, 2001). The dorsal putamen and caudate nucleus receive topographic projections from tonotopic areas of auditory cortex (Reale and Imig,

1983), and appear to have a role in sensory processing by affecting threshold and frequency responses (Sun et al., 1996). Motor behavior could be modulated by inputs from auditory cortex to the basal ganglia (Beneyto and Prieto, 2001). Auditory cortex is also positioned to affect autonomic function via the projections to amygdala (e.g. Romanski and LeDoux, 1993) and central gray (Winer et al., 1998). Other inputs to the amygdala come directly from the auditory thalamus, at least in rats (Iwata et al., 1986).

1.7 Objective

Our long term aim is to further define the functional organization of primate auditory cortex, and relate anatomical structure to neural processing of sound. By incorporating the results from a number of studies, a working model of primate auditory cortex has emerged (Kaas and Hackett, 2000; Hackett, 2002, 2010). As discussed previously in this chapter, the current working model is comprised of three levels of processing involving three cortical regions: core, belt, and parabelt. These regions can be divided into approximately thirteen different areas, distinguished by a unique set of anatomical and physiological properties that overlap in some dimensions and differ in others (reviewed in: Hackett, 2010). The current working model predicts a hierarchy of processing in two directions. The first is a strict serial processing from the core to belt to parabelt, with successive integration between levels due to converging inputs. In addition to this, there is evidence of a hierarchy of flow from caudal to rostral areas within a region.

In addition to testing the predictions made about direction of flow reviewed earlier, we are also interested in understanding the physiological signature of the many shared converging and diverging inputs in cortex. Work in anesthetized cats suggest that neuron pairs within different areas of auditory cortex have spike timing that is weakly yet similarly correlated (reviewed in: Eggermont, 2000, 2007). Though there are similarities between the auditory cortex of primates and cats (reviewed in: Hackett, 2010), correlations within and between areas are not a formal part of the primate model yet. To do this, this work needs to be extended to multiple areas of the awake primate. If the results can also be applied to the primate model, we predict that pairwise correlations will be similar for neurons within an area, irrespective of regional or caudorostal level. Additionally, we predict that overall correlation values of neuron pairs between different areas will be smaller, but also similar, irrespective of regional or caudorostal level. Timelags of cross-area peak correlations can also be used to indicate direction of flow between areas.

In this series of studies, we examine response latencies, temporal tuning measures, and pairwise spike correlations in multiple areas in core, belt, and parabelt of the auditory cortex of the awake macaque. Our aims are to examine physiological evidence for serial processing and integration of inputs along the hypothesized axes of information flow in the auditory cortex. By studying multiple areas in the same animal under the same experimental conditions, we are better able to compare responses between areas to better evaluate these aims.

1.8 Organization of the Dissertation

This chapter (Chapter I) serves as an introduction to primate auditory cortex and the cortical encoding of sound by reviewing auditory pathways and neural response properties. Chapter II addresses hypotheses about the timing of information flow in auditory cortex by examining neural response latencies to auditory stimuli in ten different areas across core, belt, and parabelt. As an additional and complementary measure, LFP latencies are also examined for evidence of the same trends. Chapter III addresses hypotheses about flow and convergence in auditory cortex by examining changes in temporal modulation tuning in five areas across core, belt, and parabelt. LFP tuning is also examined for evidence of the same trends. Chapter IV also addresses flow and convergence by examining correlations from pairs of neurons within seven areas and pairs of neurons across three sets of different areas. Evidence for correlations within and across areas may be attributed to common inputs, and as evidence for across-area correlations that have nonzero lag may be attributable to the direct driving influence of one area on another. Chapter V reviews the main findings, and synthesizes them in the context of their implications for auditory cortex and auditory information processing. It also discusses limitations and future directions of study. Lastly, in the course of the studies it became apparent that there was no tested standard to determine neural latency in auditory cortex, as popular methods used in anesthetized cortex were inappropriate. Thus, the appendix is a comparison of five different latency measures in awake auditory cortex, which was necessary preparation for Chapter II. Each chapter is written as an independent article, as some of them have been or are currently being prepared for

submission. However, references to other chapters are made where appropriate to avoid repetition of figures or method details.

1.9 References

Ahissar M, Ahissar E, Bergman H, Vaadia E (1992) Encoding of sound-source location and movement: activity of single neurons and interactions between adjacent neurons in the monkey auditory cortex. J Neurophysiol 67:203-215.

Allon N, Yeshurun Y, Wollberg Z (1981) Responses of single cells in the medial geniculate body of awake squirrel monkeys. Exp Brain Res 41:222-232.

Artchakov D, Tikhonravov D, Vuontela V, Linnankoski I, Korvenoja A, Carlson S (2007) Processing of auditory and visual location information in the monkey prefrontal cortex. Exp Brain Res 180:469-479.

Azuma M, Suzuki H (1984) Properties and distribution of auditory neurons in the dorsolateral prefrontal cortex of the alert monkey. Brain Res 298:343-346.

Barbas H (2007) Specialized elements of orbitofrontal cortex in primates. Ann N Y Acad Sci 1121:10-32.

Barbas H, Hilgetag CC, Saha S, Dermon CR, Suski JL (2005) Parallel organization of contralateral and ipsilateral prefrontal cortical projections in the rhesus monkey. BMC Neurosci 6:32.

Barlow H (1961) Possible principles underlying the transformation of sensory messages. In: Sensory Communication (Rosenblith W, ed), pp 217-234. Cambridge: MIT Press.

Barone P, Clarey JC, Irons WA, Imig TJ (1996) Cortical synthesis of azimuth-sensitive single-unit responses with nonmonotonic level tuning: a thalamocortical comparison in the cat. J Neurophysiol 75:1206-1220.

Belin P (2006) Voice processing in human and non-human primates. Philos Trans R Soc Lond B Biol Sci 361:2091-2107.

Bendor D, Wang X (2005) The neuronal representation of pitch in primate auditory cortex. Nature 436:1161-1165.

Bendor D, Wang X (2006) Cortical representations of pitch in monkeys and humans. Curr Opin Neurobiol 16:391-399.

Bendor D, Wang X (2008) Neural response properties of primary, rostral, and rostrotemporal core fields in the auditory cortex of marmoset monkeys. J Neurophysiol 100:888-906.

Bendor D, Wang X (2010) Neural coding of periodicity in marmoset auditory cortex. J Neurophysiol 103:1809-1822.

Beneyto M, Prieto JJ (2001) Connections of the auditory cortex with the claustrum and the endopiriform nucleus in the cat. Brain Res Bull 54:485-498.

Bieser A (1995) Amplitude envelope encoding as a feature for temporal information processing in the auditory cortex of squirrel monkeys. In: Primate Vocal Communication (Zimmerman E, ed), pp 221-232. New York, NY: Plenum Press.

Bieser A (1998) Processing of twitter-call fundamental frequencies in insula and auditory cortex of squirrel monkeys. Exp Brain Res 122:139-148.

Bieser A, Muller-Preuss P (1996) Auditory responsive cortex in the squirrel monkey: neural responses to amplitude-modulated sounds. Exp Brain Res 108:273-284.

Bodner M, Kroger J, Fuster JM (1996) Auditory memory cells in dorsolateral prefrontal cortex. Neuroreport 7:1905-1908.

Brodal P (1972) The corticopontine projection in the cat. The projection from the auditory cortex. Arch Ital Biol 110:119-144.

Brown C, Waser P (1988) Environmental influences on the stucture of primate vocalizations. In: Primate Vocal Communication (Todt D, Goedeking P, Symmes D, eds), pp 51-66. Berlin: Springer-Verlag.

Brown CH, Gomez R, Waser PM (1995) Old-World Monkey Vocalizations - Adaptation to the Local Habitat. Animal Behaviour 50:945-961.

Brown TJ, Handford P (2000) Sound design for vocalizations: Quality in the woods, consistency in the fields. Condor 102:81-92.

Calford MB (1983) The parcellation of the medial geniculate body of the cat defined by the auditory response properties of single units. J Neurosci 3:2350-2364.

Calford MB, Aitkin LM (1983) Ascending projections to the medial geniculate body of the cat: evidence for multiple, parallel auditory pathways through thalamus. J Neurosci 3:2365-2380.

Cavada C, Company T, Tejedor J, Cruz-Rizzolo RJ, Reinoso-Suarez F (2000) The anatomical connections of the macaque monkey orbitofrontal cortex. A review. Cereb Cortex 10:220-242.

Cheung SW, Bedenbaugh PH, Nagarajan SS, Schreiner CE (2001) Functional organization of squirrel monkey primary auditory cortex: responses to pure tones. J Neurophysiol 85:1732-1749.

Cohen YE, Hauser MD, Russ BE (2006) Spontaneous processing of abstract categorical information in the ventrolateral prefrontal cortex. Biol Lett 2:261-265.

Cohen YE, Theunissen F, Russ BE, Gill P (2007) Acoustic features of rhesus vocalizations and their representation in the ventrolateral prefrontal cortex. J Neurophysiol 97:1470-1484.

Collins CE, Lyon DC, Kaas JH (2005) Distribution across cortical areas of neurons projecting to the superior colliculus in new world monkeys. Anat Rec A Discov Mol Cell Evol Biol 285:619-627.

Crabtree JW (1998) Organization in the auditory sector of the cat's thalamic reticular nucleus. J Comp Neurol 390:167-182.

Crum P, Issa E, Hackett T, Wang X (submitted) Hierarchical processing in awake primate auditory cortex.

de la Mothe LA, Blumell S, Kajikawa Y, Hackett TA (2006a) Thalamic connections of the auditory cortex in marmoset monkeys: core and medial belt regions. J Comp Neurol 496:72-96.

de la Mothe LA, Blumell S, Kajikawa Y, Hackett TA (2006b) Cortical connections of the auditory cortex in marmoset monkeys: core and medial belt regions. J Comp Neurol 496:27-71.

de Ribaupierre F (1997) Acoustical information porcessing in the auditory thalamus and cerebral cortex. In: The Central Auditory System (Ehret G, Romand R, eds), pp 317-398. New York, NY: Oxford University Press.

Disbrow E, Litinas E, Recanzone GH, Padberg J, Krubitzer L (2003) Cortical connections of the second somatosensory area and the parietal ventral area in macaque monkeys. J Comp Neurol 462:382-399.

Dittus W (1988) An analysis of toque macaque cohesion calls from an ecological perspective. In: Primate Vocal Communication (Todt D, Goedeking P, Symmes D, eds), pp 31-49. Berlin: Springer-Verlag.

Eggermont JJ (2000) Sound-induced synchronization of neural activity between and within three auditory cortical areas. J Neurophysiol 83:2708-2722.

Eggermont JJ (2007) Correlated neural activity as the driving force for functional changes in auditory cortex. Hear Res 229:69-80.

Epple G (1968) Comparative studies on vocalization in marmoset monkeys (Hapalidae). Folia Primatol (Basel) 8:1-40.

Evans E (1974) Neural processes for the detection of acoustic patterns and for sound localization. In: The Neurosciences, third study program (Schmidt F, Wordern F, eds), pp 131-145. Cambridge: MIT Press.

Fischer J, Hammerschmidt K, Cheney DL, Seyfarth RM (2001) Acoustic features of female chacma baboon barks. Ethology 107:33-54.

Fitch WTS (2002) Primate vocal production and its implications for auditory research. In: Primate Audition: Ethology and Neurobiology (Ghazanfar A, ed), pp 87-108. London: CRC Press.

FitzPatrick KA, Imig TJ (1978) Projections of auditory cortex upon the thalamus and midbrain in the owl monkey. J Comp Neurol 177:573-555.

Fitzpatrick KA, Imig TJ (1980) Auditory cortico-cortical connections in the owl monkey. J Comp Neurol 192:589-610.

Fuster JM, Bodner M, Kroger JK (2000) Cross-modal and cross-temporal association in neurons of frontal cortex. Nature 405:347-351.

Galaburda AM, Pandya DN (1983) The intrinsic architectonic and connectional organization of the superior temporal region of the rhesus monkey. J Comp Neurol 221:169-184.

Gerbella M, Belmalih A, Borra E, Rozzi S, Luppino G (2010) Cortical connections of the macaque caudal ventrolateral prefrontal areas 45A and 45B. Cereb Cortex 20:141-168.

Ghazanfar AA, Turesson HK, Maier JX, van Dinther R, Patterson RD, Logothetis NK (2007) Vocal-tract resonances as indexical cues in rhesus monkeys. Curr Biol 17:425-430.

Gifford GW, 3rd, MacLean KA, Hauser MD, Cohen YE (2005) The neurophysiology of functionally meaningful categories: macaque ventrolateral prefrontal cortex plays a critical role in spontaneous categorization of species-specific vocalizations. J Cogn Neurosci 17:1471-1482.

Gil-da-Costa R, Martin A, Lopes MA, Munoz M, Fritz JB, Braun AR (2006) Species-specific calls activate homologs of Broca's and Wernicke's areas in the macaque. Nat Neurosci 9:1064-1070.

Griffiths TD, Rees A, Witton C, Cross PM, Shakir RA, Green GG (1997) Spatial and temporal auditory processing deficits following right hemisphere infarction. A psychophysical study. Brain 120 (Pt 5):785-794.

Gutierrez C, Cola MG, Seltzer B, Cusick C (2000) Neurochemical and connectional organization of the dorsal pulvinar complex in monkeys. J Comp Neurol 419:61-86.

Hackett T (2008) Organization and coorespondence of the auditory cortex of humans and non-human primates. In: Evolution of the Nervous System (Kaas JH, ed), pp 199-226. Oxford: Elsevier.

Hackett TA (2002) The comparative anatomy of the primate auditory cortex. In: Primate Audition: Behavior and Neurobiology (Ghanzafar A, ed). Boca Raton: CRC Press.

Hackett TA (2010) Information flow in the auditory cortical network. Hear Res.

Hackett TA, de la Mothe LA (2009) Regional and laminar distribution of the vesicular glutamate transporter, VGluT2, in the macaque monkey auditory cortex. J Chem Neuroanat 38:106-116.

Hackett TA, Stepniewska I, Kaas JH (1998a) Thalamocortical connections of the parabelt auditory cortex in macaque monkeys. J Comp Neurol 400:271-286.

Hackett TA, Stepniewska I, Kaas JH (1998b) Subdivisions of auditory cortex and ipsilateral cortical connections of the parabelt auditory cortex in macaque monkeys. J Comp Neurol 394:475-495.

Hackett TA, Stepniewska I, Kaas JH (1999) Prefrontal connections of the parabelt auditory cortex in macaque monkeys. Brain Res 817:45-58.

Hackett TA, Preuss TM, Kaas JH (2001) Architectonic identification of the core region in auditory cortex of macaques, chimpanzees, and humans. J Comp Neurol 441:197-222.

Hackett TA, Smiley JF, Ulbert I, Karmos G, Lakatos P, de la Mothe LA, Schroeder CE (2007) Sources of somatosensory input to the caudal belt areas of auditory cortex. Perception 36:1419-1430.

Hall DA, Plack CJ (2009) Pitch processing sites in the human auditory brain. Cereb Cortex 19:576-585.

Hammerschmidt K, Todt D (1995) Individual-differences in vocalizations of young barbary macaques (macaca sylvanus) - a multi-parametric analysis to identify critical cues in acoustic signaling. Behaviour 132:381-399.

Hashikawa T, Molinari M, Rausell E, Jones EG (1995) Patchy and laminar terminations of medial geniculate axons in monkey auditory cortex. J Comp Neurol 362:195-208.

Hauser MD (1996) The Evolution of Communication. Cambridge, MA: MIT Press.

Hauser MD, Fowler CA (1992) Fundamental frequency declination is not unique to human speech: evidence from nonhuman primates. J Acoust Soc Am 91:363-369.

He J, Hu B (2002) Differential distribution of burst and single-spike responses in auditory thalamus. J Neurophysiol 88:2152-2156.

Huerta M, Harting J (1984) Connectional organization of the superior colliculus. Trends in Neurosciences 7:286-289.

Imig TJ, Morel A (1984) Topographic and cytoarchitectonic organization of thalamic neurons related to their targets in low-, middle-, and high-frequency representations in cat auditory cortex. J Comp Neurol 227:511-539.

Imig TJ, Morel A (1985a) Tonotopic organization in lateral part of posterior group of thalamic nuclei in the cat. J Neurophysiol 53:836-851.

Imig TJ, Morel A (1985b) Tonotopic organization in ventral nucleus of medial geniculate body in the cat. J Neurophysiol 53:309-340.

Ito SI (1982) Prefrontal unit activity of macaque monkeys during auditory and visual reaction time tasks. Brain Res 247:39-47.

Iwata J, LeDoux JE, Meeley MP, Arneric S, Reis DJ (1986) Intrinsic neurons in the amygdaloid field projected to by the medial geniculate body mediate emotional responses conditioned to acoustic stimuli. Brain Res 383:195-214.

Jones EG (2003) Chemically defined parallel pathways in the monkey auditory system. Ann N Y Acad Sci 999:218-233.

Kaas JH, Hackett TA (1998) Subdivisions of auditory cortex and levels of processing in primates. Audiol Neurootol 3:73-85.

Kaas JH, Hackett TA (2000) Subdivisions of auditory cortex and processing streams in primates. Proc Natl Acad Sci U S A 97:11793-11799.

Kajikawa Y, de La Mothe L, Blumell S, Hackett TA (2005) A comparison of neuron response properties in areas A1 and CM of the marmoset monkey auditory cortex: tones and broadband noise. J Neurophysiol 93:22-34.

Kajikawa Y, de la Mothe LA, Blumell S, Sterbing-D'Angelo SJ, D'Angelo W, Camalier CR, Hackett TA (2008) Coding of FM sweep trains and twitter calls in area CM of marmoset auditory cortex. Hear Res 239:107-125.

Kayser C, Petkov CI, Logothetis NK (2007) Tuning to sound frequency in auditory field potentials. J Neurophysiol 98:1806-1809.

Kelly K, Metzger R, Mulette-Gillman O, Werner-Reiss U, Groh J (2002) Representation of sound location in the primate brain. In: Primate Audition: Ethology and Neurobiology (Ghazanfar A, ed), pp 177-198. London: CRC Press.

Kikuchi-Yorioka Y, Sawaguchi T (2000) Parallel visuospatial and audiospatial working memory processes in the monkey dorsolateral prefrontal cortex. Nat Neurosci 3:1075-1076.

Kosmal A, Malinowska M, Kowalska DM (1997) Thalamic and amygdaloid connections of the auditory association cortex of the superior temporal gyrus in rhesus monkey (Macaca mulatta). Acta Neurobiol Exp (Wars) 57:165-188.

Kusmierek P, Rauschecker JP (2009) Functional specialization of medial auditory belt cortex in the alert rhesus monkey. J Neurophysiol.

Lakatos P, Pincze Z, Fu KM, Javitt DC, Karmos G, Schroeder CE (2005) Timing of pure tone and noise-evoked responses in macaque auditory cortex. Neuroreport 16:933-937.

Langner G (1992) Periodicity coding in the auditory system. Hear Res 60:115-142.

Langner G, Schreiner CE (1988) Periodicity coding in the inferior colliculus of the cat. I. Neuronal mechanisms. J Neurophysiol 60:1799-1822.

LeDoux JE, Ruggiero DA, Forest R, Stornetta R, Reis DJ (1987) Topographic organization of convergent projections to the thalamus from the inferior colliculus and spinal cord in the rat. J Comp Neurol 264:123-146.

Lemus L, Hernandez A, Romo R (2009) Neural encoding of auditory discrimination in ventral premotor cortex. Proc Natl Acad Sci U S A 106:14640-14645.

Liang L, Lu T, Wang X (2002) Neural representations of sinusoidal amplitude and frequency modulations in the primary auditory cortex of awake primates. J Neurophysiol 87:2237-2261.

Lu T, Liang L, Wang X (2001) Temporal and rate representations of time-varying signals in the auditory cortex of awake primates. Nat Neurosci 4:1131-1138.

Luethke LE, Krubitzer LA, Kaas JH (1989) Connections of primary auditory cortex in the New World monkey, Saguinus. J Comp Neurol 285:487-513.

Maier JX, Ghazanfar AA (2007) Looming biases in monkey auditory cortex. J Neurosci 27:4093-4100.

Markowitsch HJ, Emmans D, Irle E, Streicher M, Preilowski B (1985) Cortical and subcortical afferent connections of the primate's temporal pole: a study of rhesus monkeys, squirrel monkeys, and marmosets. J Comp Neurol 242:425-458.

Marler P (1975) On the origin of speech from animal sounds. In: The Role of Speech in Language (Kavanaugh J, Cutting J, eds), pp 11-37. Cambridge: MIT Press.

Merzenich MM, Brugge JF (1973) Representation of the cochlear partition of the superior temporal plane of the macaque monkey. Brain Res 50:275-296.

Miller LM, Recanzone GH (2009) Populations of auditory cortical neurons can accurately encode acoustic space across stimulus intensity. Proc Natl Acad Sci U S A 106:5931-5935.

Mishkin M (1979) Analogous neural models for tactual and visual learning. Neuropsychologia 17:139-151.

Moore B (1997) The Psychology of Hearing, 4th Edition. San Diego, CA: Academic Press.

Morecraft RJ, Cipolloni PB, Stilwell-Morecraft KS, Gedney MT, Pandya DN (2004) Cytoarchitecture and cortical connections of the posterior cingulate and adjacent somatosensory fields in the rhesus monkey. J Comp Neurol 469:37-69.

Morel A, Kaas JH (1992) Subdivisions and connections of auditory cortex in owl monkeys. J Comp Neurol 318:27-63.

Oshurkova E, Scheich H, Brosch M (2008) Click train encoding in primary and non-primary auditory cortex of anesthetized macaque monkeys. Neuroscience 153:1289-1299.

Pandya DN, Rosene DL (1993) Laminar termination patterns of thalamic, callosal, and association afferents in the primary auditory area of the rhesus monkey. Exp Neurol 119:220-234.

Pandya DN, Hallett M, Kmukherjee SK (1969) Intra- and interhemispheric connections of the neocortical auditory system in the rhesus monkey. Brain Res 14:49-65.

Pandya DN, Rosene DL, Doolittle AM (1994) Corticothalamic connections of auditory-related areas of the temporal lobe in the rhesus monkey. J Comp Neurol 345:447-471.

Petkov CI, Kayser C, Augath M, Logothetis NK (2006) Functional imaging reveals numerous fields in the monkey auditory cortex. PLoS Biol 4:e215.

Petkov CI, Kayser C, Steudel T, Whittingstall K, Augath M, Logothetis NK (2008) A voice region in the monkey brain. Nat Neurosci 11:367-374.

Petrides M, Pandya DN (2002) Comparative cytoarchitectonic analysis of the human and the macaque ventrolateral prefrontal cortex and corticocortical connection patterns in the monkey. Eur J Neurosci 16:291-310.

Petrides M, Pandya DN (2007) Efferent association pathways from the rostral prefrontal cortex in the macaque monkey. J Neurosci 27:11573-11586.

Philibert B, Beitel RE, Nagarajan SS, Bonham BH, Schreiner CE, Cheung SW (2005) Functional organization and hemispheric comparison of primary auditory cortex in the common marmoset (Callithrix jacchus). J Comp Neurol 487:391-406.

Pickles J (1988) An Introduction to the Physiology of Hearing, 2nd Edition. San Diego, CA: Academic Press.

Poljak S (1926) The connections of the acoustic nerve. Journal of Anatomy 60:465-469.

Poremba A, Saunders RC, Crane AM, Cook M, Sokoloff L, Mishkin M (2003) Functional mapping of the primate auditory system. Science 299:568-572.

Poremba A, Malloy M, Saunders RC, Carson RE, Herscovitch P, Mishkin M (2004) Species-specific calls evoke asymmetric activity in the monkey's temporal poles. Nature 427:448-451.

Rauschecker JP, Tian B (2000) Mechanisms and streams for processing of "what" and "where" in auditory cortex. Proc Natl Acad Sci U S A 97:11800-11806.

Rauschecker JP, Tian B (2004) Processing of band-passed noise in the lateral auditory belt cortex of the rhesus monkey. J Neurophysiol 91:2578-2589.

Rauschecker JP, Tian B, Pons T, Mishkin M (1997) Serial and parallel processing in rhesus monkey auditory cortex. J Comp Neurol 382:89-103.

Reale RA, Imig TJ (1983) Auditory cortical field projections to the basal ganglia of the cat. Neuroscience 8:67-86.

Recanzone GH (2000a) Response profiles of auditory cortical neurons to tones and noise in behaving macaque monkeys. Hear Res 150:104-118.

Recanzone GH (2000b) Spatial processing in the auditory cortex of the macaque monkey. Proc Natl Acad Sci U S A 97:11829-11835.

Recanzone GH (2008) Representation of con-specific vocalizations in the core and belt areas of the auditory cortex in the alert macaque monkey. J Neurosci 28:13184-13193.

Recanzone GH, Cohen YE (2009) Serial and parallel processing in the primate auditory cortex revisited. Behav Brain Res.

Remedios R, Logothetis NK, Kayser C (2009) An auditory region in the primate insular cortex responding preferentially to vocal communication sounds. J Neurosci 29:1034-1045.

Rendall D, Rodman PS, Emond RE (1996) Vocal recognition of individuals and kin in free-ranging rhesus monkeys. Animal Behaviour 51:1007-1015.

Rendall D, Owren MJ, Rodman PS (1998) The role of vocal tract filtering in identity cueing in rhesus monkey (Macaca mulatta) vocalizations. Journal of the Acoustical Society of America 103:602-614.

Roberts AC, Tomic DL, Parkinson CH, Roeling TA, Cutter DJ, Robbins TW, Everitt BJ (2007) Forebrain connectivity of the prefrontal cortex in the marmoset monkey (Callithrix jacchus): an anterograde and retrograde tract-tracing study. J Comp Neurol 502:86-112.

Romanski LM (2007) Representation and integration of auditory and visual stimuli in the primate ventral lateral prefrontal cortex. Cereb Cortex 17 Suppl 1:i61-69.

Romanski LM, LeDoux JE (1993) Information cascade from primary auditory cortex to the amygdala: corticocortical and corticoamygdaloid projections of temporal cortex in the rat. Cereb Cortex 3:515-532.

Romanski LM, Goldman-Rakic PS (2002) An auditory domain in primate prefrontal cortex. Nat Neurosci 5:15-16.

Romanski LM, Averbeck BB (2009) The primate cortical auditory system and neural representation of conspecific vocalizations. Annu Rev Neurosci 32:315-346.

Romanski LM, Bates JF, Goldman-Rakic PS (1999a) Auditory belt and parabelt projections to the prefrontal cortex in the rhesus monkey. J Comp Neurol 403:141-157.

Romanski LM, Averbeck BB, Diltz M (2005) Neural representation of vocalizations in the primate ventrolateral prefrontal cortex. J Neurophysiol 93:734-747.

Romanski LM, Tian B, Fritz J, Mishkin M, Goldman-Rakic PS, Rauschecker JP (1999b) Dual streams of auditory afferents target multiple domains in the primate prefrontal cortex. Nat Neurosci 2:1131-1136.

Rouiller E (1997) Functional organization of the auditory pathways. In: The Central Auditory System (Ehret G, Romand R, eds), pp 3-65. New York, NY: Oxford University Press.

Rouiller EM, Durif C (2004) The dual pattern of corticothalamic projection of the primary auditory cortex in macaque monkey. Neurosci Lett 358:49-52.

Rouiller EM, Simm GM, Villa AE, de Ribaupierre Y, de Ribaupierre F (1991) Auditory corticocortical interconnections in the cat: evidence for parallel and hierarchical arrangement of the auditory cortical areas. Exp Brain Res 86:483-505.

Rouiller EM, Rodrigues-Dagaeff C, Simm G, De Ribaupierre Y, Villa A, De Ribaupierre F (1989) Functional organization of the medial division of the medial geniculate body of the cat: tonotopic organization, spatial distribution of response properties and cortical connections. Hear Res 39:127-142.

Russ BE, Ackelson AL, Baker AE, Cohen YE (2008) Coding of auditory-stimulus identity in the auditory non-spatial processing stream. J Neurophysiol 99:87-95.

Ryan A, Miller J (1978) Single unit responses in the inferior colliculus of the awake and performing rhesus monkey. Exp Brain Res 32:389-407.

Saleem KS, Kondo H, Price JL (2008) Complementary circuits connecting the orbital and medial prefrontal networks with the temporal, insular, and opercular cortex in the macaque monkey. J Comp Neurol 506:659-693.

Schrader L, Todt D (1993) Contact call parameters covary with social-context in common marmosets, Callithrix-j-jacchus. Animal Behaviour 46:1026-1028.

Schreiner CE, Langner G (1988) Periodicity coding in the inferior colliculus of the cat. II. Topographical organization. J Neurophysiol 60:1823-1840.

Scott BH, Malone BJ, Semple MN (2007) Effect of behavioral context on representation of a spatial cue in core auditory cortex of awake macaques. J Neurosci 27:6489-6499.

Smiley JF, Hackett TA, Ulbert I, Karmas G, Lakatos P, Javitt DC, Schroeder CE (2007) Multisensory convergence in auditory cortex, I. Cortical connections of the caudal superior temporal plane in macaque monkeys. J Comp Neurol 502:894-923.

Starr A, Don M (1972) Responses of squirrel monkey (Samiri sciureus) medial geniculate units to binaural click stimuli. J Neurophysiol 35:501-517.

Steinschneider M, Tenke CE, Schroeder CE, Javitt DC, Simpson GV, Arezzo JC, Vaughan HG, Jr. (1992) Cellular generators of the cortical auditory evoked potential initial component. Electroencephalogr Clin Neurophysiol 84:196-200.

Sudakov K, MacLean PD, Reeves A, Marino R (1971) Unit study of exteroceptive inputs to claustrocortex in awake, sitting, squirrel monkey. Brain Res 28:19-34.

Sugihara T, Diltz MD, Averbeck BB, Romanski LM (2006) Integration of auditory and visual communication information in the primate ventrolateral prefrontal cortex. J Neurosci 26:11138-11147.

Sun X, Chen QC, Jen PH (1996) Corticofugal control of central auditory sensitivity in the big brown bat, Eptesicus fuscus. Neurosci Lett 212:131-134.

Symmes D, Alexander GE, Newman JD (1980) Neural processing of vocalizations and artificial stimuli in the medial geniculate body of squirrel monkey. Hear Res 3:133-146.

Tian B, Rauschecker JP (2004) Processing of frequency-modulated sounds in the lateral auditory belt cortex of the rhesus monkey. J Neurophysiol 92:2993-3013.

Tian B, Reser D, Durham A, Kustov A, Rauschecker JP (2001) Functional specialization in rhesus monkey auditory cortex. Science 292:290-293.

Trojanowski JQ, Jacobson S (1975) A combined horseradish peroxidase-autoradiographic investigation of reciprocal connections between superior temporal gyrus and pulvinar in squirrel monkey. Brain Res 85:347-353.

Ungerleider L, Mishkin M (1982) Two cortical visual systems. In: Analysis of Visual Behavior (DJ I, MA G, RJW M, eds), pp 549-586. Cambridge, Mass: MIT Press.

Vaadia E, Gottlieb Y, Abeles M (1982) Single-unit activity related to sensorimotor association in auditory cortex of a monkey. J Neurophysiol 48:1201-1213.

Wang X, Merzenich MM, Beitel R, Schreiner CE (1995) Representation of a species-specific vocalization in the primary auditory cortex of the common marmoset: temporal and spectral characteristics. J Neurophysiol 74:2685-2706.

Wang X, Lu T, Bendor D, Bartlett E (2008) Neural coding of temporal information in auditory thalamus and cortex. Neuroscience 157:484-494.

West CD (1985) The relationship of the spiral turns of the cochlea and the length of the basilar membrane to the range of audible frequencies in ground dwelling mammals. J Acoust Soc Am 77:1091-1101.

Wiley RH, Richards DG (1978) Physical constraints on acoustic communication in atmosphere - implications for evolution of animal vocalizations. Behavioral Ecology and Sociobiology 3:69-94.

Winer JA (2005) Decoding the auditory corticofugal systems. Hear Res 207:1-9.

Winer JA, Wenstrup JJ, Larue DT (1992) Patterns of GABAergic immunoreactivity define subdivisions of the mustached bat's medial geniculate body. J Comp Neurol 319:172-190.

Winer JA, Larue DT, Diehl JJ, Hefti BJ (1998) Auditory cortical projections to the cat inferior colliculus. J Comp Neurol 400:147-174.

Winer JA, Chernock ML, Larue DT, Cheung SW (2002) Descending projections to the inferior colliculus from the posterior thalamus and the auditory cortex in rat, cat, and monkey. Hear Res 168:181-195.

Woods TM, Lopez SE, Long JH, Rahman JE, Recanzone GH (2006) Effects of stimulus azimuth and intensity on the single-neuron activity in the auditory cortex of the alert macaque monkey. J Neurophysiol 96:3323-3337.

Zatorre RJ, Evans AC, Meyer E (1994) Neural mechanisms underlying melodic perception and memory for pitch. J Neurosci 14:1908-1919.

CHAPTER II

AUDITORY RESPONSE LATENCIES ACROSS MACAQUE AUDITORY CORTEX

2.1 Abstract

Anatomical connections between regions and areas of the primate auditory cortex suggest a hierarchy of processing, but the precise timing of responses across regions and areas has yet to be fully determined. To do so, we compare distributions of response latencies from ten different areas from three regions of macaque auditory cortex. For both neurons and local field potentials (LFPs), latencies increase with regional level and also along the caudal to rostral axis within a region. Neural spiking latency differences are partially, but not completely, accounted for by similar differences in LFP latencies, which suggests that longer neuron latencies are a product of both slower inputs as well as longer integration time. These response differences are similar across multiple stimuli. Though these results show clear regional and caudorostral trends in the timing of flow, there is great overlap in the latency distributions, an indication of the strongly parallel nature of processing in auditory cortex.

2.2 Introduction

Current models propose that primate auditory cortex contains three regions: core, belt, and parabelt (see figure 2-1). These regions, which can be thought of as levels of

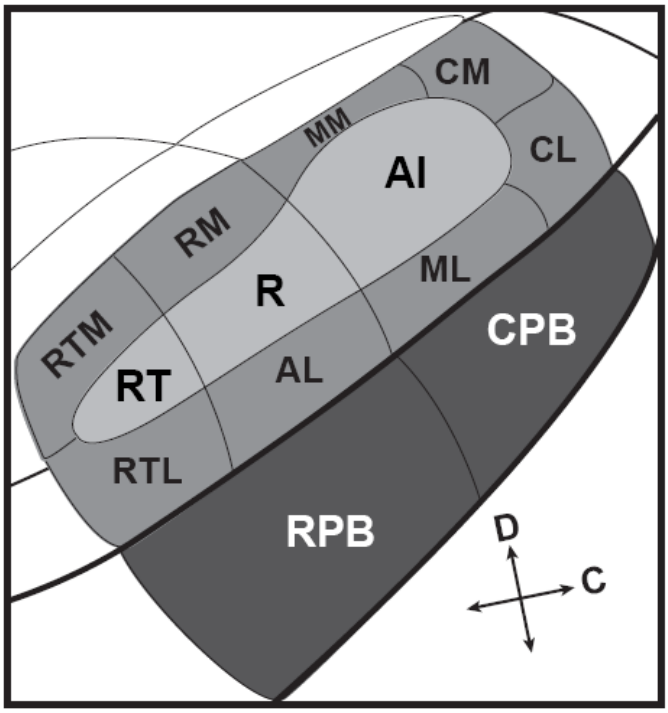

Figure 2-1. Schematic of primate auditory cortex (left hemisphere). The three areas that constitute the core region (A1, R, RT) are in light gray, the eight areas that constitute the belt region (CM, MM, RM, RTM, CL, ML, AL, RTL) are in medium gray, and the two areas that constitute the parabelt (CPB, RPB) are in dark gray. Arrows at the bottom right indicate dorsal and caudal directions.

processing, can be subdivided into approximately thirteen different areas, where each area is distinguished by a unique anatomical and physiological profile (Kaas and Hackett, 2000; Hackett, 2010). Although detailed studies of connections are lacking, evidence from connectivity patterns suggest both serial and parallel processing in auditory cortex (see figure 2-2). For example, the parabelt region receives inputs from the belt region, but not the core (Hackett et al., 1998b), suggesting that information processing between regions proceeds serially from core to belt to parabelt. In contrast, there are multiple parallel streams of input from the thalamic medial geniculate complex (MGC). Thalamic

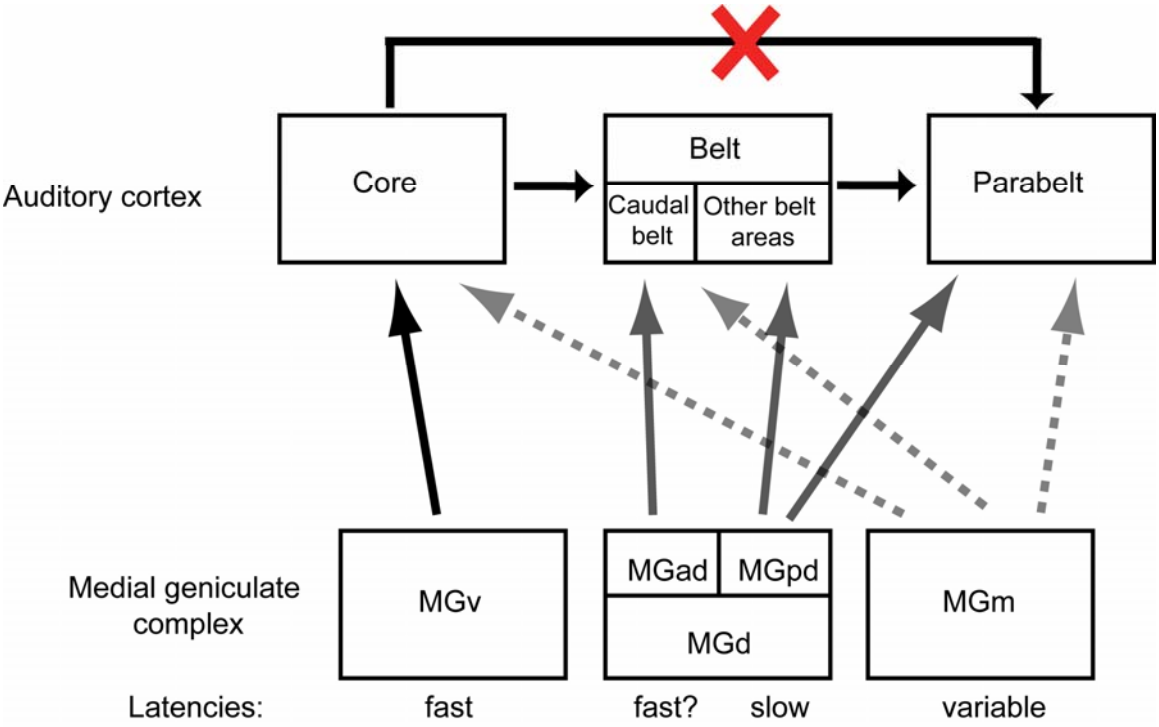

Figure 2-2. Schematic of MGC inputs by region and major feedforward ipsilateral cortical connections by region. The MGd has been further subdivided into the anterior and posterior divisions (MGad and MGpd respectively). Parallel projections from the MGC are indicated by different line conventions. Serial feedforward projections within cortex are shown with black arrows. While there are connections from core to belt, and from belt to parabelt, there are no substantial feedforward projections from core to parabelt (denoted by the red X). For comparison, known (or presumed) relative latencies for neurons in each MGC nucleus are indicated at the bottom.

input to the core mainly comes from the ventral division (MGv), input to the belt and parabelt comes from the anterior and posterior divisions of the dorsal division (MGad and MGpd), and all three regions receive input from the medial division (MGm) (Burton and Jones, 1976; Jones and Burton, 1976; Molinari et al., 1995).

To better understand the constraints under which sound is processed, it is important to characterize the direction(s) and timing of information flow in auditory cortex. Tuning and selectivity of auditory cortical neurons has been previously used to make useful predictions about direction of information flow (Rauschecker et al., 1995;

Rauschecker et al., 1997; Kaas and Hackett, 2000; Recanzone, 2000), but cannot address timing. To determine the relative timing of stimulus-related cortical activation, measures of neural onset response latency across multiple areas are quite powerful (for examples in the visual system, see: Schmolesky et al., 1998; Schroeder et al., 1998).

Based on known patterns of connectivity in the auditory cortex, what timing of cortical activation would be predicted? Serial cortical connections imply a regional flow from core to belt to parabelt, so latencies of parabelt neurons should be slower than core neurons. Corticocortical laminar projection patterns appear to favor a caudal to rostral feedforward pattern (Fitzpatrick and Imig, 1980; Galaburda and Pandya, 1983; de la Mothe et al., 2006b; reviewed in Hackett, 2010). Thus these patterns suggest that within a region neurons in caudal areas should have faster latencies than neurons in rostral areas. Estimating cortical activation timing using known cortical and thalamic connections is complicated by the incomplete characterization of the primate MGC. From work in primates and cats, it is generally believed that neurons in the MGv respond quickly, while neurons in the MGd respond slowly and more variably (Allon et al., 1981; Calford, 1983), but there is evidence from cats that neurons in the MGad subdivision may respond quickly (Imig and Morel, 1984, 1985a, b). Further complicating latency predictions is that the MGm is heterogeneous and appears to have quite variable latencies (Allon et al., 1981; Hashikawa et al., 1995).

Consistent with these predictions a comparison of latencies between core A1 and lateral belt ML reported neural response latencies in belt longer than core, (Recanzone, 2000; Crum et al., submitted). In the medial belt areas CM, MM, and RM, however, latencies have been found to be the same or shorter than in adjoining core (Recanzone,

2000; Kajikawa et al., 2005; Lakatos et al., 2005; Kusmierek and Rauschecker, 2009; but see Bieser and Muller-Preuss, 1996). Belt latencies that are the same or faster than core pose a problem for serial flow and suggest that parallel inputs arising outside of A1 may be contributing to this short latency activity in portions of the belt (Kajikawa et al., 2005). There is also increasing evidence that latencies increase within a region in a caudal to rostral direction, both in core and in medial belt (Bieser and Muller-Preuss, 1996; Bendor and Wang, 2008; Kusmierek and Rauschecker, 2009).

While some intriguing patterns are emerging, drawing meaningful cross-area and cross-region comparisons across studies is difficult due to the differences in species, stimuli, methods, and anesthetic state. Our understanding of timing also remains incomplete because many areas of auditory cortex have not been characterized physiologically. This study aims to cohesively study response latencies of neurons across multiple areas in the same species and under the same conditions. Specifically, we aim to evaluate whether latencies increase along the proposed core-belt-parabelt processing hierarchy, as well as whether latencies increase within a region in a caudal to rostral direction. As a complement to latencies derived from the unit activity, we also analyze latencies of the evoked local field potential (LFP). Initial poststimulus deflection of the LFP can be used as an estimate of the timing of incoming activity, as it is a measure of the initial current flux of the local area. By comparing patterns of neural spiking and LFP onset latencies, we generate a picture of input-output relationships across regions and areas of the majority of the macaque auditory cortex, building a more complete characterization of response timing to auditory stimuli across primate auditory cortex.

In this study, we compare distributions of response latencies from ten different areas covering all three regions of macaque auditory cortex. For both neurons and LFPs, latencies increase mediolaterally with regional level and also along the caudal to rostral axis within a region. Neural spiking latency differences are partially, but not completely, accounted for by similar differences in LFP latencies, which suggests that longer neuron latencies are a product of both slower inputs as well as longer integration time. Though these results show clear regional and caudorostral trends in the timing of flow, there is great overlap in the latency distributions, an indication of the strongly parallel nature of processing in auditory cortex.

2.3 Materials and Methods

Animal subjects

Three adult macaque monkeys PJ, SP, and DY were used for neural recordings (PJ-female bonnet macaque (*Macaca radiata*) 5.0 kg, SP-male bonnet macaque 10.0 kg, and DY-female rhesus macaque (*Macaca mulatta*) 7.0 kg). Animals were housed in an AAALAC-accredited facility under supervision of laboratory and veterinary staff. All animal care and experimental procedures were in accordance with the U.S. National Institutes of Health *Guide for the care and use of laboratory animals*, under a protocol approved by the Vanderbilt Institutional Animal Care and Use Committee.

Surgical procedure

After completing training to enter a primate chair and initial acclimatization, a headpost (in-house design) was implanted under aseptic conditions. The monkey was initially tranquilized with Ketamine (10-30 mg/kg IM) and Robinul (0.015 mg/kg IM) for intubation, catheterization and scrubbing, and premedicated with antibiotic (Cefazolin, 2.2 mg/kg IM). Through the duration of the procedure, anesthesia was maintained with inhalation Isofluorane in O_2 (2-4%). Respiration was maintained with a mechanical ventilator and body temperature was maintained at 37°C. Heart rate, blood pressure, expiratory CO_2, and peripheral oxygen levels were monitored as well. After 4-8 weeks of acclimatization to the headpost and further training to sit tranquilly in a primate chair with insert earphones, a second surgery was performed. In this surgery (details above) we implanted a recording chamber (22 mm wide; Crist Instruments, Hagerstown MD), oriented vertically over caudal auditory cortex (stereotaxic coordinates of the center of the chamber were approximately A7: L23 mm from earbar zero). For consistency, data was collected exclusively from the left hemisphere of each monkey. A craniotomy slightly smaller than the chamber was also made at this time to allow access to cortex.

Stimulus generation and neurophysiological acquisition

Stimulus generation and delivery. Recording sessions were conducted in a double walled chamber (Industrial Acoustics Corp, NY). Acoustic stimuli were generated by Tucker-Davis technologies (TDT, Gainesville, FL) System II hardware and software (SigGen), controlled by a custom software interface between the stimulus generation and acquisition setups. Stimuli were delivered using Beyer DT911 insert earphones (range

0.1-25.0 kHz), coupled to custom earmolds in both ears. These earmolds were made individually for each monkey by constructing a silicon mold of the concha and first few millimeters of the ear canal of each ear to completely seal the ear canal. A stainless steel tube (inner diameter ~ 1mm) passed through the ear mold to protrude 2-3 mm into the ear canal. The transducer tube interfaced to the mold tube to form a sealed system. Stimuli were calibrated for intensity using a ¼ inch microphone (Model 7017; ACO Pacific, CA), pistonphone (Bruel and Kjaer type 4220) and custom software (TDT, SigCal). Amplitude corrections were saved in a data file and applied to each stimulus to preequalize the response of each earphone independently.

Stimuli. All stimuli were delivered diotically with a jittered interonset interval of approximately 1000 ms, randomly interleaved with other stimulus types in the battery.

Clicks. The duration of these diphasic clicks was 0.25 ms. They were calibrated to 60 dB SPL and presented 30 times.

Wideband noise. The duration of these Gaussian white noise bands was 200 ms, with a 5 ms cosine^2 ramp at onset and offset. They were calibrated to 60 dB SPL and presented 30 times.

Tones. The center frequency of these pure tones ranged from 0.3-21.0 kHz in 1/3 octave steps. Four intensities were used, ranging from 15-60 dB SPL in 15 dB steps. Stimulus duration was 50 ms with a 5 ms cosine^2 ramp at onset and offset. Each frequency-intensity combination was presented in random order 10 times. Here, we present latencies derived from the 60 dB tones.

Electrophysiological recording. Electrode penetrations were made through a recording grid 15 mm wide with 1 mm spacing which fit over the implanted chamber

(Crist Instruments, Hagerstown MD). This ensured a replicable and roughly perpendicular trajectory through most parts of the superior temporal plane corresponding to caudal two-thirds of auditory cortex. After a local anesthetic (0.13% bupivacaine and 0.50% lidocaine in sterile saline) was topically applied and then removed, a sharpened stainless steel guide tube was inserted to puncture the dura. The use of a guide tube also ensured that the penetration ran parallel to the recording chamber. One to two tungsten microelectrodes (2-4 MOhm, FHC, Bowdoin, MA) aligned mediolaterally were advanced through the guide tube through parietal cortex and into auditory cortex using manual microdrives (Narishige, Tokyo, Japan). Somatosensory mapping of primary and secondary somatosensory cortices was performed in order to establish maps to guide subsequent electrode penetrations. For all three monkeys, maps of the SII/PV border areas showed a caudal to rostral receptive field map of leg to hand to mouth. This map corresponded to maps of somatotopy derived from anesthetized animals in these areas, though the receptive fields we found appeared to be much larger (Robinson and Burton, 1980a, b; Krubitzer et al., 1995; Disbrow et al., 2003; Coq et al., 2004). However, though the somatotopic map is consistent between monkeys, somatotopic borders do not precisely correspond to areal borders in auditory cortex and cannot be used as a guide.

From the first auditory responses until the end of auditory-responsive cortex, all isolated neurons, irrespective of apparent responsiveness, were tested with all or most of the stimulus battery to avoid biasing the sample. In between isolations the microdrives were moved at least 200 μm to avoid resampling units. For most runs, we recorded through all layers until the white matter was reached. We assigned a relative cortical depth to each penetration by normalizing the recording depth with respect to the first

auditory responses, presumably from the first layer or two of auditory cortex. While unequivocal laminar depths cannot be established, it is likely that the majority of recorded neurons are coming from the middle and upper layers, consistent with the cytoarchitecture of auditory cortex (Hackett, 2010). During recording sessions the monkey was continuously monitored via closed-circuit television for alertness.

Multichannel spike and local field potential (LFP) recordings were acquired with a 64 channel system that controls amplification, filtering and related parameters (Many Neuron Acquisition Processor, Plexon Inc, Dallas, TX). Both signals were referenced to ground. Spike signals were amplified (100x), filtered (150-8800 Hz), and digitized at 40 kHz. The signal was further DC-offset corrected with a low-cut filter (0.7 Hz). Spikes were initially sorted online for all channels using real-time window discrimination. Digitized waveforms and timestamps of stimulus events were also saved for final offline analysis and final sorting (Plexon offline sorter), and graded according to isolation quality (single or multi units). Single and multi units were analyzed separately. Since the patterns of results were similar, results from both single and multi units were included in the results. The LFP signals were acquired simultaneously with the spike data. These were amplified (500x), filtered (3.3-89.0 Hz), and digitized at 1 kHz. Again, the signal was further DC-offset corrected by with a low-cut filter (0.7 Hz). To investigate the possible effect of phase shifts introduced by the preamp and DC-correction filter (see Nelson et al., 2008), the LFP was analyzed two ways: with and without offline phase correction using custom software (Plexon FPAlign, v1.3.1). As the phase shifts did not affect results, the LFP results are presented without phase correction. To ensure timing precision, the Plexon acquisition software interfaced with the stimulus delivery system

(Tucker Davis Technologies) and both systems were controlled by custom software (SGPlay, TDT, provided by Peter Yang).

Histology and identification of cortical areas

Since electrophysiological signatures have yet to be determined for the majority of auditory cortex, it was necessary to anatomically reconstruct cortex for precision in the determining electrode locations. At the end of the electrophysiological recording, lesions were made in representative grid sites to facilitate reconstruction. Additionally, best-frequency matched sites were identified and 2-3 tracer injections were placed for a parallel anatomical study of auditory cortex. After a 12-14 day tracer transport period, the monkey was initially tranquilized with Ketamine and a lethal dose of Euthasol (120 mg/kg) was administered. Just after cardiac arrest, the monkey was perfused with 4ºC 0.1M phosphate buffered saline containing heparin (10 units/ml) , followed by 4ºC paraformaldehyde (4%) dissolved in 0.1M phosphate buffer (pH 7.4). Immediately after perfusion, the head was placed in a stereotaxic apparatus to for precise measurement of chamber placement and electrode angles. The brain was removed from the skull and photographed. The cerebral hemispheres, thalamus and brainstem were blocked and placed in 30% sucrose for 1-3 days. To facilitate reconstruction, the left hemisphere was cut at an approximately vertical angle (angle of the electrode) in 40 μm sections. Alternating series of sections were stained for Nissl substance with thionin, cytochrome oxidase (Wong-Riley, 1979), acetylcholinesterase (Geneser-Jensen and Blackstad, 1971), myelinated fibers (Gallyas, 1979), and processed for neuronal tracers. Figure 2-3 shows the cytoarchitecture (Nissl stain) and laminar organization unique to each of the 13 areas

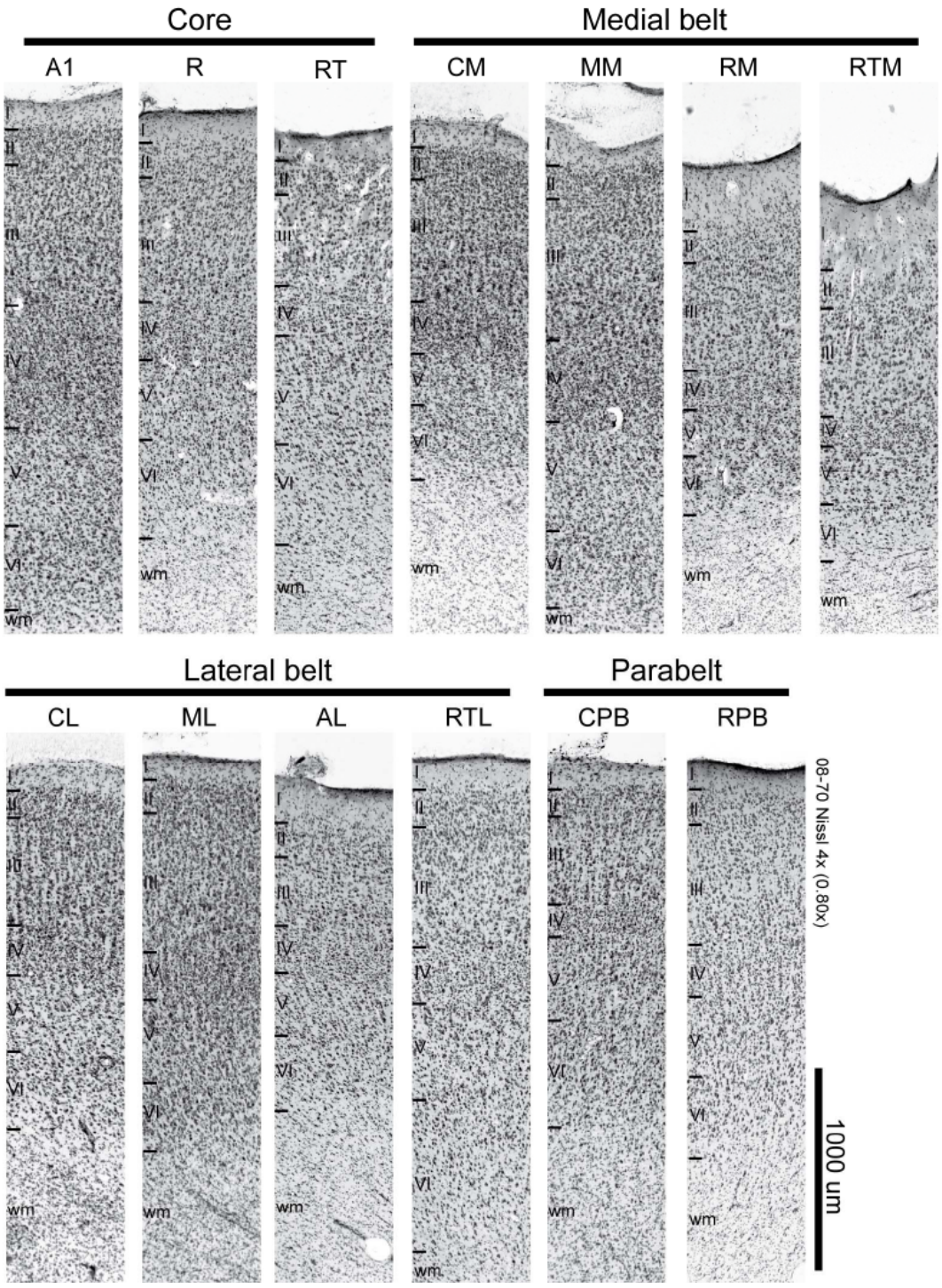

Figure 2-3. Sections of the macaque monkey superior temporal cortex stained for Nissl substance to reveal differences in cytoarchitecture and laminar patterns between areas. Top row: areas of the core and medial belt regions, arranged in a caudal to rostral direction. Bottom row: areas of the lateral belt and parabelt regions, arranged in a caudal to rostral direction. Roman numerals denote cortical layer, delimited by black lines, and wm denotes white matter.

of macaque auditory cortex. Areas were identified by architectonic criteria established in previous studies (Hackett et al., 1998a; Hackett et al., 2001; Hackett and de la Mothe, 2009). Using information from the lesions, electrode tracks, and histological reconstruction of areas, areal locations of electrodes were determined and confirmed by electrophysiological properties.

Neurophysiological data analysis

All analyses described below were done using in-house Matlab scripts (MathWorks, Natick, MA), confirmed when possible by analyses in Neuroexplorer v3.021 (Nex Technologies, Littleton, MA). Spike times were binned at 1 ms and no smoothing was used to maintain precision of timing.

Unit response onset latencies. Response onset latency of each neuron was obtained in a similar way for multiple stimulus conditions (e.g. tones, clicks, noise). Response onset latency was determined using the Gaussian standard deviation algorithm (see Appendix for discussion). This algorithm is based on the averaged neural response in the form of a peristimulus time histogram (PSTH). The neural onset latency is the first bin after stimulus presentation to cross a response threshold and remain there for some number of bins (here, 3 bins). The algorithm defines a response threshold as 3 Gaussian standard deviations of the spontaneous rate above the mean spontaneous firing rate. Spontaneous firing rate measures are derived from the period 200-0 ms before stimulus onset.

LFP response onset latencies. LFP signals are an estimate of the summed transmembrane currents in a local cortical area, possibly as discrete as 250 μm (Katzner

et al., 2009). To provide consistency between the unit and LFP analysis, response onset latency of the LFP was calculated using a similar measure. Onset latency was the first of three bins which exceeded 4 Gaussian standard deviations above or below baseline (SD derived from the variance of the absolute value of the LFP in the window from 200-0 ms before stimulus onset).

Best tone frequency (BF). For tones, latencies were derived from the group of three frequencies that produced the best response (similar to Recanzone, 2000). This reduced noise in the determination of the BF and had the additional benefit of normalizing the number of stimulus presentations to 30 for all three kinds of stimuli in this study. For units, the BF was derived by analyzing firing rates in two different windows: 1) 10-100 ms poststimulus onset and 2) from response onset latency to 100 ms after onset latency. Regardless of the analysis window, tuning was similar from each frequency + the neighboring frequencies (edge frequencies had only 1 neighbor and were normalized appropriately). At 60 dB, no neurons exhibited sideband inhibition at frequencies directly neighboring the BF. A similar method was used to determine BF for the LFP, except peak deflection was used to determine best response. As expected, BF for units and BF for LFPs were concordant (Kayser et al., 2007).

2.4 Results

Overall 1656, 1335, and 1583 units across cortex were analyzed for click, noise, and tone responses respectively. LFPs from 504, 511 and 425 sites were analyzed for click, noise and tone responses. Table 2-1 shows neuron counts, means and median

latencies for each area for all three stimulus types. These neurons and LFPs were distributed across three regions and ten areas. Except for area CM, each area contains neurons from at least two monkeys. Results between monkeys were qualitatively similar and could be combined. Due to the size of the grid, some auditory cortical areas were not covered by the grids. These included the rostral-most areas RTM, RT, RTL and the rostral tip of RPB.

Table 2-1. Counts of neurons and LFP sites analyzed and responsive for all areas and all stimulus conditions examined, divided by regional level (columns) and stimulus type (rows). For comparison, means and medians of distributions are also listed.

			Core		Medial Belt			Lateral Belt			Parabelt	
			A1	R	CM	MM	RM	CL	ML	AL	CPB	RPB
Click latencies	Unit	means	17.7	26.2	13.9	22.8	33.7	16.8	24.9	31.6	25.7	31.1
		medians	14.0	20.0	10.0	18.0	35.0	13.5	20.0	27.5	25.0	25.0
		analyzed	283	81	30	69	18	30	56	40	33	47
		total	536	282	64	158	59	55	155	114	76	157
	LFP	means	16.4	23.2	8.7	17.3	26.5	12.0	18.6	19.2	21.3	24.1
		medians	13.0	19.0	9.0	12.0	20.5	10.0	12.0	15.0	13.0	15.0
		analyzed	110	66	3	56	22	18	43	40	28	46
		total	113	80	3	63	27	21	49	47	38	63
	unit-LFP	means	4.8	8.1	7.1	9.1	10.4	6.0	10.4	15.0	11.9	13.9
		medians	1.0	1.5	4.5	4.0	11.5	2.0	7.0	10.0	11.0	6.0
		analyzed	161	56	8	62	16	27	49	34	31	33
Noise latencies	Unit	means	22.2	31.3	16.7	27.6	35.8	23.0	35.7	33.3	31.1	29.3
		medians	18.0	28.0	16.0	24.0	33.0	20.0	31.0	28.0	25.5	25.0
		analyzed	210	120	9	79	30	37	73	80	44	75
		total	301	256	9	169	66	58	130	124	83	139
	LFP	means	18.0	24.8	11.3	23.9	30.7	13.5	20.3	19.9	29.9	22.5
		medians	15.0	20.0	12.0	18.0	21.0	13.0	15.5	17.0	25.0	16.5
		analyzed	106	77	3	69	27	20	48	47	35	46
		total	110	85	3	70	31	22	51	48	38	53
	unit-LFP	means	6.5	11.1	5.3	9.9	8.6	9.8	18.6	13.3	9.3	11.9
		medians	2.0	9.0	4.0	5.5	11.0	5.0	16.0	8.0	6.5	8.0
		analyzed	193	96	9	78	27	36	66	73	36	59
Tones (BF+2) latencies	Unit	means	27.9	35.3	22.3	28.5	40.3	24.0	35.0	33.8	31.8	40.2
		medians	26.0	32.5	17.5	26.0	34.0	19.5	30.0	32.0	27.5	37.0
		analyzed	175	88	14	35	10	16	33	38	16	29
		total	551	299	49	148	46	47	129	108	67	139
	LFP	means	21.4	28.8	13.7	28.4	35.8	16.5	27.0	27.2	28.8	29.0
		medians	19.0	26.5	13.0	24.0	34.0	15.0	23.0	22.0	23.0	24.0
		analyzed	96	64	3	44	15	17	35	45	27	42
		total	99	70	3	48	20	18	38	45	29	45
	unit-LFP	means	9.7	10.6	5.5	6.1	9.8	8.4	11.0	10.3	9.1	15.1
		medians	6.0	9.0	2.0	5.0	6.5	4.0	8.0	5.5	6.5	8.5
		analyzed	116	63	6	26	9	17	21	37	14	22

Click Latencies

Figure 2-4A shows a boxplot of the response onset latencies for clicks across the three regions and ten areas. Boxplots were chosen over simple means because it is a more

compete description of the distribution. However for reference, means are listed in table 2-1. For ease of comparison, the y-axis is the same for all unit and LFP latencies for all three stimuli. Each region is separated by a vertical line (the belt is separated into medial and lateral sub-regions), and the areas within are arranged from caudal to rostral level left to right. To ease comparison of areas across regions, the shadowing of the boxplot indicates relative caudorostral level (e.g. all the light-gray are A1, MM, ML and CPB). Given predictions about axis of flow, it is most straightforward to compare latencies from areas at the same caudorostral level. Note that there is no core region that corresponds to the caudorostral level of belt CM and CL. Also, since CPB receives projections from belt areas at both the first and second caudorostral level, for visualization purposes it is placed in between the tick marks. To be conservative in the statistical analysis, CPB was put in the first caudorostral level, the same as MM and ML. Overall the experimental design was a two factor with three regional levels (1-core, 2-belt, and 3-parabelt) and three caudorostral levels (1-level of CM/CL, 2-level of MM/A1/ML/CPB, 3-level of RM/R/AL/RPB). Before selecting these groupings, we additionally demonstrated that the medial and lateral belt subregions were not different and could be combined. This was done separately for each stimulus and was true for each comparison (results below).

In examining figure 2-4A, a number of trends become evident. First, the medial and lateral belt areas do not appear to be different from each other. A separate planned ANOVA also did not demonstrate differences between the subregions (2x3 subregion x caudorostral level ANOVA, subregion $p > 0.05$). Secondly, upon examination of all of the areas, we can examine two additional trends. The first trend is that indeed, latencies increase with increasing hierarchical region. For example latencies in A1 are faster than

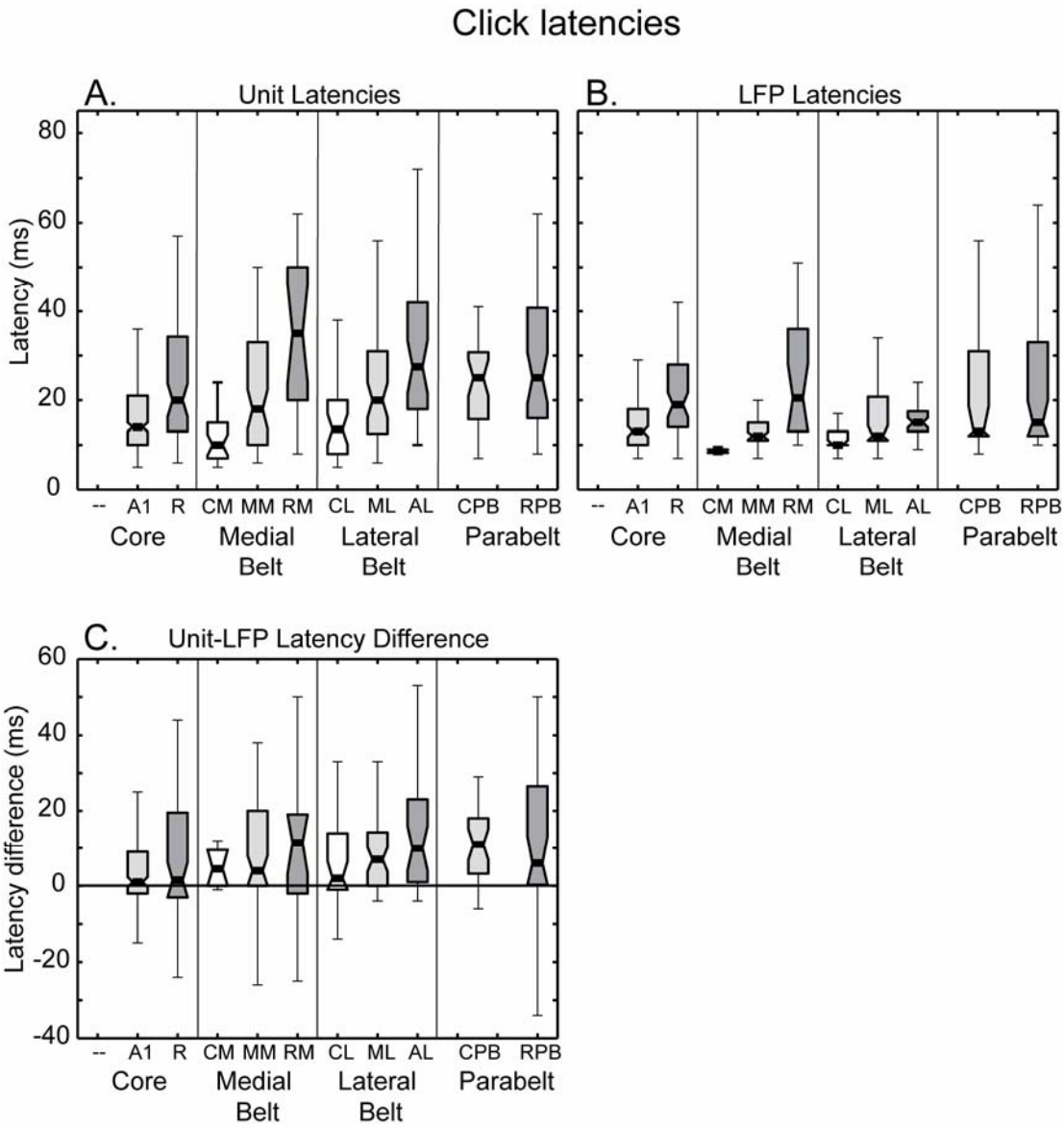

Figure 2-4. Click latencies. A. Boxplots of unit latencies per area. Each region is separated by a vertical line (the belt is separated into medial and lateral subregions), and the areas within each region are arranged in a caudal to rostral direction. The color of the boxplot indicates relative caudorostral level. The box denotes the upper quartile, median, and lower quartile of the distribution. Whiskers denote the extent of the rest of the data. Notches indicate an estimate of the uncertainty about the median. If notches do not overlap, the medians differ at the α level of $p < 0.05$. B. Boxplots of LFP latencies per area. Conventions as in part A. C. Boxplots of 'transformation time': Unit latency-LFP latency. Conventions as in part A.

MM latencies, which are approximately equal to those in ML, which are faster than those in CPB. The second striking result is that latencies increase with increasing rostral level. These results were confirmed by a two factor 3x3 region x caudorostral level ANOVA (region $p<0.05$; caudorostral level $p<0.05$).

Figure 2-4B shows a boxplot of the response onset latencies for LFPs across the three regions and ten areas, conventions are the same as for part A. Note that generally LFP latencies are faster than unit latencies, consistent with the interpretation that they indicate input activity. Again, the medial and lateral belt areas do not appear to be different from each other. A separate planned ANOVA also did not demonstrate differences between the subregions (2x3 subregion x caudorostral level ANOVA, subregion $p > 0.05$). Secondly, upon examination of all of the areas, we found two additional trends. In contrast to the units, LFP latencies do not increase with increasing hierarchical region. Similar to the units, LFP latencies do increase with increasing rostral level. There results were confirmed by a two factor 3x3 region x caudorostral level ANOVA (region $p>0.05$; caudorostral level $p<0.05$).

To get a more precise estimate of the differences in LFP and spike timing, we took each unit's latency and subtracted the simultaneous recorded LFP latency. For example, if a recording site yielded three neurons, it has 1 LFP and yields three different unit-LFP difference values. This difference in latency is the time between the onset of the LFP and onset of the neural response, and can roughly be considered to be 'transformation time'. An important caveat is that since cell bodies and their related dendritic arborization can be hundreds of micrometers apart, this subtraction indicates the input-output timing of a discrete piece of cortex a few hundred microns in diameter

(Katzner et al., 2009), not the input-output timing of a given neuron. However, this method is more precise than collapsing across different penetrations since it compares measures with the same behavioral state and areal location. Figure 2-4C shows a boxplot of the transformation times across the three regions and ten areas, conventions are the same as for part A. A number of trends are worth noting. Note that at a single neuron level, generally LFPs are shorter than unit latencies, but not always. Again, the medial and lateral belt areas do not appear to be different from each other. A separate planned ANOVA also did not demonstrate differences between the subregions (2x3 subregion x caudorostral level ANOVA, subregion $p > 0.05$). Upon examination of all of the areas, we can examine two additional trends. The first trend is that indeed, transformation time increases with increasing hierarchical region. The second trend, though weaker, is that transformation time increases with increasing rostral level. These results were confirmed by a two factor 3x3 region x caudorostral level ANOVA (region $p<0.05$; caudorostral level $p<0.10$).

Noise Latencies

Figure 2-5A shows a boxplot of the response onset latencies for broadband noise across the three regions and ten areas. As with the clicks, a number of trends become evident. First, the medial and lateral belt areas do not appear to be different from each other. A separate planned ANOVA also did not demonstrate differences between the subregions (2x3 subregion x caudorostral level ANOVA, subregion $p > 0.05$). Secondly, upon examination of all of the areas revealed two additional trends. Again, latencies increase with increasing hierarchical region and latencies increase with increasing rostral

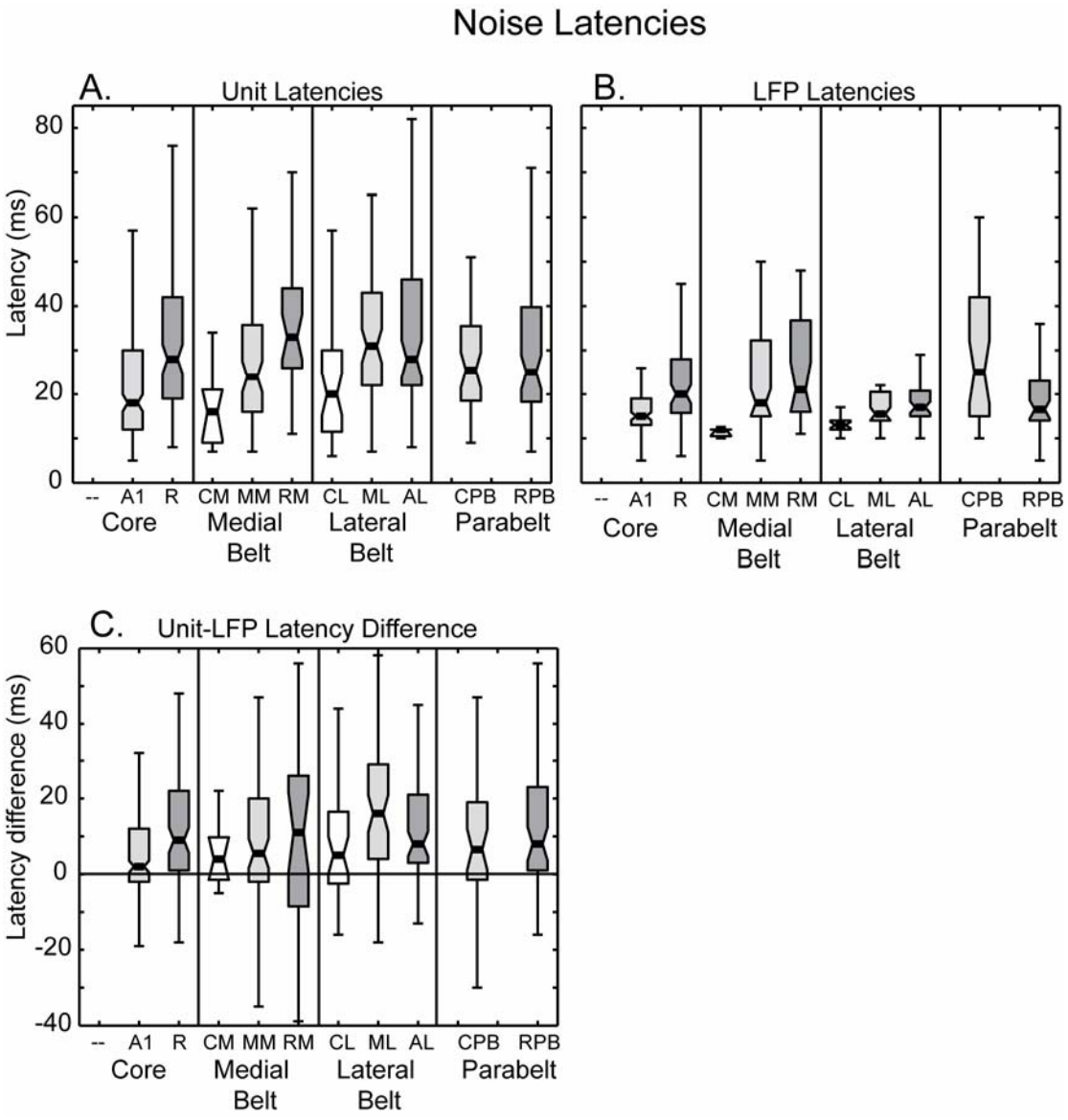

Figure 2-5. Noise latencies. A. Boxplots of unit latencies per area. Conventions as in figure 2-4. B. Boxplots of LFP latencies per area. C. Boxplots of 'transformation time': Unit latency-LFP latency.

level. These results were confirmed by a two factor 3x3 region x caudorostral level ANOVA (region $p<0.05$; caudorostral level $p<0.05$).

Figure 2-5B shows a boxplot of the response onset latencies for LFPs. Again, the medial and lateral belt areas do not appear to be different from each other. A separate planned ANOVA also did not demonstrate differences between the subregions (2x3 subregion x caudorostral level ANOVA, subregion $p > 0.05$). Secondly, upon examination of all of the areas, we found two additional trends. Consistent with the units, latencies increase with increasing hierarchical region and increase with increasing rostral level. There results were confirmed by a two factor 3x3 region x caudorostral level ANOVA (region $p<0.05$; caudorostral level $p<0.05$).

Again, we took each unit's latency and subtracted the simultaneous recorded LFP latency to show transformation times in figure 2-5C. This time, a separate planned ANOVA showed differences between the medial and lateral belt subregions (2x3 subregion x caudorostral level ANOVA, subregion $p = 0.04$), probably due to the different patterns. However, since the medial and lateral belt areas displayed no difference between each other for the majority of tests, so this difference is probably artifactual, and so we continued to collapse latencies across the caudorostral levels of medial and lateral belt.

We can examine two additional trends using all of the areas. The first trend is that indeed, transformation time increases with increasing hierarchical region. However, transformation time does not increase with increasing rostral level. These results were confirmed by a two factor 3x3 region x caudorostral level ANOVA (region $p<0.05$; caudorostral level $p>0.05$).

Tone Latencies

Figure 2-6A shows a boxplot of the response onset latencies for broadband noise across the three regions and ten areas. As with the clicks, a number of trends become evident. First, the medial and lateral belt areas do not appear to be different from each other. A separate planned ANOVA also did not demonstrate differences between the subregions (2x3 subregion x caudorostral level ANOVA, subregion $p > 0.05$). Secondly, we can examine two additional trends across all of the areas,. In this case, latencies do not increase with increasing hierarchical region. However, consistent with the results testing latencies to stimuli, latencies increase with increasing rostral level. These results were confirmed by a two factor 3x3 region x caudorostral level ANOVA (region $p=0.12$; caudorostral level $p<0.05$).

Figure 2-6B shows a boxplot of the response onset latencies for LFPs. Again, the medial and lateral belt areas do not appear to be different from each other. A separate planned ANOVA also did not demonstrate differences between the subregions (2x3 subregion x caudorostral level ANOVA, subregion $p > 0.05$). Secondly, upon examination of all of the areas, we can examine two additional trends. Consistent with the units, latencies increase with increasing hierarchical region and also increase with increasing rostral level. These results were confirmed by a two factor 3x3 region x caudorostral level ANOVA (region $p<0.05$; caudorostral level $p<0.05$).

Again, we took each unit's latency and subtracted the simultaneous recorded LFP latency to show transformation times in figure 2-6C. As for tones, a separate planned ANOVA showed differences between the medial and lateral belt subregions

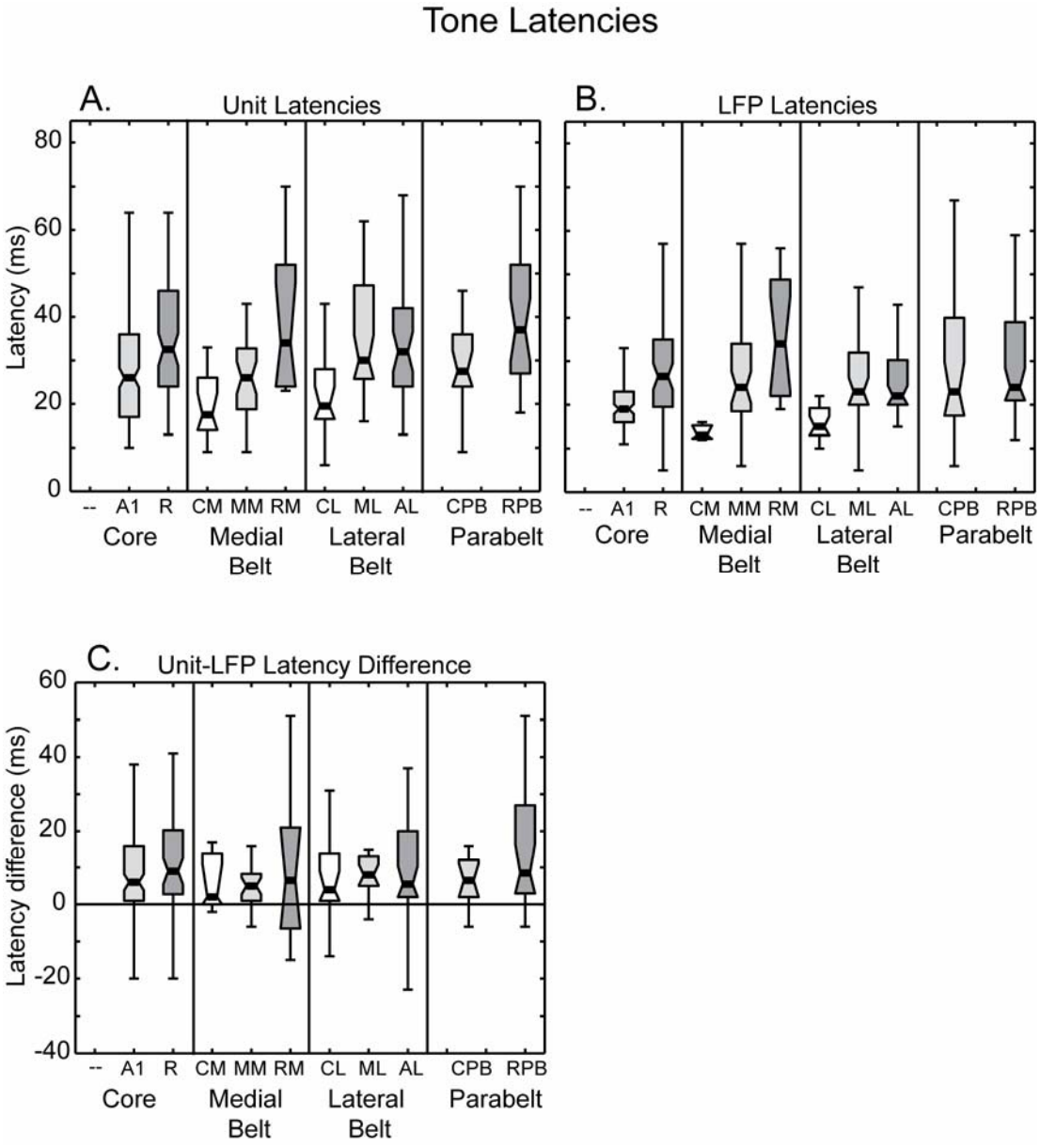

Figure 2-6. Tone latencies at BF + neighboring frequencies. A. Boxplots of unit latencies per area. Conventions as in figure 2-4. B. Boxplots of LFP latencies per area. C. Boxplots of 'transformation time': Unit latency-LFP latency.

(2x3 subregion x caudorostral level ANOVA, subregion $p > 0.05$), but since this difference was the exception we continued to collapse latencies across the caudorostral levels of medial and lateral belt. Upon examination of all of the areas, we noted two

additional trends. The first trend is that, different from the other stimuli, transformation time does not appear to increase with increasing hierarchical region. However, transformation time does increase with increasing rostral level. These results were confirmed by a two factor 3x3 region x caudorostral level ANOVA (region $p>0.05$; caudorostral level $p<0.05$).

Responsiveness

A further question is whether units' general responsiveness decreases with region and caudorostral level. Overall, responsiveness does differ with stimulus type. Noise elicits the most responses, then clicks, and then tones (see table 2-1). However, for most stimuli percent responsiveness does not appear to change with regional or caudorostral level. The sole exception was for click responsiveness, which varied with caudorostral level (two factor 3x3 region x caudorostral level ANOVA; caudorostral level $p<0.05$).

2.5 Discussion

In a survey of ten areas across three regions of the primate auditory cortex, we find that both neuron (single- and multi-unit) and LFP latencies generally increase as a function of both regional level and caudorostral level, regardless of stimulus type. The LFP differences are not as strong, as confirmed by the unit-LFP difference analysis, which indicates that the unit latency differences are incompletely accounted for by the LFP differences. This suggests that these rostral areas with longer unit latencies may also have a longer integration time window. Other than absolute latencies, there are few

differences between results from broadband (click, noise) and pure tone responses, despite differences in envelope, duration and bandwidth. This indicated that our results are probably generally reflective of timing information for the majority of ethologically relevant stimuli. Given the proposed differences in the way that tone information is propagated compared to broadband information, this may be surprising. However, at these suprathreshold levels, often narrowly tuned neurons respond to a broad range of frequencies, so it is not surprising that pure tones and broadband noise activate the same sequence of pathways.

Comparisons of latencies between studies is difficult due to the differences in species, stimuli, methods, and anesthetic state - all of these factors can affect absolute latency reported (reviewed in the Appendix). For example primate A1 latency estimates range from 10-40 ms depending on the study (Vaadia et al., 1982; Steinschneider et al., 1992; Bieser and Muller-Preuss, 1996; Recanzone, 2000; Cheung et al., 2001; Kajikawa et al., 2005; Bendor and Wang, 2008; Oshurkova et al., 2008; Kusmierek and Rauschecker, 2009; Crum et al., submitted). With that caveat, results from this study fit both absolute latencies of similar studies and patterns of latency differences in unit activity found between areas (Recanzone, 2000; Cheung et al., 2001; Kajikawa et al., 2005; Lakatos et al., 2005; Philibert et al., 2005; Bendor and Wang, 2008; Kusmierek and Rauschecker, 2009; Crum et al., submitted). Studies have shown that neurons in belt areas adjacent to A1 have later responses (Vaadia et al., 1982; Bieser and Muller-Preuss, 1996; Recanzone, 2000; Crum et al., submitted). An important exception to this core-belt-parabelt hierarchy is that we found latencies in the caudal most portion of belt (CM, CL) that are are as fast or faster than latencies of neurons in A1, even in response to

tones. The functional implications of this are discussed below. One study of core and medial belt did not show that medial belt latencies (MM and RM) were slower than core at the same caudorostral level (Kusmierek and Rauschecker, 2009). The difference between this study and our results may be that the latency reported in that study was the fastest latency from either tone or noise. The results here are from a single stimulus type, so differences between latencies to tone and noise may explain the differences between studies. Reports of parabelt latencies are rare in the literature, but a recent study finds that parabelt (probably CPB) is also slower than core (Crum et al., submitted). An even more striking trend is that rostral areas are indeed slower than caudal areas within the same region, consistent with results of neural latencies from both the core and medial belt (Bieser and Muller-Preuss, 1996; Bendor and Wang, 2008; Kusmierek and Rauschecker, 2009).

Reports of LFP latencies in auditory cortex are also rare, but one study also finds that LFPs are faster than unit activity (Crum et al., submitted). That study also reports that parabelt latencies are slower, but found no difference between core and lateral belt. Latencies have also been reported from a continuous measure of 'multi-unit activity' (MUA) (Steinschneider et al., 1992; Lakatos et al., 2005). The MUA is not derived from spikes, but is a high-frequency rectified LFP. Similar to the LFP, MUA latencies are extremely fast. However, Lakatos 2005 reported a dissociation of tone and noise based latencies, where belt neurons respond faster and less variably than A1 to broadband noise. Their stimuli were also delivered at levels well above threshold, so it is unclear why we do not see this dissociation in our study. Further interpretation is complicated because the area of the lateral belt they were recording from is unclear.

Limitations to the current study include that the interpretation of the local field potential should be done with caution. Some latency differences in the LFP between areas could be due to the differential cytoarchitecture between areas. This is unlikely given the strong correlation between units and LFP patterns. Additionally, area CM had a low number of units sampled, as recordings from this area came from only one monkey. However, we included it in this study because CM has been characterized in a number of studies (Recanzone, 2000; Kajikawa et al., 2005; Oshurkova et al., 2008) and our results are consistent with the upper end of the absolute latency values, and more importantly, consistent with relative latency differences with A1.

Click stimulation provides some unique advantages in the assay of latencies across areas. First, it is broadband and activates neurons well. Second, because it has a sharp and quick onset and offset, long latency responses will not be complicated by offset responses. A similar reasoning was applied to the choice of visual stimuli in studies investigating response latencies across the visual system (Schmolesky et al., 1998; Schroeder et al., 1998), and in the auditory potentials in cortex (Steinschneider et al., 1992; Inui et al., 2006). For this reason, the click latencies are probably most representative of the lower limits of how fast information can reach various areas across auditory cortex.

How do these results fit with anatomical predictions made for cortical activation timing? Thalmocortical and corticocortical connectivity predicts core, belt, and parabelt latency differences. We indeed observed the predicted latency differences with regional level. This is consistent with the chemoarchitectural gradients with regional level (e.g. Hackett and de la Mothe, 2009). Cytochrome oxidase expression, a marker of metabolic

activity often seen in fast cortices and pathways, is most dense in core and least dense in parabelt. Additionally, consistent with anatomical predictions, we also see almost no differences in the timing of cortical activation between medial and lateral belt, supporting the notion that they are subparts of the same regional level.

Are the latency differences seen with regional level evidence for truly strict serial flow? Studies based in the cortical visual system concluded that serial interareal transfer time should be approximately 10 ms (reviewed in Nowak and Bullier, 1997). In the auditory cortex, latency differences between regions do not appear to be of such magnitude. However, neural onset latencies in the belt and parabelt are in response to a mix of inputs from separate cortical but overlapping thalamic sources. Given the numerous parallel pathways from the MGC, the more parallel timing of processing in cortex is perhaps unsurprising.

A significant challenge to the core-belt-parabelt direction of flow are the extremely fast latencies seen in caudal belt CM and CL compared to neighboring core A1. Fast latencies have previously been demonstrated in CM (Recanzone, 2000; Kajikawa et al., 2005; Oshurkova et al., 2008). A resolution may lay in closer examination of the topography of thalamic inputs. Caudal belt, particularly CM and CL, receive projections from an anterior portion of the MGd, the MGad. This region has not been well characterized in primates, but a possibly corresponding structure in cats exhibits fast latencies much like the MGv (Imig and Morel, 1984, 1985a, b). Projections from the MGad to both the medial and lateral belt decrease in strength as one progresses rostrally and are almost absent at the level of RM (de la Mothe et al., 2006a; Hackett et al., 2007), which is then characterized by a dense projection from the MGpd. Thus it is

possible that the belt receives some of its inputs serially, but that the fastest latencies in the caudal-most portion may be driven by this extremely fast direct thalamic input from MGad. The connections and response properties of the divisions of the MGC need to be better characterized.

Another striking pattern in this study is that within the same region, rostral latencies are slower than caudal latencies. This result is not immediately predicted by known thalamocortical connectivity patterns. However, the patterns of laminar connectivity are still being elucidated, and quantitative studies of thalamocortical connectivity are also lacking (for example, does A1 receive more MGv input than R?). While the thalamocortical connections do not immediately account for these caudorostral latency trends, the chemoarchitecture of the caudal areas indicates that these areas should be very fast. Caudal areas are marked by being cytochrome oxidase dense, a marker of metabolic activity often seen in fast cortices and pathways (e.g. Hackett and de la Mothe, 2009). Additionally, corticocortical connectivity of some areas is suggestive of feedforward activity in the rostral direction (connections to layer 4) (Fitzpatrick and Imig, 1980; Galaburda and Pandya, 1983), but his has not been demonstrated conclusively for all areas (see de la Mothe et al., 2006b). Our finding that the differences between LFP and unit latencies are more pronounced in rostral than caudal areas appear to help resolve some of the apparent discrepancy between the anatomical predictions and physiological timing. In rostral areas neuron latencies are much later (compared to caudal areas) than the corresponding LFP latency , indicating that the units in these area may have a longer integration time window to generate a response, which will result in longer unit latencies in the rostral areas.

Almost 20 years ago, known connections were used to make predictions about the processing hierarchy of another sensory system, the visual system (Felleman and Van Essen, 1991). This work identified levels of hierarchy and divided processing into dorsal/ventral streams. Based on known connectivity at the time (primarily Galaburda and Pandya, 1983), it also attempted to extend reasoning to the auditory system. They noted suggestions of a hierarchy between core and belt, as well as a caudal to rostral flow, but noted that root (medial belt) connectivity did not fit into an 'internally consistent hierarchy'. In the intervening decades, work from many labs is filling in these gaps, indicating that there is flow from core to belt to parabelt (Vaadia et al., 1982; Bieser and Muller-Preuss, 1996; Recanzone, 2000; Crum et al., submitted), as well as a caudorostral flow (Bieser and Muller-Preuss, 1996; Bendor and Wang, 2008; Kusmierek and Rauschecker, 2009). Based on the topography of prefrontal cortical projections from auditory cortex, it has been suggested that there is functional correspondence between the dorsal/ventral streams of the visual system and proposed caudal/rostral streams in the auditory system (e.g. Romanski et al., 1999; Rauschecker and Tian, 2000). It is striking that areas of the putative caudal 'what' stream in auditory cortex have a distinct temporal advantage, similar to the fast latencies found in the dorsal 'what' streams of the visual system (e.g. Schroeder et al., 1998). However, functional correspondence between the streams of the visual system and the auditory system remains to be determined.

Through comparison of both units and LFP latencies, we are able to develop a broad schema of timing of information flow. However, the hierarchy of auditory processing is still indeterminate. What is perhaps most striking is that though there are clear regional and caudorostral trends in the flow of information, there is enormous

overlap in the latency distributions. This is no doubt indicative of the massively parallel inputs coming in from the subdivisions of the primary thalamic nuclei. Because of the ongoing nature of sound, auditory stimuli must be processed very rapidly. A system that is wired to process information in many streams at once is best suited for fast processing. The auditory cortical system processes in serial, but its stunning feature is massively parallel processing. We would argue that this is a hallmark of the auditory system, imposed by timing constraints on the processing of auditory stimuli.

Never before has auditory cortical timing from so many areas been compared using identical conditions, but we are still far from determining the existence of hierarchy in the auditory system. Though it is expected that they will follow the same trends, we need data from more rostral areas RTM, RT, and RTL for a more complete picture. Clearly, there is a need for more studies characterizing laminar patterns of connectivity and timing, and characterization of response specificity in different areas to understand mechanisms for auditory processing. Only through combining information from connectivity (the how?), tuning properties (the what?), and response latencies (the when?) can we build a picture of how auditory information reaches and flows though cortex to form the basis of auditory perception.

2.6 References

Allon N, Yeshurun Y, Wollberg Z (1981) Responses of single cells in the medial geniculate body of awake squirrel monkeys. Exp Brain Res 41:222-232.

Bendor D, Wang X (2008) Neural response properties of primary, rostral, and rostrotemporal core fields in the auditory cortex of marmoset monkeys. J Neurophysiol 100:888-906.

Bieser A, Muller-Preuss P (1996) Auditory responsive cortex in the squirrel monkey: neural responses to amplitude-modulated sounds. Exp Brain Res 108:273-284.

Burton H, Jones EG (1976) The posterior thalamic region and its cortical projection in New World and Old World monkeys. J Comp Neurol 168:249-301.

Calford MB (1983) The parcellation of the medial geniculate body of the cat defined by the auditory response properties of single units. J Neurosci 3:2350-2364.

Cheung SW, Bedenbaugh PH, Nagarajan SS, Schreiner CE (2001) Functional organization of squirrel monkey primary auditory cortex: responses to pure tones. J Neurophysiol 85:1732-1749.

Coq JO, Qi H, Collins CE, Kaas JH (2004) Anatomical and functional organization of somatosensory areas of the lateral fissure of the New World titi monkey (Callicebus moloch). J Comp Neurol 476:363-387.

Crum P, Issa E, Hackett T, Wang X (submitted) Hierarchical processing in awake primate auditory cortex.

de la Mothe LA, Blumell S, Kajikawa Y, Hackett TA (2006a) Thalamic connections of the auditory cortex in marmoset monkeys: core and medial belt regions. J Comp Neurol 496:72-96.

de la Mothe LA, Blumell S, Kajikawa Y, Hackett TA (2006b) Cortical connections of the auditory cortex in marmoset monkeys: core and medial belt regions. J Comp Neurol 496:27-71.

Disbrow E, Litinas E, Recanzone GH, Padberg J, Krubitzer L (2003) Cortical connections of the second somatosensory area and the parietal ventral area in macaque monkeys. J Comp Neurol 462:382-399.

Felleman DJ, Van Essen DC (1991) Distributed hierarchical processing in the primate cerebral cortex. Cereb Cortex 1:1-47.

Fitzpatrick KA, Imig TJ (1980) Auditory cortico-cortical connections in the owl monkey. J Comp Neurol 192:589-610.

Galaburda AM, Pandya DN (1983) The intrinsic architectonic and connectional organization of the superior temporal region of the rhesus monkey. J Comp Neurol 221:169-184.

Gallyas F (1979) Silver staining of myelin by means of physical development. Neurol Res 1:203-209.

Geneser-Jensen FA, Blackstad TW (1971) Distribution of acetyl cholinesterase in the hippocampal region of the guinea pig. I. Entorhinal area, parasubiculum, and presubiculum. Z Zellforsch Mikrosk Anat 114:460-481.

Hackett TA (2010) Information flow in the auditory cortical network. Hear Res.

Hackett TA, de la Mothe LA (2009) Regional and laminar distribution of the vesicular glutamate transporter, VGluT2, in the macaque monkey auditory cortex. J Chem Neuroanat 38:106-116.

Hackett TA, Stepniewska I, Kaas JH (1998a) Thalamocortical connections of the parabelt auditory cortex in macaque monkeys. J Comp Neurol 400:271-286.

Hackett TA, Stepniewska I, Kaas JH (1998b) Subdivisions of auditory cortex and ipsilateral cortical connections of the parabelt auditory cortex in macaque monkeys. J Comp Neurol 394:475-495.

Hackett TA, Preuss TM, Kaas JH (2001) Architectonic identification of the core region in auditory cortex of macaques, chimpanzees, and humans. J Comp Neurol 441:197-222.

Hackett TA, De La Mothe LA, Ulbert I, Karmos G, Smiley J, Schroeder CE (2007) Multisensory convergence in auditory cortex, II. Thalamocortical connections of the caudal superior temporal plane. J Comp Neurol 502:924-952.

Hashikawa T, Molinari M, Rausell E, Jones EG (1995) Patchy and laminar terminations of medial geniculate axons in monkey auditory cortex. J Comp Neurol 362:195-208.

Imig TJ, Morel A (1984) Topographic and cytoarchitectonic organization of thalamic neurons related to their targets in low-, middle-, and high-frequency representations in cat auditory cortex. J Comp Neurol 227:511-539.

Imig TJ, Morel A (1985a) Tonotopic organization in lateral part of posterior group of thalamic nuclei in the cat. J Neurophysiol 53:836-851.

Imig TJ, Morel A (1985b) Tonotopic organization in ventral nucleus of medial geniculate body in the cat. J Neurophysiol 53:309-340.

Inui K, Okamoto H, Miki K, Gunji A, Kakigi R (2006) Serial and parallel processing in the human auditory cortex: a magnetoencephalographic study. Cereb Cortex 16:18-30.

Jones EG, Burton H (1976) Areal differences in the laminar distribution of thalamic afferents in cortical fields of the insular, parietal and temporal regions of primates. J Comp Neurol 168:197-247.

Kaas JH, Hackett TA (2000) Subdivisions of auditory cortex and processing streams in primates. Proc Natl Acad Sci U S A 97:11793-11799.

Kajikawa Y, de La Mothe L, Blumell S, Hackett TA (2005) A comparison of neuron response properties in areas A1 and CM of the marmoset monkey auditory cortex: tones and broadband noise. J Neurophysiol 93:22-34.

Katzner S, Nauhaus I, Benucci A, Bonin V, Ringach DL, Carandini M (2009) Local origin of field potentials in visual cortex. Neuron 61:35-41.

Kayser C, Petkov CI, Logothetis NK (2007) Tuning to sound frequency in auditory field potentials. J Neurophysiol 98:1806-1809.

Krubitzer L, Clarey J, Tweedale R, Elston G, Calford M (1995) A redefinition of somatosensory areas in the lateral sulcus of macaque monkeys. J Neurosci 15:3821-3839.

Kusmierek P, Rauschecker JP (2009) Functional specialization of medial auditory belt cortex in the alert rhesus monkey. J Neurophysiol.

Lakatos P, Pincze Z, Fu KM, Javitt DC, Karmos G, Schroeder CE (2005) Timing of pure tone and noise-evoked responses in macaque auditory cortex. Neuroreport 16:933-937.

Molinari M, Dell'Anna ME, Rausell E, Leggio MG, Hashikawa T, Jones EG (1995) Auditory thalamocortical pathways defined in monkeys by calcium-binding protein immunoreactivity. J Comp Neurol 362:171-194.

Nelson MJ, Pouget P, Nilsen EA, Patten CD, Schall JD (2008) Review of signal distortion through metal microelectrode recording circuits and filters. J Neurosci Methods 169:141-157.

Nowak L, Bullier J (1997) The timing of information transfer in the visual system. In: Cerebral Cortex (Rockand K, Jones EG, Peters A, Kaas JH, eds), pp 205-241. New York: Plenum Press.

Oshurkova E, Scheich H, Brosch M (2008) Click train encoding in primary and non-primary auditory cortex of anesthetized macaque monkeys. Neuroscience 153:1289-1299.

Philibert B, Beitel RE, Nagarajan SS, Bonham BH, Schreiner CE, Cheung SW (2005) Functional organization and hemispheric comparison of primary auditory cortex in the common marmoset (Callithrix jacchus). J Comp Neurol 487:391-406.

Rauschecker JP, Tian B (2000) Mechanisms and streams for processing of "what" and "where" in auditory cortex. Proc Natl Acad Sci U S A 97:11800-11806.

Rauschecker JP, Tian B, Hauser M (1995) Processing of complex sounds in the macaque nonprimary auditory cortex. Science 268:111-114.

Rauschecker JP, Tian B, Pons T, Mishkin M (1997) Serial and parallel processing in rhesus monkey auditory cortex. J Comp Neurol 382:89-103.

Recanzone GH (2000) Response profiles of auditory cortical neurons to tones and noise in behaving macaque monkeys. Hear Res 150:104-118.

Robinson CJ, Burton H (1980a) Somatic submodality distribution within the second somatosensory (SII), 7b, retroinsular, postauditory, and granular insular cortical areas of M. fascicularis. J Comp Neurol 192:93-108.

Robinson CJ, Burton H (1980b) Organization of somatosensory receptive fields in cortical areas 7b, retroinsula, postauditory and granular insula of M. fascicularis. J Comp Neurol 192:69-92.

Romanski LM, Tian B, Fritz J, Mishkin M, Goldman-Rakic PS, Rauschecker JP (1999) Dual streams of auditory afferents target multiple domains in the primate prefrontal cortex. Nat Neurosci 2:1131-1136.

Schmolesky MT, Wang Y, Hanes DP, Thompson KG, Leutgeb S, Schall JD, Leventhal AG (1998) Signal timing across the macaque visual system. J Neurophysiol 79:3272-3278.

Schroeder CE, Mehta AD, Givre SJ (1998) A spatiotemporal profile of visual system activation revealed by current source density analysis in the awake macaque. Cereb Cortex 8:575-592.

Steinschneider M, Tenke CE, Schroeder CE, Javitt DC, Simpson GV, Arezzo JC, Vaughan HG, Jr. (1992) Cellular generators of the cortical auditory evoked potential initial component. Electroencephalogr Clin Neurophysiol 84:196-200.

Vaadia E, Gottlieb Y, Abeles M (1982) Single-unit activity related to sensorimotor association in auditory cortex of a monkey. J Neurophysiol 48:1201-1213.

Wong-Riley M (1979) Changes in the visual system of monocularly sutured or enucleated cats demonstrable with cytochrome oxidase histochemistry. Brain Res 171:11-28.

CHAPTER III

MODULATION FREQUENCY TUNING IN AUDITORY CORTEX OF THE ALERT MACAQUE: EVIDENCE FOR HIERARCHICAL PROCESSING AND IMPLICATIONS FOR STIMULUS ENCODING

3.1 Abstract

The current working model of primate auditory cortex designates three interconnected regions which in turn can be subdivided into multiple areas, distinguished by unique anatomical and physiological profiles. Though regions are generally considered to be levels of processing, the direction and flow of information within primate auditory cortex remains an active area of study. An influential hypothesis is that modulation frequency tuning can imply flow: as the stimulus-related neural response ascends the auditory hierarchy, entrainment-based (i.e. temporal) modulation frequency tuning decreases due to variability introduced by successive synaptic delays. To evaluate temporal tuning, we collected neural responses from five areas in core, lateral belt, and parabelt to amplitude modulated noise in the awake macaque. Temporal best tuning was lower in lateral belt and parabelt than in core for both units and the LFP. This decrease in temporal tuning provides support for hierarchical processing in a regional direction. In addition, we see that for all areas a rate based code covers all the modulation frequencies tested, showing that a rate code is sufficient to encode the modulation frequencies that cannot be accounted for by temporal measures, particularly at later levels of processing.

3.2 Introduction

The current working model of primate auditory cortex designates three interconnected regions (core, belt, and parabelt) which are thought to represent different levels of processing. Each region is subdivided into multiple areas, distinguished by unique anatomical and physiological profiles (see figure 2-1, chapter 2). The direction and flow of information within and between regions and areas remains an active area of study. Patterns of connectivity from the ventral division of the medial geniculate (MGv) and the absence of significant connections from core to parabelt suggest a serial flow of information from core to belt to parabelt (Rauschecker et al., 1997; Kaas and Hackett, 2000; Hackett, 2010). However, there are strong elements of parallel processing both from other medial geniculate complex (MGC) inputs as well as within regions (reviewed in chapter 1 and 2). In this study, we seek to evaluate tuning to temporally modulated sounds in neurons across multiple areas of core, belt, and parabelt. We have two separate but complementary aims. The first is to characterize modulation frequency tuning across multiple areas of auditory cortex. The second is to evaluate the implications of those findings for hierarchical flow between regions and areas in auditory cortex of the primate.

Temporally modulated sounds are sounds for which the waveform envelope is subject to repeated amplitude modulation. Temporal envelope modulations are common, especially in vocalizations; hence detection of temporally modulated sound is critical for communication and survival. Perception of temporal modulation appears to be dependent on an intact auditory cortex (Whitfield, 1980; Heffner and Heffner, 1986; Zatorre, 1988; Phillips and Farmer, 1990; Kelly et al., 1996; Griffiths, 1999). Given its obvious

importance, the encoding of modulated sounds in the primate cortex has been under active investigation in a variety of primate species, particularly in core area A1 (Sudakov et al., 1971; Bieser, 1995; Bieser and Muller-Preuss, 1996; Steinschneider et al., 1998; Fishman et al., 2000a, b; Lu et al., 2001a, b; Liang et al., 2002; Tian and Rauschecker, 2004; Bendor and Wang, 2007; Malone et al., 2007; Phan and Recanzone, 2007; Bendor and Wang, 2008; Kajikawa et al., 2008; Oshurkova et al., 2008; Bendor and Wang, 2010; Crum et al., submitted). Studies suggest that the frequency of modulated sound (temporal frequency) can be encoded in two ways in cortex (e.g. Schreiner and Urbas, 1986; Lu et al., 2001a).

The first, which we will refer to as temporal tuning, is a measure of how phase-locked, or entrained, the neuronal response is with respect to particular features of the envelope of the stimulus. Temporal tuning is additionally of interest because it can be used to infer processing hierarchy in the auditory system. A prominent hypothesis is that as the stimulus-related neural response ascends the auditory hierarchy, entrainment-based (i.e. temporal) modulation frequency tuning decreases as a consequence of variability introduced by successive synaptic delays (Joris et al., 2004). This has been observed through the subcortical processing stream in mammals (reviewed in: Langner, 1992), including the transition from medial geniculate to A1 in primates (Wang et al., 2008). The connectivity between areas in the primate auditory cortex suggests that temporal tuning may be a useful physiological signature of hierarchical position. Based on both connectivity and physiological studies, it is hypothesized that information flows both in a regional (core-belt-parabelt) and caudorostral direction (Hackett 2010). If this is true,

then we should see gradients or shifts in temporal modulation frequencies along both axes.

To represent the modulation frequencies that can no longer be encoded by entrainment, it has been proposed that another type of code emerges (e.g. Bendor and Wang, 2007; Wang et al., 2008). This second type of code, called rate coding, is a measure of the firing rate evoked by a given modulation frequency. Rate based codes for modulation frequency tuning have been observed in mammalian subcortical structures such as the inferior colliculus and medial geniculate complex (e.g. Langner and Schreiner, 1988; Schreiner and Langner, 1988; Bartlett and Wang, 2007), as well as in primate cortex (Liang et al., 2002; Bendor and Wang, 2007; Phan and Recanzone, 2007; Bendor and Wang, 2008; Oshurkova et al., 2008; Crum et al., submitted). Although temporal and rate based codes had originally been proposed to be two wholly separate codes in primate cortex (Bendor and Wang, 2007), it has been increasingly accepted that a single neuron can encode modulation frequencies in both temporal and rate based ways (Phan and Recanzone, 2007; Bendor and Wang, 2008, 2010). Neurons in cortex can encode in a rate based way regardless of high modulation frequency, and it is expected that, concomitant with limitations that may be imposed by the processing hierarchy, a rate based code will be increasingly used at later processing stages. This has been seen in many mammalian species (reviewed in Langner, 1992; Wang et al., 2008). We are interested in evaluating rate-based modulation frequency tuning across multiple areas and regions of macaque cortex.

This study aims to better characterize modulation frequency tuning across regions and areas using the same stimuli, as well as to look for evidence of processing flow in the

form of differences in temporal tuning . Measures of entrainment limitations (tMAX) should be particularly sensitive to differences in stimulus-locked synchronization ability between areas. As an additional measure of temporal tuning, LFPs are presumed to be the summed dendritic input over a local area, and have been shown to exhibit tuning. Local field potential (LFP) tuning measures have been explored previously in both human and nonhuman primate (Rees et al., 1986; Steinschneider et al., 1998; Fishman et al., 2000a, b; Liegeois-Chauvel et al., 2004; Brugge et al., 2009; Crum et al., submitted). We are interested in examining temporal tuning of the LFP as an additional measure to evaluate processing flow in the primate auditory cortex.

In this study, we collected neural responses from five areas in core, lateral belt, and parabelt to amplitude modulated noise in the awake macaque. Modulation rates from 3.1-957 Hz were evaluated. Entrainment based best tuning was mainly 13 Hz and below in core. In lateral belt and parabelt, best modulation tuning is lower. This decrease in entrainment based modulation frequency tuning provides support for hierarchical processing in a regional direction. Temporal tuning measures derived from the LFP support the same patterns. In addition, we see that for all areas a rate based code covers all the modulation frequencies tested in a parauniform way. This shows that a rate code is sufficient to encode the modulation frequencies that cannot be accounted for by temporal measures, particularly at later levels of processing.

3.3 Materials and Methods

General surgical procedures, histological processing, anatomical reconstruction, and experimental methods have been reported previously (see chapter 2), but details pertinent to this investigation are included below.

Animal subjects

Two adult macaque monkeys SP and DY were used for neural recordings (SP male bonnet macaque (*Macaca radiata*) 10.0 kg, and DY female rhesus macaque (*Macaca mulatta*) 7.0 kg). Animals were housed in an AAALAC-accredited facility under supervision of laboratory and veterinary staff. All animal care and experimental procedures were in accordance with the U.S. National Institutes of Health *Guide for the care and use of laboratory animals*, under a protocol approved by the Vanderbilt Institutional Animal Care and Use Committee.

Stimulus generation and neurophysiological acquisition

Stimulus generation and delivery. Recording sessions were conducted in a double walled chamber (Industrial Acoustics Corp, NY) that attenuated sounds, particularly at the mid to high frequencies. Acoustic stimuli were generated by Tucker-Davis technologies (TDT, Gainesville, FL) System II hardware and software (SigGen), controlled by a custom software interface between the stimulus generation and acquisition setups. Stimuli were delivered using Beyer DT911 insert earphones (range 0.10-25 kHz), coupled to custom earmolds in both ears. Stimuli were calibrated for

intensity using a ¼ inch microphone (Model 7017; ACO Pacific, CA), pistonphone (Bruel and Kjaer type 4220) and custom software (TDT, SigCal). Amplitude corrections were saved in a data file and applied to each stimulus to pre-equalize the response of each earphone independently.

Stimuli: Amplitude modulated noise**.** AM noise was constructed using Gaussian white noise convolved with a sine wave of 100% depth, yielding sinusoidally amplitude modulated white noise. Other studies have used pure tones as carriers, but for this study, the choice of white noise as a carrier yields threefold benefit. First, amplitude modulation of pure tones creates spectral sidebands which are nonconstant at different modulation frequencies and may introduce spectral cues unrelated to modulation frequency tuning. In contrast modulated white noise yields an essentially flat frequency spectrum irrespective of modulation frequency. Second, this study was designed to examine differences between areas and regions known to have different spectral tuning functions. Despite differences in best tuning frequency and width, all regions respond robustly to wideband noise. Thus it is the best carrier to use when one is aiming to compare across areas and regions. Third, wideband noise has a spectrum more similar to ethologically relevant sounds that are often wideband in character and is thus useful for assaying the encoding of more generalized stimuli.

Temporal modulation frequencies ranged from 3.1-957 Hz. Each stimulus type had a duration of 1000 ms, was calibrated to 50 dB SPL, and each modulation frequency was presented diotically 10 times with a jittered interonset interval of approximately 3000 ms, randomly interleaved with other stimulus types in the battery (e.g. clicks, noise). These stimuli contain a 5 ms cosine^2 ramp at onset and offset. The modulation rates were

chosen to be the closest prime to roughly equal steps between 3 and 100 Hz, and four faster modulation frequencies, also primes, to cover much higher modulation frequencies (251, 503, 751, 957). Prime frequencies are computationally useful because they do not contain common multiples with each other or with 60 Hz (e.g. AC line noise). This avoids spurious vector strength due to entrainment or power sources at lower multiples.

Electrophysiological recording. Electrode penetrations were made through a recording grid 15 mm wide with 1 mm spacing which fit over the implanted chamber (Crist Instruments, Hagerstown MD). This ensured a replicable and roughly perpendicular trajectory through most parts of the superior temporal plane corresponding to the caudal two-thirds of auditory cortex. After a local anesthetic (0.13% bupivacaine and 0.5% lidocaine in sterile saline) was topically applied and then removed, a sharpened stainless steel guide tube was used to puncture through the dura. The use of a guide tube also ensured that the penetration ran parallel to the recording chamber. One to two tungsten microelectrodes (2-4 MOhm, FHC, Bowdoin, MA) aligned mediolaterally were advanced through somatosensory cortices and into auditory cortex using manual microdrives (Narishige, Tokyo, Japan).

From the first auditory responses until the end of auditory-responsive cortex, all isolated neurons, irrespective of responsiveness, were tested with all or most of the stimulus battery. This avoids introducing bias to our sample. In between isolations the microdrives were moved at least 200 μm to avoid resampling units. For most runs, we recorded through all layers until the white matter was reached. We assigned a relative cortical depth to each penetration by normalizing the recording depth with respect to the first auditory responses, presumably from the first layer or two of auditory cortex. While

unequivocal laminar depths cannot be established, it is likely that the majority of recorded neurons are coming from the middle and upper layers, consistent with the cytoarchitecture of auditory cortex (see Hackett, 2010). During recording sessions the monkey was continuously monitored for alertness via closed-circuit television.

Multichannel spike and local field potential (LFP) recordings were acquired with a 64-channel system that controls amplification, filtering and related parameters (Many Neuron Acquisition Processor, Plexon Inc, Dallas, TX). Both signals were referenced to ground. Spike signals were amplified (100x), filtered (150-8800 Hz), and digitized at 40 kHz. The signal was further DC-offset corrected with a low-cut filter (0.7Hz). Spikes were sorted online for all channels using real-time window discrimination. Digitized waveforms and timestamps of stimulus events were also saved for final offline analysis and sorting (Plexon offline sorter), and graded according to isolation quality (single or multi units). Single and multi units were analyzed separately and the tuning results and patterns across areas were qualitatively and quantitatively indistinguishable. Thus both single and multi units were included in this study. The LFP signals were acquired simultaneously with the spike data. These were amplified (500x), filtered (3.3-89.0 Hz), and digitized at 1 kHz. Again, the signals were further DC-offset corrected by with a low-cut filter (0.7 Hz). To ensure timing precision, the Plexon acquisition software interfaced with the stimulus delivery system (Tucker Davis Technologies) and both systems were controlled by custom software (SGPlay, provided by Peter Yang).

Neurophysiological data analysis

All analyses described below were performed using in-house Matlab scripts (MathWorks, Natick, MA).

Unit: Rate and temporal modulation transfer functions (rMTF and tMTF), best modulation frequencies (rBMF and tBMF), and maximum temporal entrainment frequency (tMAX). From responses to AM noise, two measures were used to calculate a unit's modulation frequency tuning: the rate and temporal modulation transfer functions (rMTF and tMTF respectively). Figure 3-1 shows the steps involved in calculating these measures. An enduring question is whether stimulus onset response should be removed. On the one hand, onset response is similar for many neurons irrespective of modulation frequency and does not reliably indicate tuning (e.g. neuron in figure 3-1). On the other hand, the onset is an integral part of the response and it is difficult to imagine a cortical mechanism by which it is ignored. Thus, for thoroughness, we analyzed responses both ways. Tuning and trends between areas did not change when the onset was included, perhaps because our stimuli were sufficiently long. Since the results were similar, for brevity we present results from responses with the onset removed.

The peristimulus time histogram (PSTH) of an exemplar response is shown on the left side of figure 3-1. To remove the onset, the first ~100 ms of response was removed (specifically, the closest number of whole cycles in 100 ms), and then averaged responses per period were calculated. Each response was divided into 20 bins to create the cycle histogram from which the rate and temporal tuning measures were derived. Note that each period was a different duration (x-axis); for improved visualization the lengths were normalized.

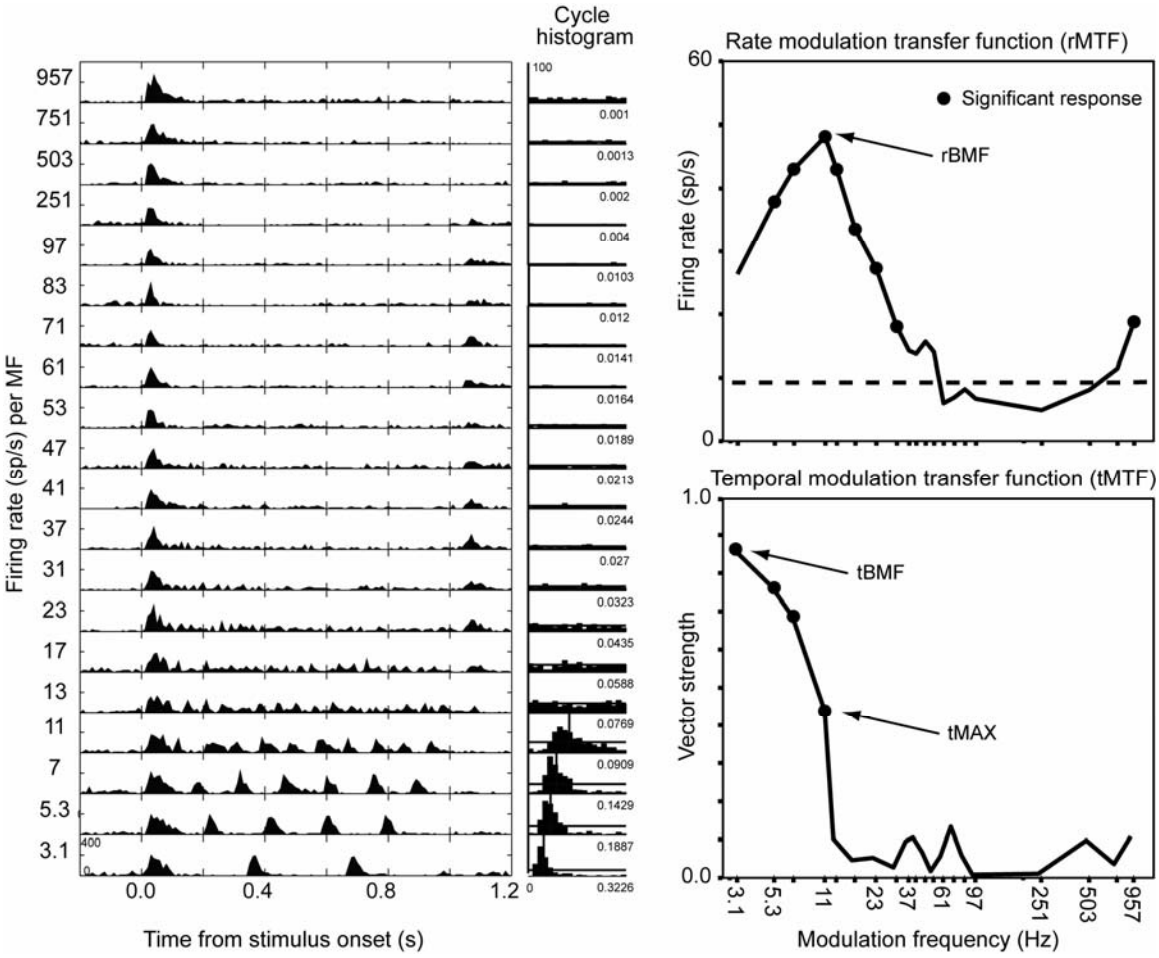

Figure 3-1. Unit: Derivation of rate and temporal tuning measures. Left side, peristimulus time histogram of responses for each of the 20 modulation frequencies presented. To the right of this is the cycle histogram, the average response per cycle (timebase is one period long). Vertical bars on the cycle histogram indicate where the vector strength was significant and at what part of the phase. Horizontal lines indicate the average firing rate. Top right, derivation of the rate modulation transfer function (rMTF) and rate best modulation frequency (rBMF). Circles indicate firing rates that are significantly elevated from baseline firing rate (dotted line). Bottom right, derivation of the vector strength-based temporal modulation transfer function (tMTF), temporal best modulation frequency (tBMF), and temporal maximum entrainment frequency (tMAX). Circles indicate vector strengths that are significant.

The rate modulation transfer function (rMTF), shown in the top right of figure 3-1, measured the firing rate of a neuron in response to a given modulation frequency, plotted as a solid line. Spontaneous firing rate was plotted as a dashed line. Significance of response was determined by a t-test with an α level of $p < 0.05$. Each significant response is denoted with a solid circle. Only a minority of neurons showed significant inhibition at all or a portion of the modulation frequencies tested, so inhibitory tuning was not included in this analysis. The best rate-based modulation frequency (rBMF) was defined as the highest significant value of the rMTF (arrow on figure).

The temporal modulation transfer function (tMTF), shown in the bottom right of figure 3-1, was a measure of the strength of phase-locking of the neuron at different modulation frequencies. A common measure of entrainment is vector strength (but see Kajikawa and Hackett, 2005). This vector strength measure quantified the magnitude of regularity in phase-locking to cyclic stimulation (Goldberg and Brown, 1969; Batschelet, 1981). The tMTF is the relationship between the modulation rate of the AM noise stimulus and the vector strength. Significance of vector strength was determined by the Rayleigh test at the α level of $p < 0.001$. As before, each significant response is denoted with a circle. The best temporal-based modulation frequency (tBMF) was defined as the highest significant value of the tMTF (arrow on figure). The maximum entrainment frequency (tMAX) was defined as the highest modulation frequency at which the vector strength was significant (arrow on figure).

LFP: Temporal modulation transfer function (tMTF), best modulation frequency (tBMF), and maximum temporal entrainment frequency (tMAX). As an additional way to test our hypotheses about hierarchical organization of primate auditory cortex, we

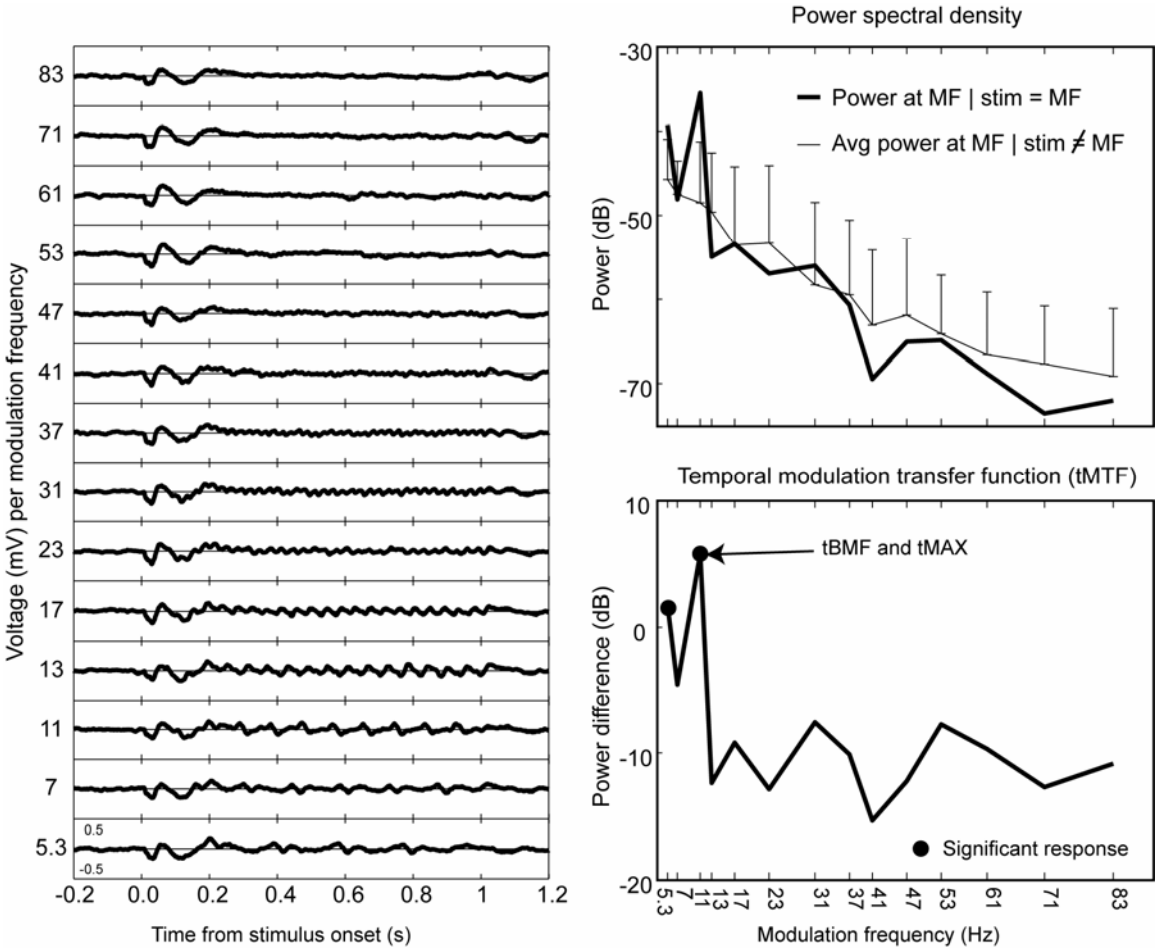

Figure 3-2. LFP: Derivation of temporal tuning measure. Left side, stimulus locked averaged evoked LFP for each of the 14 modulation frequencies analyzed. Top right, thick lines indicate 'evoked power' power spectral density at that modulation frequency for that stimulus. Thin lines indicate the 'expected power' (see methods for details). Error bars are the significance criteria. Bottom right, temporal modulation transfer functions derived for the subtraction of the expected power from the evoked power. Anything that is greater than zero indicates a significant evoked power (circle). For this LFP site, the temporal best modulation frequency (tBMF), and temporal maximum entrainment frequency (tMAX) are the same value.

analyzed the local field potential for temporal tuning. A restricted range of modulation frequencies (5.3-87.0) was used due to cutoffs from the LFP filter settings. Thus it was not possible to directly compare unit and LFP tuning at all frequencies, but any patterns within the LFP could be compared to patterns within the units. Again, for thoroughness, we performed all of the analyses with and without onset. Tuning and trends between areas did not change when the onset was included. An exemplar LFP response is shown in figure 3-2 to illustrate calculation of temporal tuning. The leftmost graph shows across trial averaged evoked potential aligned on stimulus onset for each modulation frequency analyzed.

To preserve similarity with the unit calculation, the first 100 ms of onset response was removed (specifically, the closest number of whole cycles that was at least 100 ms). The following analysis was inspired by methods developed using depth electrodes in human auditory cortex (Rees et al., 1986; Liegeois-Chauvel et al., 2004), with some important modifications listed below. To calculate the tMTF, LFPs were analyzed for stimulus-locked modulation by first characterizing the power spectral density for a given modulation frequency. In the top right graph, the thick line indicates 'evoked power', or the power spectral density at that modulation frequency for that stimulus (e.g. power at 5.3 Hz when the stimulus presented is 5.3 Hz). For comparison, the thin line indicates the estimate of the 'expected power', or the averaged power spectral density at that modulation frequency for all other stimuli (e.g. average power at 5.3 Hz when the stimulus is any other frequency besides 5.3 Hz). Error bars are the significance criterion, here 1.5 times the standard deviation of the 'expected power' estimate. If the evoked

power was greater than the criteria developed from the expected power, the stimulus locked modulation was determined to be significant.

The bottom right graph of figure 3-2 shows the derived tMTF, which is the power difference between the evoked power and the criterion. Values greater than zero indicate a significant evoked power (circles). tBMF and tMAX are derived analogously to the unit data, and for this LFP site, the temporal best modulation frequency (tBMF), and temporal maximum synchronization frequency (tMAX) are the same value.

LFP method development: Welch modification and choice of criterion

This method is similar to methods used in human depth electrodes (Rees et al., 1986; Liegeois-Chauvel et al., 2004; Brugge et al., 2009) but, because it normalizes power within modulation frequencies, it avoids an overemphasis of low powers that may simply be an artifact of the 1/f power spectrum falloff common to stochastic signals. When characterizing the power at a given frequency, the power spectral density (PSD) is a commonly used metric. The PSD is simply the Fourier transform of the square of the signal. However, since PSD estimation using just the Fourier transform is known to be both biased and inconsistent (neither mean nor variance improves with sample size increase (Allen and Mills, 2004)), a modification using the Welch method was adopted. This is another nonparametric method which allows the fast Fourier transform time domain windows to overlap. During method development, a subset of LFP data were analyzed separately using both the Fourier transform and Welch methods. It became apparent that PSDs generated by the Fourier transform method were noisier than those generated by the Welch method. Power curves do show differences, yielding differences

in tuning curves. The two methods did not commonly yield different best tuning estimates (only 2/57 LFPs had different BMFs). However, since the Welch modification addresses some of the problems of biased and inconsistent estimation, the Welch was adopted for further analyses (details of method described in Camalier and Hackett, 2008).

Additionally, when determining significance criterion for the expected power when calculating the tMTF, we used both 95% confidence bounds, bootstrapped 95% confidence bounds, and 1.5 times the standard deviation of the expected power values. Tuning measures of tBMF did not change with significance criterion. As expected, the values for tMAX do change with strictness of criteria: the stricter the criteria, the closer the tMAX is to tBMF. Importantly however, tuning trends between areas do not change with choice of criterion.

3.4 Results

Yield and cortical location

In total, 728 units from five different areas from two core (A1 and R), the two adjacent lateral belt areas (ML and AL), and the adjacent rostral parabelt (RPB) were included. 182 LFPs from four different areas were included in this analysis from the core and belt areas above. There was an insufficient yield of LFP sites to include RPB in the LFP analyses. The numbers of collected and analyzed units and LFPs for each area are summarized in table 3-1.

Table 3-1. Neuron and LFP counts (total, rate-, and temporal-responsive) for each cortical area examined.

		A1	R	ML	AL	RPB
UNITS	rate tuned	140	105	42	46	65
	temporally tuned	198	144	62	71	76
	both	127	83	35	37	46
	TOTAL	243	191	87	93	114
LFP	temporally tuned	56	40	25	19	
	TOTAL	72	52	29	29	

Temporal tuning: evidence for decreased entrainment

Figure 3-3 shows temporal maximum entrainment distributions of units for the five areas examined. For ease of comparison across regions, the caudal-most areas (A1 and ML) and the rostral areas (R, AL, and RPB) were plotted together in separate panels. For each plot, areas within a region are plotted using the same conventions (i.e. distributions from A1 and R are both thick solid lines). For the caudal areas, maximum entrainment (tMAX) indeed decreases from core to belt: the mode of the A1 distribution is at a faster modulation frequency than the mode of the ML distribution. To infer differences we found that measures of medians and means (i.e. Wilcoxon rank sum) were insensitive to these subtle but important differences in the distributions, so we chose to examine modes of the distribution. For the rostral areas, the same is true: the mode of R is at a faster modulation frequency than the mode of the adjacent lateral belt area AL. The mode of the parabelt area RBP is the same as AL, thought it proportionally contains more units synchronized to the slowest modulation frequency. While tMAX decreases with regional level, it does not appear to decrease with rostrocaudal level: the core areas have the same mode and the belt areas have the same mode.

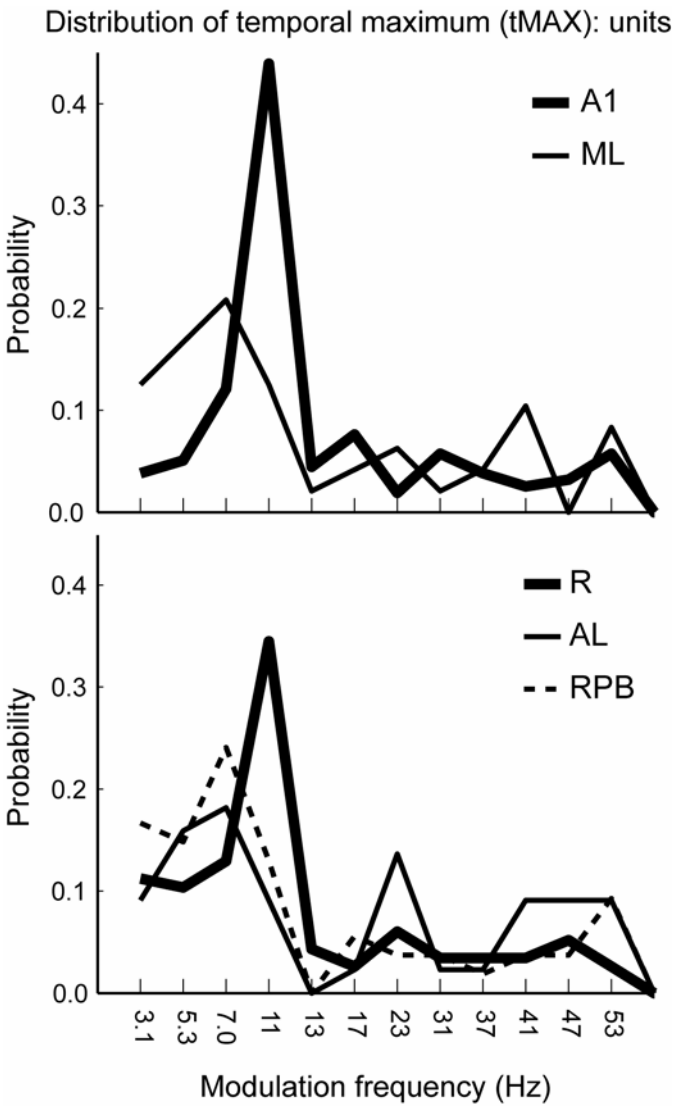

Figure 3-3. Distribution of temporal maximum (tMAX) values: units. Top graph, core and lateral belt: A1 and ML. Bottom graph, next-most rostral level of core, lateral belt and parabelt: R, Al, and RPB. For ease of comparison, areas of the core region are indicated by thick lines, areas of the belt region are indicated by thin lines and the area of the parabelt region is indicated by a dashed line.

As a further test of decreased entrainment, figure 3-4 shows distributions of temporal best modulation frequencies (tBMF) of units in the five areas, conventions preserved from figure 3-3. For all areas, tBMFs were clustered at the lowest frequency (3.1 Hz) and drop off by 13 Hz. Modes for all distributions were clustered at 3.3 or 5.3, the lowest frequencies tested. These tuning curves were very similar; there was no trend either as a function of regional level or rostrocaudal level.

Next, we examined entrainment and tuning of the LFP from four areas (core A1 and R, and lateral belt ML and AL) for evidence of decreasing entrainment. Figure 3-5 shows distributions of tMAX of LFPs for these areas. Similar to the units, there was evidence for decreased entrainment from core to belt. A1 and ML had the same mode, but ML had proportionately more units whose maximum synchrony was at lower frequencies. R had a mode at a higher modulation frequency than AL. In a caudorostral direction, both core areas had a distribution mode that occurred around 11 Hz, whereas the belt areas' mode is lower at 7. Similar to the units, there as no difference in modes for core areas in a caudorostral dimension, but ML had a higher mode than AL.

Figure 3-6 shows distributions of tBMF for the LFPs. Along the regional axis, A1 and ML had the same mode, but R had a mode at a higher modulation frequency than AL. In a caudorostral direction, for both core areas the mode of the distribution occurs around 11 Hz, whereas ML's mode is slightly higher than the mode at AL, possibly indicating a weak decrease in entrainment.

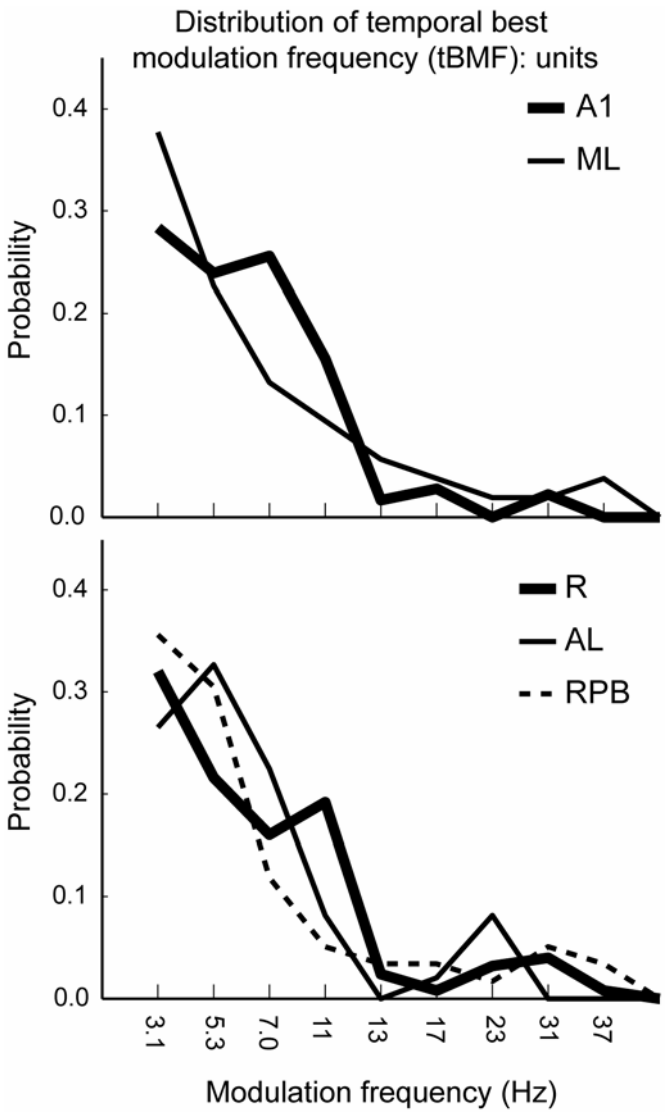

Figure 3-4. Distribution of temporal best modulation frequency (tBMF) values: units. Conventions are preserved from figure 3-3.

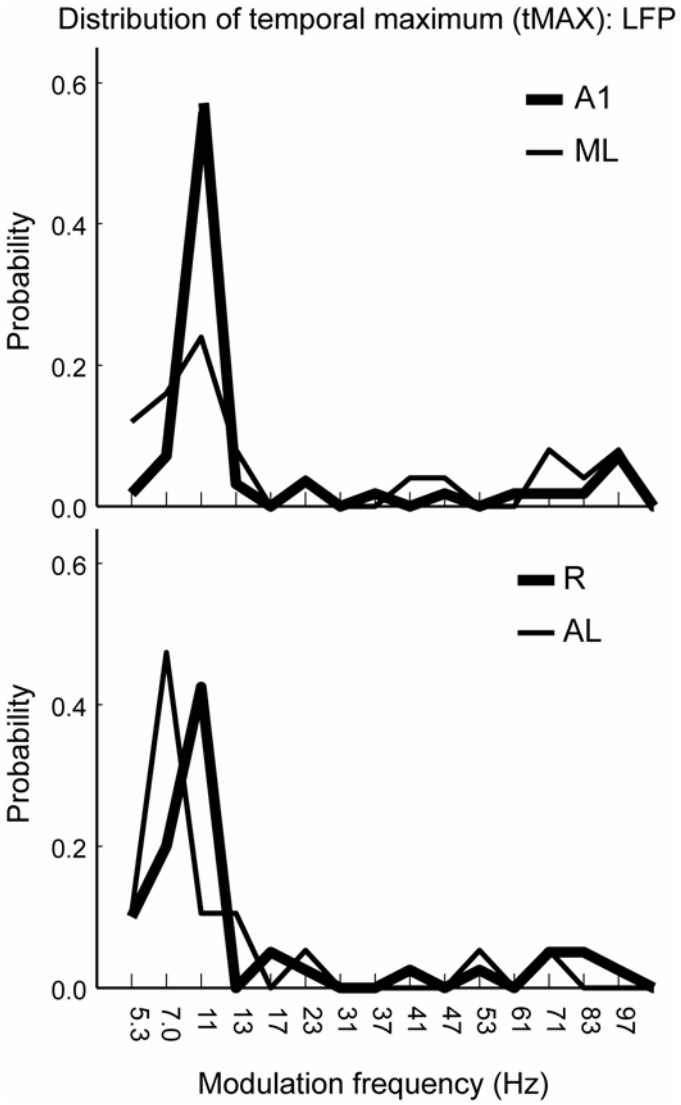

Figure 3-5. Distribution of temporal maximum (tMAX) values: LFP. Top graph, caudal levels of core and lateral belt: A1 and ML. Bottom graph, next-most rostral level of core and lateral belt: R, Al. All other conventions preserved from figure 3-3.

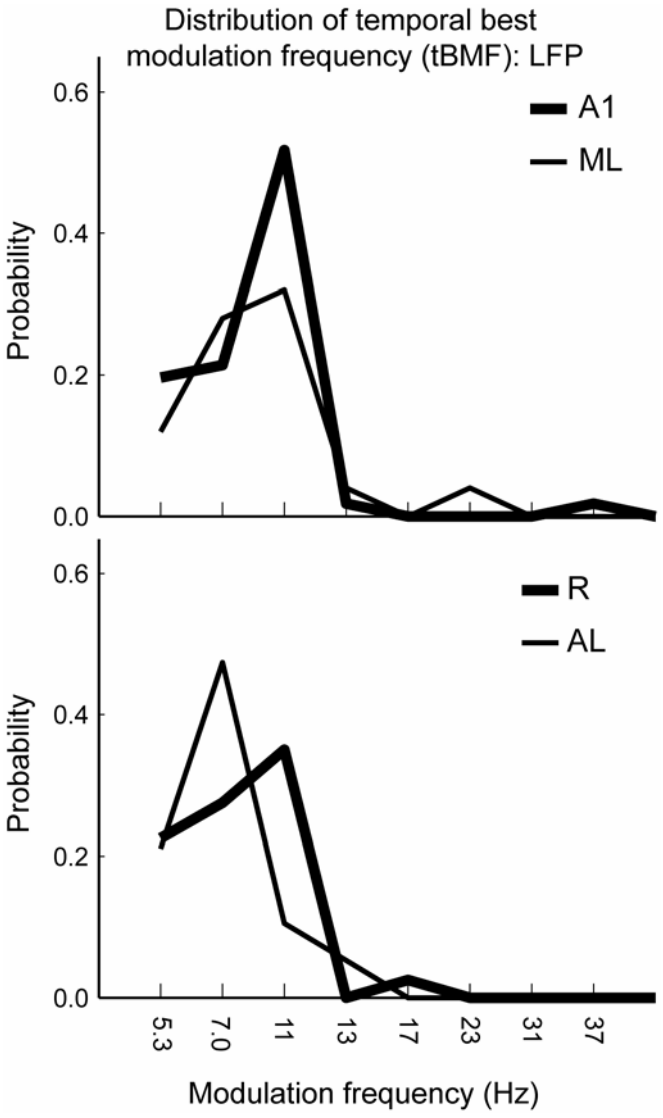

Figure 3-6. Distribution of temporal best modulation frequency (tBMF) values: LFP. Conventions preserved from figure 3-5.

Rate based tuning of units and relative responsiveness in a temporal versus rate code

Figure 3-7 shows distributions of best modulation tuning in a rate based manner (rBMFs) for units in the five areas examined. Distributions are similar for all areas, and are relatively flat. Modulation frequencies appear to be coded in a uniform way with a slight overrepresentation of frequencies < 23 Hz. The distribution appears to increase at the highest modulation frequencies (> 100). Above 60 Hz, however, the bin sizes are also increasing, consequently this finding may be an artifact of larger bin size.

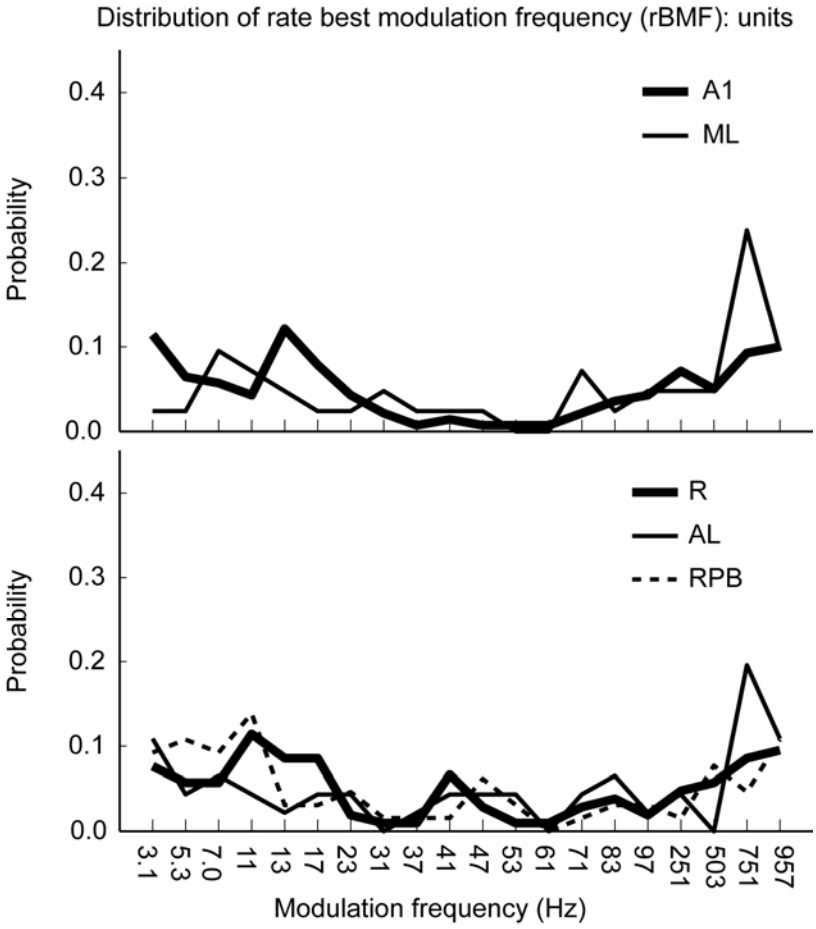

Figure 3-7. Distribution of rate best modulation frequency (rBMF) values: units. Conventions are preserved from figure 3-3.

To examine how many units are responding in a rate or temporal manner, figure 3-8 shows the percent rate, or temporal responsiveness for each area. A unit was considered responsive in a rate or temporal code if it exhibited at least one modulation frequency with a significantly elevated firing rate or vector strength. Also plotted is the percent of units that exhibited responsiveness in both a rate and temporal code. There are no consistent trends as a function of regional level or a rostrocaudal level. For areas examined, more of the units respond in a temporal code than a rate based code, but many of the neurons are coding in both ways.

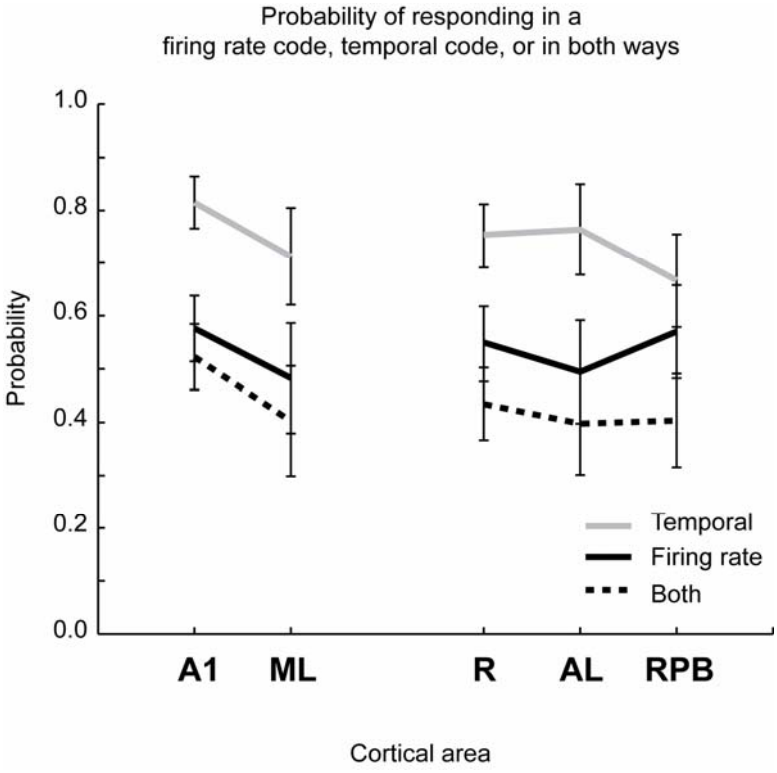

Figure 3-8. Probability of responding in a firing rate or temporal code, or in both ways. For each area, line graphs show the probability of a neuron having at least one modulation frequency with a significant rate or temporal response, or with both kinds of significant responses. For ease of comparison, lines connect areas from core, belt, or parabelt regions across the same caudorostral level. Error bars denote 95% binomial confidence intervals.

3.5 Discussion

Temporal tuning: evidence for processing hierarchy

In conclusion, we examined tuning of both units and LFPs to different modulation frequencies to look for evidence for a decrease in temporal entrainment that would be predicted by hierarchical processing (Joris et al., 2004). Unit responses from five areas were considered in core A1 and R, lateral belt ML and AL, and parabelt RPB. We found evidence for decreased entrainment from core to belt at both caudorostral levels examined, but only for tMAX, not tBMF. A maximum synchrony measure is most sensitive to changes in entrainment capacity among areas, since the limits of entrainment are where desynchronization will have the most effect.

For LFP tuning, we found evidence for decreased entrainment from core to belt, both for tMAX and tBMF. Additionally, there was evidence for decreased entrainment in a caudorostral direction, but it was only for the belt areas. Given that the belt areas had the least number of LFPs analyzed, and this result is not consistent either with core LFP trends or core or belt unit trends, evidence for decreased entrainment in a caudorostral direction in this dataset is weak.

Our estimates of A1 unit tuning are similar to other studies examining responses to amplitude modulation or click trains in a variety of primate species. Studies find that tBMFs of A1 usually cluster at frequencies 16 Hz or lower in squirrel monkeys, marmoset and macaques (Sudakov et al., 1971; Bieser, 1995; Bieser and Muller-Preuss, 1996; Liang et al., 2002; Malone et al., 2007; Bendor and Wang, 2008; Oshurkova et al., 2008; Crum et al., submitted). Studies comparing responses across regions are rarer, but

there is evidence for decreased tBMF and tMAX from A1 to belt CM (Oshurkova et al., 2008), and a recent study comparing A1, ML, and CPB found that vector strength generally decreases with increasing regional level, though tuning measures were not discussed (Crum et al., submitted). Lower vector strength and tuning are due to variability in inputs, either longer, more variable latencies, variability introduced by successive synaptic delays, or variability introduced by convergence of inputs (Eggermont and Smith, 1995; Wang and Sachs, 1995; Joris et al., 2004). Thus, these decreases in entrainment rates and vector strengths in belt and parabelt are consistent with both the increased synaptic delays introduced in belt and parabelt as well as the convergence of inputs from cortical (core, belt) and thalamocortical (MGd) sources that belt and parabelt share. There appears to be decrease in measures of entrainment after the core level, consistent with the Joris hypothesis.

In our dataset, peak tMAX and tBMF measures do not indicate decreased entrainment in parabelt RPB compared to adjacent lateral belt AL, as would be expected. However, RPB has proportionately more of its tMAX and tBMF distributions at the lowest modulation frequencies tested, which could indicate a preference towards lower modulation frequencies. Because the degree of convergence would not be expected to differ in the belt and parabelt, just in the number of synaptic delays from core, belt-parabelt differences in entrainment would consequently not be expected to be as large as core-belt differences.

Previous estimates of LFP tuning report that neurons in A1 entrain to very high modulation frequencies, as high or higher than 100 Hz (Steinschneider et al., 1998; Fishman et al., 2000b; Crum et al., submitted). These tMAX estimates are higher than our

tMAX estimates, but may be due to methodological differences, since the stricter the criterion for significance, the closer tMAX will be to tBMF (and lower). Distributions of LFP-derived tBMF are generally not reported in earlier studies, which limits comparisons that can be made. Again, studies comparing regions are rare, but Crum et al (Crum et al., submitted) report that mean tMAX values do decrease in a regional manner from A1 to ML to CPB.

Contrary to expectations, there was little evidence for hierarchical processing in a caudorostral direction for both units and LFPs. This is surprising given that some early studies have shown differences in distributions and median tBMF between A1 and R in squirrel monkey cortex (Sudakov et al., 1971; Bieser, 1995; Bieser and Muller-Preuss, 1996). These earlier studies use tones as the carrier for the amplitude modulations, so it may be a methodological difference. Additionally, differences in tBMF between the areas were slight in some later marmoset studies (median of 12 Hz in A1 and 11 Hz in R for Bendor and Wang, 2008) so it is possible that the effect size in this direction is smaller than the effect size along the regional axis. For example, tBMF distributions between adjoining core areas A1 and R show no significant differences in that study, but differences are seen between nonadjacent core A1 and RT (Bendor and Wang, 2008). Differences in tMAX are seen between A1 and R, but only when a specific subset of synchronized neurons was examined, and modal values of the tMAX distributions are slightly lower by one step-size in R than A1 (Bendor and Wang, 2008). If these patterns are valid, why would the effect size be smaller in the rostrocaudal direction? One would expect lower entrainment rates because latencies are longer in the rostral direction, and it is possible that there may be more convergence in rostral areas due to feedforward

projections from caudal areas (i.e. A1 onto R). However, the difference in the amount of convergence is probably not as large as from core to belt. To test for differences in entrainment that may not be reflected in tBMF and tMAX distributions, one might look at magnitude of VS with modulation frequency (e.g. Bendor and Wang, 2008; Crum et al., submitted).

Implications for stimulus encoding: rate and temporal codes

Given that tBMFs were generally quite low in all areas examined, how are higher modulation frequencies encoded? Across all five areas, we found that BMFs in a rate based code covered all of the modulation frequencies examined in an approximately uniform fashion. The distributions were remarkably similar across regional level and caudorostral direction. These findings are consistent with the hypothesis that a rate code emerges to encode modulation frequencies that are too high to be temporally encoded by cortex (Lu et al., 2001a; Wang et al., 2008). This predicts that a rate code represents proportionally more of the modulation frequency tuning as areas lose the ability to encode it in a temporal fashion. This effect has been reported previously in a caudorostral direction in marmoset cortex between core A1 and the undifferentiated R/RT fields (Bendor and Wang, 2007) as well as in a regional direction between core A1 and parabelt CPB (Crum et al., submitted). We did not see strong differences in the differential rate vs temporal responsiveness with regional or caudorostral area, but his is probably because our lowest modulation frequency presented is quite slow and many neurons can still temporally entrain to it, which elevates estimates of temporal responsiveness. If a set of

higher modulation frequencies were examined (as in Bendor and Wang, 2007), we would expect to see these trends.

Consistent with our findings, other studies have found that rate based distributions are not different between A1 and R, or between core and belt regions in awake squirrel monkey (Bieser and Muller-Preuss, 1996) and marmoset (Bendor and Wang, 2008). In many other studies examining rBMFs, distributions are not shown, so it is more difficult to determine if the distributions show the same characteristics (Lu et al., 2001a; Liang et al., 2002; Bendor and Wang, 2007; Crum et al., submitted). One study in macaques does not show uniform distributions of core A1 or belt CM, but it was performed in the anesthetized preparation (Oshurkova et al., 2008) which tends to reflect different dynamics for sustained responses (Wang et al., 2005).

The percept of a given modulation frequency can vary with rate. Low frequencies (< 20 Hz) correspond to perception of rhythm, mid frequencies (~10-50 Hz) correspond to roughness/flutter and higher frequencies correspond to pitch percepts (~> 50-3000 Hz) (Miller and Taylor, 1948; Terhardt, 1974; Krumbholtz et al., 2000). Strict perceptual frequency boundaries are approximate, as they can differ with carrier type and individual differences, but appear to be similar for humans and primates (Moody and Stebbins, 1989). Though different, these distinct percepts can all be encoded with the rate code.

Though the rate based distributions are approximately uniform, there may be a slight overrepresentation of lower modulation frequencies (i.e. < 20 Hz). Given the emphasis on the lower frequencies in the temporal code, there is an overrepresentation of modulation frequencies less than 20 Hz. This may be epiphenomenal, but it is striking that these are also the frequencies common to communication sounds in Old and New

World primates (macaque < 20 Hz (Hammerschmidt and Todt, 1995; Hammerschmidt and Fischer, 1998; Hauser et al., 1998; Rendall et al., 1998), squirrel monkey 6-46 Hz (Schott, 1975) , marmoset 7-15 Hz (Epple, 1968)).

Despite differences in evolutionary history and ecological niche, there appears to be a common primate schema for processing modulated sounds. Strikingly, results from this study and others suggest that modulation frequency tuning appears to be similar for marmoset, squirrel monkey, and macaque. These similarities across Old and New world primate species suggests that frequency tuning is not a function of ethological niche, but appears to reflect a general primate schema that is probably more subject to the bounds put on it by a common primate organization. This modulation frequency tuning decrease also has been demonstrated in humans (fMRI: Giraud et al., 2000; depth electrode: Brugge et al., 2009). Additionally, the temporal cues in human speech are critical for its comprehension (e.g. Shannon et al., 1995; Ahissar et al., 2001) and are limited to similar low modulation frequencies. It is likely that the temporal specializations necessary for language processing also develop under similar structural constraints.

Clearly, neurons respond to more than just the frequency in the context of temporal envelope frequency tuning, and are also responsive to other aspects. such as envelope shape (Malone et al., 2007; Zheng and Escabi, 2008). It is known that neural responses are especially sensitive to depth and periodicity, so whether these tuning curves generalize to other stimulus types is being currently explored (see Camalier et al., 2008; Bendor and Wang, 2010). More studies that look at coding in the awake behaving animal are needed to better understand the neural correlates of modulation frequency perception and discrimination. For example, in a pitch discrimination study of ferrets, it was

concluded that a spike count code was sufficiently fast to describe pitch discrimination performance, but that an ensemble code is required (Bizley et al., 2010). This emphasis on ensemble coding is consistent with a theoretical analysis that also suggests ensembles are necessary (Gourevitch and Eggermont, 2009). One limitation is that both of these studies were performed in A1 only. Another set of recent flutter discrimination studies in macaques suggest that firing rates in A1 neurons are sufficient to predict performance behavior (Lemus et al., 2009b), but that A1 responses are limited to the sensory encoding and that higher order decision and working memory components are encoded in the ventral premotor cortex (Lemus et al., 2009a). Belt and parabelt are located between A1 and prefrontal cortex – perhaps there is more to be learned about the sensory-motor transformations necessary for behavior in the investigation of the higher order cortices. Clearly more work is needed in higher levels and more areas of auditory cortex. Ultimately, information about tuning must be combined with behavioral studies to inform what aspects of the stimulus are most important for perceptions of modulated sounds such as communication.

3.6 References

Ahissar E, Nagarajan S, Ahissar M, Protopapas A, Mahncke H, Merzenich MM (2001) Speech comprehension is correlated with temporal response patterns recorded from auditory cortex. Proc Natl Acad Sci U S A 98:13367-13372.

Allen R, Mills D (2004) Signal Analysis: Time, frequency, scale and structure. Piscataway, NJ: IEEE Press.

Bartlett EL, Wang X (2007) Neural representations of temporally modulated signals in the auditory thalamus of awake primates. J Neurophysiol 97:1005-1017.

Batschelet E (1981) Circular statistics in biology. New York: Academic Press.

Bendor D, Wang X (2007) Differential neural coding of acoustic flutter within primate auditory cortex. Nat Neurosci 10:763-771.

Bendor D, Wang X (2008) Neural response properties of primary, rostral, and rostrotemporal core fields in the auditory cortex of marmoset monkeys. J Neurophysiol 100:888-906.

Bendor D, Wang X (2010) Neural coding of periodicity in marmoset auditory cortex. J Neurophysiol 103:1809-1822.

Bieser A (1995) Amplitude envelope encoding as a feature for temporal information processing in the auditory cortex of squirrel monkeys. In: Primate Vocal Communication (Zimmerman E, ed), pp 221-232. New York, NY: Plenum Press.

Bieser A, Muller-Preuss P (1996) Auditory responsive cortex in the squirrel monkey: neural responses to amplitude-modulated sounds. Exp Brain Res 108:273-284.

Bizley JK, Walker KM, King AJ, Schnupp JW (2010) Neural ensemble codes for stimulus periodicity in auditory cortex. J Neurosci 30:5078-5091.

Brugge JF, Nourski KV, Oya H, Reale RA, Kawasaki H, Steinschneider M, Howard MA, 3rd (2009) Coding of repetitive transients by auditory cortex on Heschl's gyrus. J Neurophysiol 102:2358-2374.

Camalier CR, Hackett TA (2008) Modulation rate tuning of LFPs in macaque auditory cortex: comparison to single unit data. In: Annual meeting of the Society for Neuroscience. Washington, DC.

Camalier CR, D'Angelo WR, Sterbing-D'Angelo SJ, Hackett TA (2008) Modulation rate tuning in core and belt of macaque: effects of carrier duty cycle. In: Midwinter meeting of the Association for Research in Otolaryngology. Phoenix, AZ.

Crum P, Issa E, Hackett T, Wang X (submitted) Hierarchical processing in awake primate auditory cortex.

Eggermont JJ, Smith GM (1995) Synchrony between single-unit activity and local field potentials in relation to periodicity coding in primary auditory cortex. J Neurophysiol 73:227-245.

Epple G (1968) Comparative studies on vocalization in marmoset monkeys (Hapalidae). Folia Primatol (Basel) 8:1-40.

Fishman YI, Reser DH, Arezzo JC, Steinschneider M (2000a) Complex tone processing in primary auditory cortex of the awake monkey. II. Pitch versus critical band representation. J Acoust Soc Am 108:247-262.

Fishman YI, Reser DH, Arezzo JC, Steinschneider M (2000b) Complex tone processing in primary auditory cortex of the awake monkey. I. Neural ensemble correlates of roughness. J Acoust Soc Am 108:235-246.

Giraud AL, Lorenzi C, Ashburner J, Wable J, Johnsrude I, Frackowiak R, Kleinschmidt A (2000) Representation of the temporal envelope of sounds in the human brain. J Neurophysiol 84:1588-1598.

Goldberg JM, Brown PB (1969) Response of binaural neurons of dog superior olivary complex to dichotic tonal stimuli: some physiological mechanisms of sound localization. J Neurophysiol 32:613-636.

Gourevitch B, Eggermont JJ (2009) Maximum decoding abilities of temporal patterns and synchronized firings: application to auditory neurons responding to click trains and amplitude modulated white noise. J Comput Neurosci.

Griffiths TD (1999) Human complex sound analysis. Clin Sci (Lond) 96:231-234.

Hackett TA (2010) Information flow in the auditory cortical network. Hear Res.

Hammerschmidt K, Todt D (1995) Individual-differences in vocalizations of young barbary macaques (macaca sylvanus) - a multi-parametric analysis to identify critical cues in acoustic signaling. Behaviour 132:381-399.

Hammerschmidt K, Fischer J (1998) The vocal repertoire of Barbary macaques: a quantitative analysis of a graded vocalizazation signal system. Ethology 104:203-216.

Hauser M, Agnetta B, Perez C (1998) Orienting asymmetries in rhesus monkeys: the effect of time-domain changes on acoustic perception. Anim Behav 56:41-47.

Heffner HE, Heffner RS (1986) Hearing loss in Japanese macaques following bilateral auditory cortex lesions. J Neurophysiol 55:256-271.

Joris PX, Schreiner CE, Rees A (2004) Neural processing of amplitude-modulated sounds. Physiol Rev 84:541-577.

Kaas JH, Hackett TA (2000) Subdivisions of auditory cortex and processing streams in primates. Proc Natl Acad Sci U S A 97:11793-11799.

Kajikawa Y, Hackett TA (2005) Entropy analysis of neuronal spike train synchrony. J Neurosci Methods 149:90-93.

Kajikawa Y, de la Mothe LA, Blumell S, Sterbing-D'Angelo SJ, D'Angelo W, Camalier CR, Hackett TA (2008) Coding of FM sweep trains and twitter calls in area CM of marmoset auditory cortex. Hear Res 239:107-125.

Kelly JB, Rooney BJ, Phillips DP (1996) Effects of bilateral auditory cortical lesions on gap-detection thresholds in the ferret (Mustela putorius). Behav Neurosci 110:542-550.

Krumbholtz K, Patterson RD, Pressnitzer D (2000) The lower limit of pitch as determined by rate discrimination. Journal of the Acoustical Society of America 108:1170-1180.

Langner G (1992) Periodicity coding in the auditory system. Hear Res 60:115-142.

Langner G, Schreiner CE (1988) Periodicity coding in the inferior colliculus of the cat. I. Neuronal mechanisms. J Neurophysiol 60:1799-1822.

Lemus L, Hernandez A, Romo R (2009a) Neural encoding of auditory discrimination in ventral premotor cortex. Proc Natl Acad Sci U S A 106:14640-14645.

Lemus L, Hernandez A, Romo R (2009b) Neural codes for perceptual discrimination of acoustic flutter in the primate auditory cortex. Proc Natl Acad Sci U S A 106:9471-9476.

Liang L, Lu T, Wang X (2002) Neural representations of sinusoidal amplitude and frequency modulations in the primary auditory cortex of awake primates. J Neurophysiol 87:2237-2261.

Liegeois-Chauvel C, Lorenzi C, Trebuchon A, Regis J, Chauvel P (2004) Temporal envelope processing in the human left and right auditory cortices. Cereb Cortex 14:731-740.

Lu T, Liang L, Wang X (2001a) Temporal and rate representations of time-varying signals in the auditory cortex of awake primates. Nat Neurosci 4:1131-1138.

Lu T, Liang L, Wang X (2001b) Neural representations of temporally asymmetric stimuli in the auditory cortex of awake primates. J Neurophysiol 85:2364-2380.

Malone BJ, Scott BH, Semple MN (2007) Dynamic amplitude coding in the auditory cortex of awake rhesus macaques. J Neurophysiol 98:1451-1474.

Miller GA, Taylor WG (1948) The perception of repeated bursts of noise. Journal of the Acoustical Society of America 20:171-182.

Moody DB, Stebbins WC (1989) Salience of frequency modulation in primate communication. In: The comparative psychology of audition: processing complex sounds (Dooling R, Holse S, eds). Hillsdale, NJ: Erlbaum.

Oshurkova E, Scheich H, Brosch M (2008) Click train encoding in primary and non-primary auditory cortex of anesthetized macaque monkeys. Neuroscience 153:1289-1299.

Phan ML, Recanzone GH (2007) Single-neuron responses to rapidly presented temporal sequences in the primary auditory cortex of the awake macaque monkey. J Neurophysiol 97:1726-1737.

Phillips DP, Farmer ME (1990) Acquired word deafness, and the temporal grain of sound representation in the primary auditory cortex. Behav Brain Res 40:85-94.

Rauschecker JP, Tian B, Pons T, Mishkin M (1997) Serial and parallel processing in rhesus monkey auditory cortex. J Comp Neurol 382:89-103.

Rees A, Green GG, Kay RH (1986) Steady-state evoked responses to sinusoidally amplitude-modulated sounds recorded in man. Hear Res 23:123-133.

Rendall D, Owren MJ, Rodman PS (1998) The role of vocal tract filtering in identity cueing in rhesus monkey (Macaca mulatta) vocalizations. Journal of the Acoustical Society of America 103:602-614.

Schott D (1975) Quantitative analysis of the vocal repertoire of squirrel monkeys (Saimiri sciureus). Zeitschrift für Tierpsychologie 38:225-250.

Schreiner CE, Urbas JV (1986) Representation of amplitude modulation in the auditory cortex of the cat. I. The anterior auditory field (AAF). Hear Res 21:227-241.

Schreiner CE, Langner G (1988) Periodicity coding in the inferior colliculus of the cat. II. Topographical organization. J Neurophysiol 60:1823-1840.

Shannon RV, Zeng FG, Kamath V, Wygonski J, Ekelid M (1995) Speech recognition with primarily temporal cues. Science 270:303-304.

Steinschneider M, Reser DH, Fishman YI, Schroeder CE, Arezzo JC (1998) Click train encoding in primary auditory cortex of the awake monkey: evidence for two mechanisms subserving pitch perception. J Acoust Soc Am 104:2935-2955.

Sudakov K, MacLean PD, Reeves A, Marino R (1971) Unit study of exteroceptive inputs to claustrocortex in awake, sitting, squirrel monkey. Brain Res 28:19-34.

Terhardt E (1974) On the perception of periodic sound fluctuations (roughness). Acustica 20:210-214.

Tian B, Rauschecker JP (2004) Processing of frequency-modulated sounds in the lateral auditory belt cortex of the rhesus monkey. J Neurophysiol 92:2993-3013.

Wang X, Sachs MB (1995) Transformation of temporal discharge patterns in a ventral cochlear nucleus stellate cell model: implications for physiological mechanisms. J Neurophysiol 73:1600-1616.

Wang X, Lu T, Snider RK, Liang L (2005) Sustained firing in auditory cortex evoked by preferred stimuli. Nature 435:341-346.

Wang X, Lu T, Bendor D, Bartlett E (2008) Neural coding of temporal information in auditory thalamus and cortex. Neuroscience 157:484-494.

Whitfield IC (1980) Auditory cortex and the pitch of complex tones. J Acoust Soc Am 67:644-647.

Zatorre RJ (1988) Pitch perception of complex tones and human temporal-lobe function. J Acoust Soc Am 84:566-572.

Zheng Y, Escabi MA (2008) Distinct roles for onset and sustained activity in the neuronal code for temporal periodicity and acoustic envelope shape. J Neurosci 28:14230-14244.

CHAPTER IV

A COMPARISON OF CORRELATED NEURAL ACTIVITY WITHIN AND ACROSS MULTIPLE AREAS OF AUDITORY CORTEX IN THE AWAKE MACAQUE

4.1 Abstract

In order to refine and extend current theories of primate auditory cortical organization, there is a need to characterize neural synchrony, or correlations, between pairs of neurons both within and across areas. Such pairwise correlations are often interpreted as a measure of 'effective' connectivity. In this study, we measured correlations in seven areas of auditory cortex in core, belt and parabelt, and find that correlation measures in within-area pairs do not differ with area, even for areas at different regional levels. We measured correlation in three sets of across-area pairs and find that they are lower than those measured between areas, but are not different from each other. Additionally, correlation strength does not generally change from spontaneous to stimulation conditions, except for tone stimulation. Correlation lags of within-area pairs were all zero, as was the core-core across-area pair. Additionally, there was only weak evidence for a bias towards nonzero lags in the two sets of core-belt across-area pairs. Awake macaque auditory cortex appears to be weakly, yet isotopically correlated, observations which support previous studies of functional assemblies in the auditory cortex of the anesthetized cat.

4.2 Introduction

The current working model of primate auditory cortex designates three interconnected regions (core, belt, and parabelt) which are thought to represent different levels of processing. Each region is subdivided into multiple areas, distinguished by unique anatomical and physiological profiles (for schematic, see figure 2-1 of chapter 2). We are interested in characterizing the direction and flow of information within and between regions and areas to better understand auditory cortical processing of sounds. One important aspect of this is the characterization of neural synchrony, or correlations, between pairs of neurons both within and across areas. Such pairwise correlations are often interpreted as a measure of 'effective' connectivity (e.g Dickson and Gerstein, 1974; Toyama et al., 1981a, b; Frostig et al., 1983; Ts'o et al., 1986; Aertsen et al., 1989; Stevenson et al., 2008). Correlations in auditory cortex have been best described in the anesthetized cat, where both within and across area correlations have been measured (Dickson and Gerstein, 1974; Frostig et al., 1983; Espinosa and Gerstein, 1988; Eggermont, 1992; Eggermont et al., 1993; Eggermont, 1994; Eggermont and Smith, 1995; Brosch and Schreiner, 1999; Eggermont, 2000; Miller et al., 2001b; Miller et al., 2001a; Valentine and Eggermont, 2001; Tomita and Eggermont, 2005; Eggermont, 2006). In the primate, a few studies have looked at correlation in A1 (Vaadia and Abeles, 1987; Ahissar et al., 1992; deCharms and Merzenich, 1996; Ahissar et al., 1998; Bieser, 1998; Brosch et al., 2002; Brosch and Scheich, 2002), but there is an incomplete understanding of the correlation within other areas and between different areas of primate auditory cortex, especially in the cortex of awake animals (Brosch and Scheich, 2002).

Thus, in an effort to better understand the interactions between multiple areas of awake primate auditory cortex, we characterize correlations of pairs of neurons both under different kinds of stimulation (tones, noise, temporally modulated noise) and under silence (spontaneous). We are interested in whether within-area correlations differ between areas and between regions. Also, we are interested in whether these correlations within areas are stronger than between areas, and whether they are affected by stimulus condition or presence. Lastly, we look for any evidence of correlation lags in across-region pairs (i.e. adjacent core-belt). Correlation lags are often interpreted as flow from one area to another (reviewed in: Ts'o et al., 1986; see also: Perkel et al., 1967a, b; Moore et al., 1970; Bryant et al., 1973; Miller et al., 2001b) and would be supporting evidence for a processing hierarchy.

We measured correlations in seven areas of auditory cortex in core, belt and parabelt, and find that correlation measures in within-area pairs do not differ with area, even for areas at different regional levels. We measured correlation in three sets of across-area pairs and find that they are lower than those measured between areas, but are not different from each other. Additionally, correlation strength does not generally change from spontaneous to stimulation conditions, except for tone stimulation. Correlation lags of within-area pairs were all zero, as was the core-core across-area pair. Additionally, there was only weak evidence for a bias towards nonzero lags in the two sets of core-belt across-area pairs.

4.3 Materials and Methods

General surgical procedures, histological processing, anatomical reconstruction, and experimental methods have been reported previously (see chapter 2), but details pertinent to this investigation are included below.

Animal subjects

Two adult macaque monkeys SP and DY were used for neural recordings (SP male bonnet macaque (*Macaca radiata*) 10.0 kg, and DY female rhesus macaque (*Macaca mulatta*) 7.0 kg). Animals were housed in an AAALAC-accredited facility under supervision of laboratory and veterinary staff. All animal care and experimental procedures were in accordance with the U.S. National Institutes of Health *Guide for the care and use of laboratory animals*, under a protocol approved by the Vanderbilt Institutional Animal Care and Use Committee.

Stimulus generation and neurophysiological acquisition

Stimulus generation and delivery. Recording sessions were conducted in a double walled chamber (Industrial Acoustics Corp, NY) that attenuated sounds, particularly at the mid to high frequencies. Acoustic stimuli were generated by Tucker-Davis technologies (TDT, Gainesville, FL) System II hardware and software (SigGen), controlled by a custom software interface between the stimulus generation and acquisition systems. Stimuli were delivered using Beyer DT911 insert earphones (range 0.1-25.0 kHz) coupled to custom earmolds in both ears.

Stimuli. All stimuli were delivered diotically. Descriptions are below:

Tones. Pure tones of 50 ms duration had a 5 ms cosine^2 ramp at onset and offset, and were calibrated to 60 dB SPL. The center frequency of these tones ranged from 0.3-21.0 kHz in 1/3 octave steps (24 frequencies). Each frequency was presented in random order 10 times, interleaved with other stimuli (e.g. clicks, noise, 45dB SPL tones) with a jittered interonset interval of approximately 1000 ms.

Wideband noise. Gaussian white noise bands of 250 ms duration had a 5 ms cosine^2 ramp at onset and offset, and were calibrated to 60 dB SPL. They were presented 30 times, interleaved with other stimuli, with a jittered interonset interval of approximately 1000 ms.

Amplitude modulated noise. AM noise was constructed using Gaussian white noise convolved with a sine wave of 100% depth, yielding sinusoidally amplitude modulated white noise. Twenty temporal modulation frequencies ranged from 3.1-957 Hz. The duration of these stimuli was 1000 ms, calibrated to 50 dB SPL, with a 5 ms cosine^2 ramp at onset and offset. Each modulation frequency was presented 10 times with a jittered interonset interval of approximately 3000 ms, randomly interleaved with other stimulus types in the battery.

Spontaneous. To measure spontaneous correlation, approximately 1 minute of neural activity recorded in silence was divided into 35 ‘trials’ of 1000 ms.

Electrophysiological recording. Electrode penetrations were made through a recording grid 15 mm wide with 1 mm spacing which fit over the implanted chamber (Crist Instruments, Hagerstown MD). This ensured a replicable and roughly perpendicular trajectory through most parts of the superior temporal plane corresponding

to the caudal two-thirds of auditory cortex. After a local anesthetic (0.13% bupivacaine and 0.5% lidocaine in sterile saline) was topically applied and then removed, a sharpened stainless steel guide tube was used to puncture through the dura. The use of a guide tube also ensured that the penetration ran parallel to the recording chamber. One to two tungsten microelectrodes (2-4 MOhm, FHC, Bowdoin, MA) aligned roughly mediolaterally were advanced through somatosensory cortices and into auditory cortex using manual microdrives (Narishige, Tokyo, Japan).

From the first auditory responses until the end of auditory-responsive cortex, all isolated neurons, irrespective of responsiveness, were tested with all or most of the stimulus battery to avoid biasing the sample. In between isolations, the microdrives were moved at least 200 μm to avoid resampling units. For most runs, we recorded through all layers until the white matter was reached. We assigned a relative cortical depth to each penetration by normalizing the recording depth with respect to the first auditory responsive hash, presumably from the first layer or two of auditory cortex. While unequivocal laminar depths cannot be established, it is likely that the majority of recorded neurons came from the middle and upper layers, consistent with the cytoarchitecture of auditory cortex (Hackett, 2010). During recording sessions the monkey sat quietly alert and was continuously monitored via closed-circuit television. Multichannel spike and local field potential (LFP) recordings were acquired with a 64-channel system that controls amplification, filtering and related parameters (Many Neuron Acquisition Processor, Plexon Inc, Dallas, TX). Both signals were referenced to ground. Spike signals were amplified (100x), filtered (150-8800 Hz), and digitized at 40 kHz. The signal was further DC-offset corrected with a low-cut filter (0.7 Hz). To ensure

timing precision between stimulus delivery and data acquisition, the Plexon software interfaced with the stimulus delivery system (Tucker Davis Technologies) and both systems were controlled by custom software (SGPlay, provided by Peter Yang).

Spikes were sorted online for all channels using real-time window discrimination. Digitized waveforms and timestamps of stimulus events were also saved for final offline analysis and sorting (Plexon offline sorter), and graded according to isolation quality (single or multi units). Neural pairs that contained single or multi units, or both, were analyzed in this study. Multi units often show higher correlation values than single units, but multi unit and single unit correlations are themselves positively correlated (but not in a linear fashion; Eggermont, 2000; Tomita and Eggermont, 2005; Eggermont, 2007). Thus we chose to combine pairs across both single and multi units. We also replicated the analyses restricted to only single unit pairs and found that correlation values and percentages were only slightly lower, and all the trends were preserved (see results).

Histology and identification of cortical areas

Since electrophysiological signatures have yet to be determined for the majority of auditory cortex, it was necessary to anatomically reconstruct cortex for precision in determining electrode locations. Using information from the lesions, electrode tracks, and histological reconstruction of areas, areal locations of electrodes were determined and confirmed by electrophysiological properties.

Neurophysiological data analysis

Analysis code to calculate the joint peristimulus time histogram (JPSTH) was a set of Matlab scripts (MathWorks, Natick, MA) provided by Pierre Pouget of the Schall Laboratory (Vanderbilt University). All other analyses were done using in-house Matlab scripts.

Pairwise spike correlation measured via the joint peristimulus time histogram (JPSTH). Correlation between two spike trains was measured using the joint peristimulus time histogram (JPSTH) (Aertsen et al., 1989). This method has been described in detail before (Aertsen et al., 1989; Brody, 1999a), and has been used to study auditory cortical correlations in awake macaque (Ahissar et al., 1992) and anesthetized cat (Eggermont, 1994). In brief, this method determines bin by bin covariance of two spike trains, with bins ranging over all possible temporal offsets (lags) of the spike trains. Each element in this covariance matrix is then normalized by the product of the standard deviations of each spike train from that bin to produce the normalized JPSTH matrix, whose values can be treated as a coefficient of correlation and range from -1 to +1 (see figure 4-1). Two measures can be taken from this: the coincidence histogram and the crosscorrelogram. The coincidence histogram is the sum from lag -5 to +5 on either side of the lag 0 bin diagonal, and measures the correlation over trial time. We did not formally analyze correlation time course in this study, but used it to corroborate that, regardless of stimulation, correlations are present at many time points through the length of the trial. The crosscorrelogram is the average correlation value for each lag summed along all timepoints of the trial. Peak correlation was the highest value in a window between +/-50 ms of lag zero. This time window was chosen

because the width of the correlation in auditory cortex is reported to rarely be more than +/-50 ms (Ahissar et al., 1998).

To correct for increases in correlation due to concomitant increases in firing rate we used a shuffle correction. In this, we repeated the JPSTH with a shuffled trial order for one of the neurons. Significance of the crosscorrelogram peak (peak correlation) was determined twofold. Only pairs whose peak that was both 1) 2 SD above the average shuffled crosscorrelogram in the time window +/- 50 ms (e.g. Reed et al., 2008; Ghoshal et al., 2009) and 2) 2 SD above zero in the time window +/- 50 ms were considered significant (Brody, 1999a). The time at which this peak correlation occurred is the time lag, which relates the timing of the correlated activity. In the example in figure 4-1, neuron 1 generally fires before neuron 2, giving a time lag of -5 ms. It is important to note that regardless of the methods of correction, correlation measures are not conclusive evidence for nonrandom associations of activity, and a number of corrections measures have been proposed (e.g. Perkel et al., 1967b; Gerstein and Perkel, 1969, 1972; Brody, 1999a, b; Smith and Kohn, 2008). On the other hand, it has been argued that no correction should be used since it is neurally implausible (Eggermont, 2007). For our purposes, we choose to use the normalized, shuffle corrected JPSTH in these experiments since it corrects for correlations due to stimulus locked firing rate increases and also allows for an evaluation of correlation over time.

For all stimuli, the spike trains were analyzed from stimulus onset to 150 ms after stimulus offset. This window allowed for the end of the response for even sluggish neurons. These spike trains were binned by 5 ms, a bin size that is sufficiently small to examine correlations over short time scales. Smaller and larger bin sizes were examined

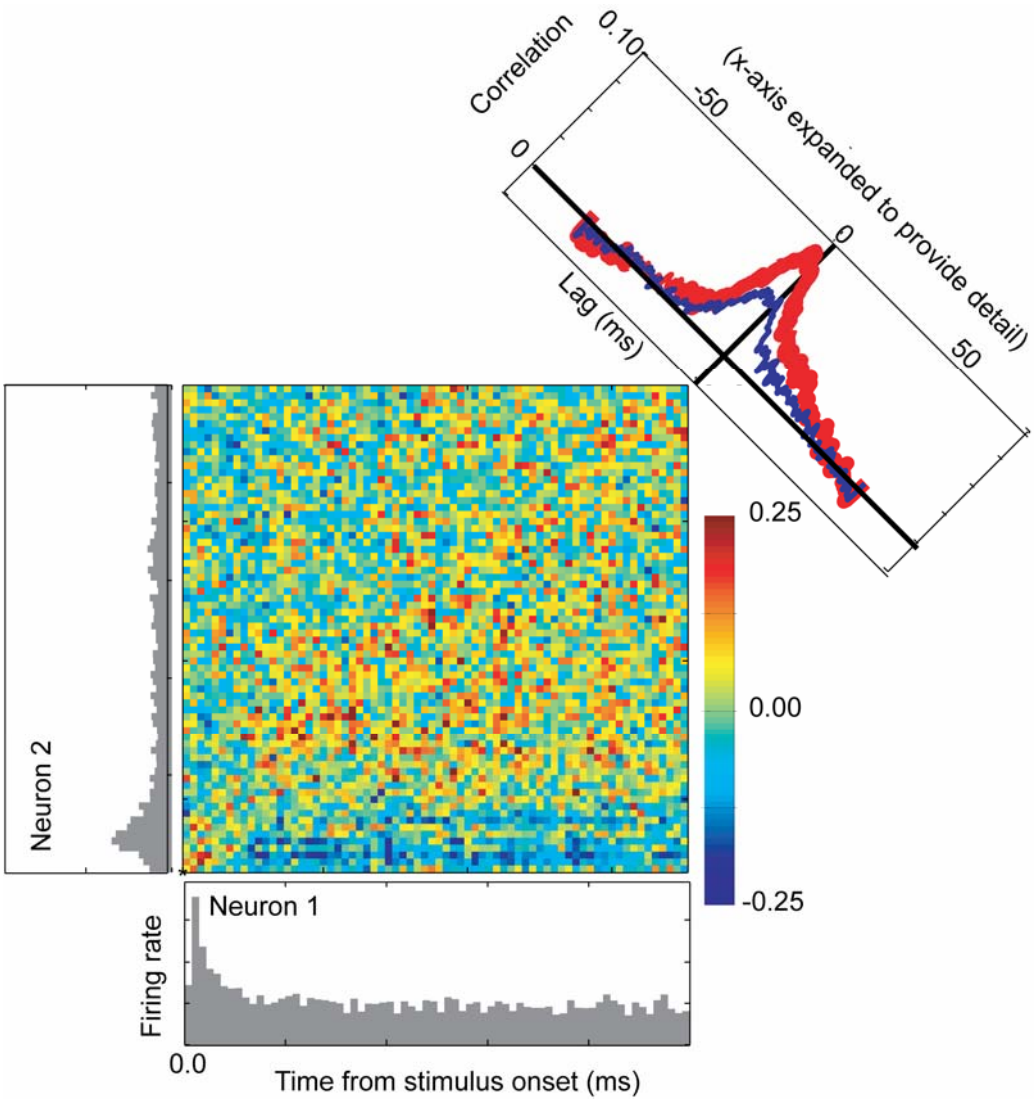

Figure 4-1. The calculation of the JPSTH: an illustrative example (see methods). PSTHs of neuron 1 and neuron 2 are the gray histograms in the x and y axis respectively. The normalized JPSTH matrix is the color plot between the PSTHs, where red values are positive correlation and blue are negative correlations (color scalebar of correlation values to the right). The crosscorrelogram, calculated by collapsing across all timebins of the trial from lag -50 to +50, is shown to the top right, with x-axis expanded to show detail. Normalized crosscorrelogram is in red (thick line) and shuffled is superimposed in blue (thin line). Here, the peak correlation of 0.09 is significant and is located at lag -5 ms, where neuron 1 firing leads neuron 2 by about 5 ms.

(2 ms and 10 ms bins); while the magnitude of peak correlation values covary with

binsize, the percent that are deemed significant does not change, and trends across areas

do not change. Similar trends of correlation values with bin size have been previously described (Eggermont, 1992). In this study we only analyze positive correlations, as negative correlations were rare.

4.4 Results

In total, within-area correlations from 7 areas were examined. These included pairs of neurons from core A1 and R, medial belt MM, lateral belt ML and AL, and parabelt CPB and RPB. The vast majority of these within-area pairs were from the same electrode. In addition, three types of across-area correlations were examined: one within core A1-R, and two from core to lateral belt A1-ML and R-AL. These were all collected from two different electrodes spaced between 3-7 mm apart. Data from other areal combinations did not yield enough pairs to be included in the analyses. Total pair counts and yield of the number of significant pairs examined are listed in table 4-1. For convenience, number of single unit only pairs is also listed.

Figure 4-2 shows the percent significant correlation and mean correlation values for the within and cross area pairs under spontaneous conditions (silence). A number of trends are evident. First, there was a difference between the within-area pairs and the across-area pairs. The probability of significance for the within-area pairs (left side) is generally higher than the across-area pairs (right side). This is true for the spontaneous condition as well as for all three stimulation conditions (noise, tones, and AM noise), confirmed by a t-test ($p<0.01$ for all four conditions). Within-area correlation strength (mean correlation) is also higher for the within-area pairs than the across-area pairs.

Table 4-1. Counts of pairs analyzed and significant for all areas and all stimulus conditions examined. For reference, counts of single unit only pairs are also listed.

			Silence		Noise		AM Noise		Tones	
			all	significant	all	significant	all	significant	all	significant
All pairs	A1	A1	255	187	274	151	258	154	266	89
	R	R	158	130	208	114	165	143	156	60
	MM	MM	106	59	172	98	112	61	139	27
	ML	ML	79	59	105	69	81	50	75	29
	AL	AL	77	54	89	45	81	59	67	15
	CPB	CPB	36	28	67	42	39	34	51	13
	RPB	RPB	104	72	102	61	107	73	94	29
	A1	R	48	17	53	18	48	9	39	2
	A1	ML	95	49	139	52	98	10	111	10
	R	AL	73	27	85	25	74	19	72	3
Single unit pairs	A1	A1	79	45	74	31	77	33	70	23
	R	R	40	29	59	23	44	35	41	24
	MM	MM	36	16	63	29	40	15	53	6
	ML	ML	28	20	35	19	28	18	26	15
	AL	AL	23	11	22	7	26	17	13	2
	CPB	CPB	12	11	27	14	13	12	18	8
	RPB	RPB	35	22	28	11	37	20	25	8
	R	A1	25	9	26	6	26	6	21	1
	ML	A1	54	25	82	29	58	7	59	3
	AL	R	36	8	33	6	38	5	32	2

Again, this is true for the spontaneous, noise, and AM noise conditions (t-test $p< 0.01$ for these three conditions). Though similar trends were evident in the tone condition, statistical significance was not met. Second, there was not a difference in within-area probability of significance or correlation strength by region or caudorostral level (two 3x2 region x caudorostral level ANOVA, $p >0.05$ both factors). Third, there was not a difference in across-area correlation probability of significance or strength between the across-area pairs from within a region (core A1-R) and the across-area pairs between regions (core-belt A1-ML and R-AL) (two t-tests, $p > 0.05$). Figure 4-3 shows results for the spontaneous condition where the pairs are restricted to single units only. Note that the trends are still very similar. This is true for the other stimulation conditions as well (not shown).

To examine the effects of stimulus type on percent and correlation strength we

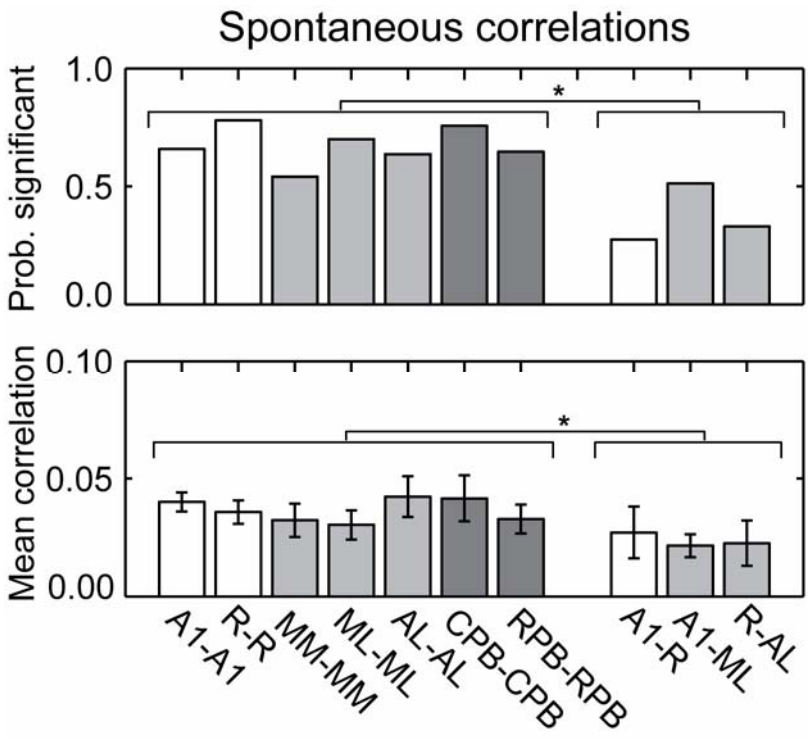

Figure 4-2. Correlation measures (probability of significance and mean correlation) by for the within-area pairs (left side) and across-area pairs (right side). For ease of comparison, shading denotes areas within a regional level or similar cross regional type (e.g. core-belt A1-ML and R-AL). Asterisks above groups indicate comparisons that were different at $p < 0.01$.

looked at measures of correlation with stimulus type, separated by within-area and across-area pairs. The left side of figure 4-4 shows the probability of significant correlation and mean correlation values for the within-area pairs. Since the within-area effects were consistent for all areas, we could collapse across them. The spontaneous condition showed the most pairs with a significant correlation, with slightly less for AM noise, less still for noise and the least number of significant pairs for pure tone stimulation. With regard to strength of correlation, the tones showed the highest strength of correlation, while the others had approximately equal magnitudes. Only the tones were different than spontaneous (multiple t-test, Bonferonni corrected $p < 0.05$).

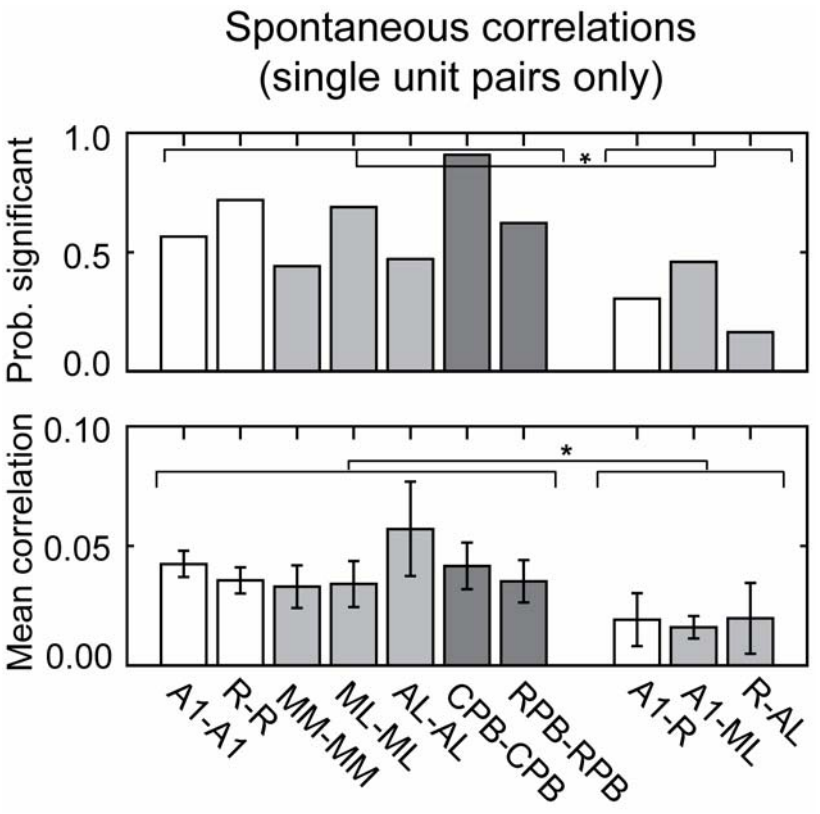

Figure 4-3. Correlation measures (probability of significance and mean correlation) for the within-area pairs (left side) and across-area pairs (right side), restricted to single unit pairs. Conventions preserved from figure 4-2. Asterisks above groups indicate comparisons that were different at $p < 0.01$.

The right side of figure 4-4 shows the probability of significant correlation and mean correlation values for the across-area pairs. Since the across-area effects were consistent for all comparisons, we could collapse across them. Similar to the within-area pairs, the spontaneous condition showed the most pairs with a significant correlation, with slightly less for AM noise, slightly less for wideband noise and the least pairs for pure tone stimulation. With regard to strength of correlation, again the tones showed the highest strength of correlation, and the others had approximately the same strengths. Only

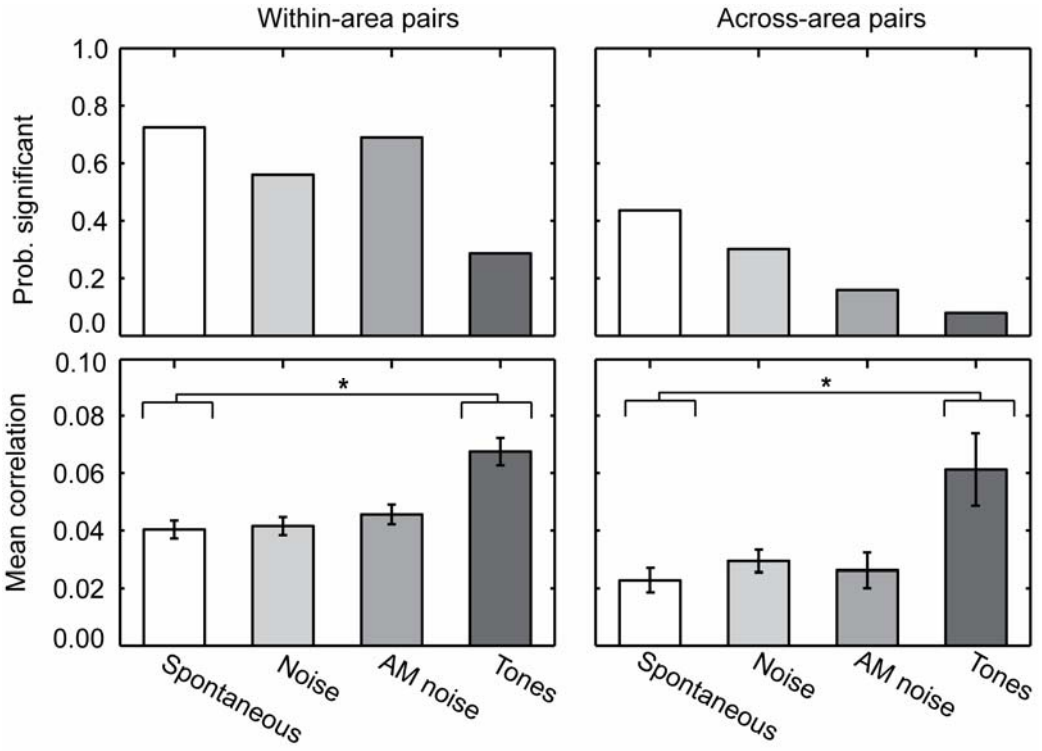

Figure 4-4. Correlation measures by stimulation type. Left side, probability of significance and mean correlation for the within-area pairs. Right side, probability of significance and mean correlation for the across-area pairs. For ease of comparison each stimulation type is shaded differently. Asterisks above groups indicate comparisons that were different at $p < 0.01$.

the tones were different than spontaneous (multiple t-test, Bonferonni corrected $p < 0.05$). When restricted to single units only the same trends were seen (data not shown). Correlation strength patterns also remain the same if the significance criteria is lifted, so these patterns are not due to the corrections used. Correlation strength patterns are also not due to firing rate differences among the stimuli: the overall firing rates for noise tend to be equal to or greater then overall firing rates for tones (data not shown).

Lastly, we looked at the distribution of the lag time of peak correlation coefficients of the within-area pairs and the across-area pairs. The left side of figure 4-5

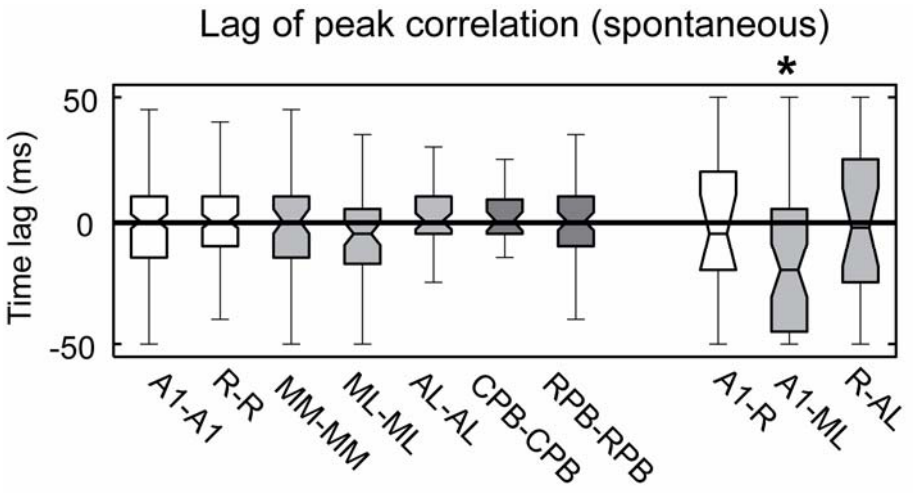

Figure 4-5. Boxplots of peak correlation lag distributions for the within-area pairs (left side) and across-area pairs (right side). The box denotes the upper quartile, median, and lower quartile of the distribution. Whiskers denote the extent of the rest of the data. Notches indicate an estimate of the uncertainty about the median. For ease of comparison, conventions preserved from figure 4-2. Asterisks above groups indicate comparisons that were different at $p < 0.01$.

shows distributions of time lags of the within-area pairs for the spontaneous condition. The distributions of peak correlation coefficients for the within-area pairs were centered around zero and were not different than zero. This was true for all four conditions (spontaneous, tones, noise, and AM noise: t-test for all area-condition pairs, $p < 0.01$). The across-area pairs are shown in the right side of figure 4-5. Due to small numbers of pairs, lags for only the spontaneous and noise burst conditions could be examined. The distribution of lags for the within-region pairs (core A1-R) was not different than zero (t-test $p < 0.01$); this was also true for the noise condition. For the pairs that cross regions the results were more mixed. In the spontaneous condition, there was a tendency for neurons in the belt areas to fire after neurons in the adjacent core areas, but only the distribution of A1-ML lags was significantly different from zero (t-test, $p < 0.01$). This effect was not consistent, however. In the noise condition both distributions tended

towards the opposite effect (not shown), where neurons in the belt areas led the adjacent core area, but this trend was not significant at the $p < 0.01$ level.

4.5 Discussion

We measured pairwise correlations across seven areas of auditory cortex in core, belt and parabelt, and find that, despite known areal differences in neurophysiological responses and source of thalamic and cortical inputs (see earlier chapters, also reviewed in Hackett, 2010), correlation measures do not differ for within-area pairs, even between areas at different regional levels or caudorostral levels. We measured correlation in three sets of across-area pairs and found that they are lower than those measured within areas, but were not different from each other. These findings are consistent with what has been found in auditory cortex of anesthetized cats (Eggermont, 2000), who also found that correlation strength did not differ for within-area pairs from different areas. Similar to our study, Eggermont also found that correlation was generally stronger in the within-area, pairs recorded from the same electrode than in the across-area pairs. Additionally, this pattern held true even for within-area pairs recorded from different electrodes, though correlation strength was weaker than for same electrode pairs. Thus, the weaker correlation in the across-area pairs seen in this study is not simply an artifact of recording from separate electrodes, though distance does have an effect on correlation.

Additionally, mean correlation strength does not generally change from spontaneous to stimulation conditions for most stimuli, except for an increase in mean correlation during tone stimulation. Tones are also the least probable to show a

significant correlation (see figure 4-4). The increase during tone stimulation is not due to higher firing rates in this condition or the use of significance criteria. This seems to suggest that during tone stimulation a small percentage of neurons are highly correlated compared to the spontaneous or noise conditions, where a higher percentage is more weakly correlated. It is unclear exactly why this is true, but the trend holds across all areas and regional levels and even for the across-area pairs. The tones are also the shortest duration stimulus used, but stimulus duration is an unlikely explanation given that the noise is a shorter stimulus than the AM noise and they exhibit similar correlation measures. Further analyses examining the time course of the correlation (i.e. coincidence histogram) or restricting the correlation measures to a shorter window for other stimuli may help resolve this. If robust, these results suggest that functionally connected networks in auditory cortex can behave differently for different stimuli, as has been suggested by a number of studies (Dickson and Gerstein, 1974; Espinosa and Gerstein, 1988; Ahissar et al., 1992; Eggermont, 1994; Brosch and Schreiner, 1999; Eggermont, 2006), and even behavioral state (Vaadia and Abeles, 1987). It may be surprising that measures of average correlation in the spontaneous condition were not different from those for the wideband stimulus conditions. However, evidence for this is mixed: spontaneous conditions has been shown to have both higher (especially for widely separated pairs) (Eggermont, 1994, 2000) and lower (Brosch and Schreiner, 1999) correlation strength than stimulation conditions.

In the present study, the distribution of correlation lags of within-area pairs are centered around zero. This is consistent with what has been seen previously for within-area pairs, particularly when recorded from the same electrode (Dickson and Gerstein,

1974; Frostig et al., 1983; Eggermont, 1992, 1994; Brosch and Schreiner, 1999; Eggermont, 2000; Brosch et al., 2002; Brosch and Scheich, 2002). This may indicate that most within-area correlations are driven by common inputs whose origin could be either thalamic or cortical (see Smith and Kohn, 2008). This explanation is consistent with the zero-centered lags within core, where the members of the across-area (A1-R) pair both receive inputs from the same thalamic nuclei, though this explanation cannot account for the latency results that suggest that input and neural response timing may be different between A1 and R (see Chapter II).

Based on anatomical and physiological evidence of information flow along the caudorostral and core-belt-parabelt axes, a reasonable prediction would be that correlation lags would also be observed between areas at different hierarchical levels. Such lags have been identified previously between the MGC and A1 in the cat, and used to infer inheritance of features (Miller et al., 2001b; Miller et al., 2001a). We found inconsistent evidence for a bias towards nonzero lags in the two sets of core-belt across-area pairs. This may be consistent with the fact that pairs showing clear evidence of unidirectional functional connectivity are infrequent in the literature (Frostig et al., 1983; Vaadia and Abeles, 1987; Eggermont, 1992; Brosch et al., 2002; Brosch and Scheich, 2002). This may be ascribed to the effects of thalamocortical convergence on auditory cortex, where a greater effect of common inputs could mask direct driving corticocortical peaks in the crosscorrelograms. All areas of auditory cortex receive projections from at least two different medial geniculate nuclei, and any two areas are receiving common input from at least one, and possibly multiple medial geniculate and other thalamic nuclei.

It is generally agreed that common inputs (stimulation or neural) or synaptic interactions can give rise to correlated activity (e.g. Aertsen et al., 1989; Usrey and Reid, 1999). Functional connections based on correlations should be distinguished from anatomical connections, though they are often interpreted as supporting evidence. For example, crosscorrelograms have commonly been interpreted as evidence for synaptic coupling if they have a narrow peak, or for common input if they have a broader peak (Perkel et al., 1967a, b; Moore et al., 1970; see also Bryant et al., 1973; reviewed in: Ts'o et al., 1986). There are important caveats to this interpretation. Correlations are biased and are more sensitive to excitatory than inhibitory effects (Aertsen and Gerstein, 1985). Even with corrections (Perkel et al., 1967b; Brody, 1999b; Smith and Kohn, 2008), it is possible to get correlations without synchrony from trial to trial covariations in latency or excitability (Brody, 1999a). Lastly, even with shared connections between a neuron pair, it is possible to get no correlation (Renart et al., 2010). Instead of assuming that correlations necessarily reflect connectivity, functional connections based on correlation are better thought of as reflecting at least some portion of the dynamic statistical efficacy of neural coupling. This coupling is no doubt predicated on some kind of anatomical connectivity. Our focus in this study has been on implications of correlation for the functional connectivity of auditory cortex, but note that correlation is thought to have important implications for stimulus coding and processing (Malsberg, 1981; Abbott and Dayan, 1999; Gray, 1999; Shadlen and Movshon, 1999; Salinas and Sejnowski, 2001; Rolls et al., 2003; Johnson, 2004; Tabareau et al., 2010; but see Shadlen and Movshon, 1999) and synchrony is also purported to underlie oscillations (Averbeck and Lee, 2004).

In summary, in this study we present evidence that across a large portion of primate auditory cortex, neurons are consistently but weakly connected within areas, and consistently but even more weakly connected across areas. This effective connectivity appears to vary somewhat with simulation condition. Thus, awake macaque auditory cortex appears to be weakly yet isotopically correlated, supporting what has been found in the auditory cortex of the anesthetized cat (Eggermont, 2000, 2006). Though there are important caveats to the interpretation of correlations, this suggests that there are large weakly correlated assemblies both within and across areas of auditory cortex (Eggermont, 2006). The weak synchronization of these assemblies allows for independence of processing, but an imbalance in this synchronization is thought to underlie clinical conditions such as tinnitus and even epilepsy (Eggermont and Roberts, 2004; Eggermont, 2007). However, within reasonable ranges, these assemblies may dynamically change, allowing for flexible stimulus processing using population codes over distinct but overlapping neural assemblies within and across the same areas. Further anatomical and physiological studies are needed to evaluate this and shed light on the source and network architecture that could underlie these assemblies.

4.6 References

Abbott LF, Dayan P (1999) The effect of correlated variability on the accuracy of a population code. Neural Comput 11:91-101.

Aertsen AM, Gerstein GL (1985) Evaluation of neuronal connectivity: sensitivity of cross-correlation. Brain Res 340:341-354.

Aertsen AM, Gerstein GL, Habib MK, Palm G (1989) Dynamics of neuronal firing correlation: modulation of "effective connectivity". J Neurophysiol 61:900-917.

Ahissar E, Abeles M, Ahissar M, Haidarliu S, Vaadia E (1998) Hebbian-like functional plasticity in the auditory cortex of the behaving monkey. Neuropharmacology 37:633-655.

Ahissar M, Ahissar E, Bergman H, Vaadia E (1992) Encoding of sound-source location and movement: activity of single neurons and interactions between adjacent neurons in the monkey auditory cortex. J Neurophysiol 67:203-215.

Averbeck BB, Lee D (2004) Coding and transmission of information by neural ensembles. Trends Neurosci 27:225-230.

Bieser A (1998) Processing of twitter-call fundamental frequencies in insula and auditory cortex of squirrel monkeys. Exp Brain Res 122:139-148.

Brody CD (1999a) Correlations without synchrony. Neural Comput 11:1537-1551.

Brody CD (1999b) Disambiguating different covariation types. Neural Comput 11:1527-1535.

Brosch M, Schreiner CE (1999) Correlations between neural discharges are related to receptive field properties in cat primary auditory cortex. Eur J Neurosci 11:3517-3530.

Brosch M, Scheich H (2002) Neural representation of sound patterns in the auditory cortex of monkeys. In: Primate Audition: Ethology and Neurobiology (Ghazanfar A, ed), pp 151-176. London: CRC Press.

Brosch M, Budinger E, Scheich H (2002) Stimulus-related gamma oscillations in primate auditory cortex. J Neurophysiol 87:2715-2725.

Bryant HL, Jr., Marcos AR, Segundo JP (1973) Correlations of neuronal spike discharges produced by monosynaptic connections and by common inputs. J Neurophysiol 36:205-225.

deCharms RC, Merzenich MM (1996) Primary cortical representation of sounds by the coordination of action-potential timing. Nature 381:610-613.

Dickson JW, Gerstein GL (1974) Interactions between neurons in auditory cortex of the cat. J Neurophysiol 37:1239-1261.

Eggermont JJ (1992) Neural interaction in cat primary auditory cortex. Dependence on recording depth, electrode separation, and age. J Neurophysiol 68:1216-1228.

Eggermont JJ (1994) Neural interaction in cat primary auditory cortex II. Effects of sound stimulation. J Neurophysiol 71:246-270.

Eggermont JJ (2000) Sound-induced synchronization of neural activity between and within three auditory cortical areas. J Neurophysiol 83:2708-2722.

Eggermont JJ (2006) Properties of correlated neural activity clusters in cat auditory cortex resemble those of neural assemblies. J Neurophysiol 96:746-764.

Eggermont JJ (2007) Correlated neural activity as the driving force for functional changes in auditory cortex. Hear Res 229:69-80.

Eggermont JJ, Smith GM (1995) Separating local from global effects in neural pair correlograms. Neuroreport 6:2121-2124.

Eggermont JJ, Roberts LE (2004) The neuroscience of tinnitus. Trends Neurosci 27:676-682.

Eggermont JJ, Smith GM, Bowman D (1993) Spontaneous burst firing in cat primary auditory cortex: age and depth dependence and its effect on neural interaction measures. J Neurophysiol 69:1292-1313.

Espinosa IE, Gerstein GL (1988) Cortical auditory neuron interactions during presentation of 3-tone sequences: effective connectivity. Brain Res 450:39-50.

Frostig RD, Gottlieb Y, Vaadia E, Abeles M (1983) The effects of stimuli on the activity and functional connectivity of local neuronal groups in the cat auditory cortex. Brain Res 272:211-221.

Gerstein GL, Perkel DH (1969) Simultaneously recorded trains of action potentials: analysis and functional interpretation. Science 164:828-830.

Gerstein GL, Perkel DH (1972) Mutual temporal relationships among neuronal spike trains. Statistical techniques for display and analysis. Biophys J 12:453-473.

Ghoshal A, Pouget P, Popescu M, Ebner F (2009) Early bilateral sensory deprivation blocks the development of coincident discharge in rat barrel cortex. J Neurosci 29:2384-2392.

Gray CM (1999) The temporal correlation hypothesis of visual feature integration: still alive and well. Neuron 24:31-47, 111-125.

Hackett TA (2010) Information flow in the auditory cortical network. Hear Res.

Johnson DH (2004) Neural population structures and consequences for neural coding. J Comput Neurosci 16:69-80.

von der Malsberg (1981) The correlation theory of brain function. MPI Biophysical Chemistry, Internal Report 81-2. In: Reprinted in: Models of Neural Networks (Domany E, JL vh, K S, eds). Berlin: Springer.

Miller LM, Escabi MA, Schreiner CE (2001a) Feature selectivity and interneuronal cooperation in the thalamocortical system. J Neurosci 21:8136-8144.

Miller LM, Escabi MA, Read HL, Schreiner CE (2001b) Functional convergence of response properties in the auditory thalamocortical system. Neuron 32:151-160.

Moore GP, Segundo JP, Perkel DH, Levitan H (1970) Statistical signs of synaptic interaction in neurons. Biophys J 10:876-900.

Perkel DH, Gerstein GL, Moore GP (1967a) Neuronal spike trains and stochastic point processes. II. Simultaneous spike trains. Biophys J 7:419-440.

Perkel DH, Gerstein GL, Moore GP (1967b) Neuronal spike trains and stochastic point processes. I. The single spike train. Biophys J 7:391-418.

Reed JL, Pouget P, Qi HX, Zhou Z, Bernard MR, Burish MJ, Haitas J, Bonds AB, Kaas JH (2008) Widespread spatial integration in primary somatosensory cortex. Proc Natl Acad Sci U S A 105:10233-10237.

Renart A, de la Rocha J, Bartho P, Hollender L, Parga N, Reyes A, Harris KD (2010) The asynchronous state in cortical circuits. Science 327:587-590.

Rolls ET, Franco L, Aggelopoulos NC, Reece S (2003) An information theoretic approach to the contributions of the firing rates and the correlations between the firing of neurons. J Neurophysiol 89:2810-2822.

Salinas E, Sejnowski TJ (2001) Correlated neuronal activity and the flow of neural information. Nat Rev Neurosci 2:539-550.

Shadlen MN, Movshon JA (1999) Synchrony unbound: a critical evaluation of the temporal binding hypothesis. Neuron 24:67-77, 111-125.

Smith MA, Kohn A (2008) Spatial and temporal scales of neuronal correlation in primary visual cortex. J Neurosci 28:12591-12603.

Stevenson IH, Rebesco JM, Miller LE, Kording KP (2008) Inferring functional connections between neurons. Curr Opin Neurobiol 18:582-588.

Tabareau N, Slotine JJ, Pham QC (2010) How synchronization protects from noise. PLoS Comput Biol 6:e1000637.

Tomita M, Eggermont JJ (2005) Cross-correlation and joint spectro-temporal receptive field properties in auditory cortex. J Neurophysiol 93:378-392.

Toyama K, Kimura M, Tanaka K (1981a) Organization of cat visual cortex as investigated by cross-correlation technique. J Neurophysiol 46:202-214.

Toyama K, Kimura M, Tanaka K (1981b) Cross-Correlation Analysis of Interneuronal Connectivity in cat visual cortex. J Neurophysiol 46:191-201.

Ts'o DY, Gilbert CD, Wiesel TN (1986) Relationships between horizontal interactions and functional architecture in cat striate cortex as revealed by cross-correlation analysis. J Neurosci 6:1160-1170.

Usrey WM, Reid RC (1999) Synchronous activity in the visual system. Annu Rev Physiol 61:435-456.

Vaadia E, Abeles M (1987) Temporal firing patterns of single units, pairs and triplets of units in the auditory cortex. Isr J Med Sci 23:75-83.

Valentine PA, Eggermont JJ (2001) Spontaneous burst-firing in three auditory cortical fields: its relation to local field potentials and its effect on inter-area cross-correlations. Hear Res 154:146-157.

CHAPTER V

DISCUSSION: OVERVIEW OF RESULTS, IMPLICATIONS, AND FUTURE DIRECTIONS

5.1 Overview of Main Findings

Our long term aim is to further define the functional organization of primate auditory cortex, and relate anatomical structure and pathways to neural processing and information flow. In this series of studies, we examined response latencies, temporal tuning measures, and pairwise spike correlations in multiple areas in core, belt, and parabelt of the auditory cortex of the awake macaque. The current working model of primate auditory cortex predicts a hierarchy of processing in two directions: along regional level (core to belt to parabelt) and along a caudorostral direction (within a region). In addition to the questions about direction of flow, we were also interested in extending the primate model to include effective connectivity (measured by correlation strength) within and between areas of auditory cortex.

Differences in auditory response latencies across areas of primate auditory cortex

The first study (Chapter II) investigated latency increases to evaluate hierarchy of flow. Given their obvious significance, areal latencies in primate have been reported and compared between areas before (Vaadia et al., 1982; Bieser and Muller-Preuss, 1996; Recanzone, 2000; Cheung et al., 2001; Kajikawa et al., 2005; Lakatos et al., 2005; Philibert et al., 2005; Bendor and Wang, 2008; Oshurkova et al., 2008; Kusmierek and Rauschecker, 2009; Crum et al., submitted). However, this study represents the first time

that so many areas representing multiple caudorostral levels and all three regional levels have been compared simultaneously, and is the first report of latencies from CL, AL, and RPB, as well as the first report of LFP latencies for RM, MM, R, Al, CL, and RPB. In a survey of ten areas across three regions of the primate auditory cortex, we found that both unit and LFP latencies generally increased as a function of both regional level and caudorostral level, regardless of stimulus type.

It was interesting that the LFP differences between areas, especially along the caudorostral axis, were not as robust as the unit latency differences, as confirmed by a unit-LFP difference analysis, which indicated that the unit latency differences are incompletely accounted for by LFP 'input' differences. This suggested that the rostral areas that have longer unit latencies may also have a longer integration time window to respond. Other than absolute latencies, there were few differences between results from broadband and pure tone responses, despite differences in envelope, duration and bandwidth. This indicated that our results were probably generally reflective of timing information for many ethologically relevant stimuli.

Differences in tuning to temporally modulated sound across areas of primate auditory cortex

The second study (Chapter III) investigated tuning to temporally modulated sounds in neurons across auditory cortex. We collected neural responses from five areas in core, lateral belt, and parabelt to amplitude modulated noise in the awake macaque for two aims. The first was to better characterize modulation frequency tuning across multiple areas of auditory cortex. The second was to evaluate the implications of tuning for hierarchical flow between regions and areas in auditory cortex of the primate. An

influential hypothesis states that temporal modulation frequency tuning decreases as a consequence of variability introduced by successive synaptic delays along the auditory hierarchy (Joris et al., 2004). In primate auditory cortex, such decreases have been reported in samples of areas along a regional level axis (Bieser and Muller-Preuss, 1996; Crum et al., submitted) and weaker trends have been reported along the rostrocaudal axis (Sudakov et al., 1971; Bieser, 1995; Bieser and Muller-Preuss, 1996; Bendor and Wang, 2008), but this study represents one of the first times that tuning measures could be directly compared among so many areas, as well as the first time that LFP tuning was analyzed in R, Al, and RPB.

Entrainment based maximum synchronization and tuning rates were lower in lateral belt and parabelt than in core. This decrease in temporal modulation frequency tuning provides support for hierarchical processing in a regional direction. Surprisingly, we did not see a decrease in tuning measures in a caudorostral direction, the possible reasons for which are discussed below. Temporal tuning measures derived from the LFP support the same patterns. In addition, we saw that for all areas a rate based code covered all the modulation frequencies, demonstrating that a rate code was sufficient to encode the modulation frequencies that cannot be accounted for by temporal measures, particularly at later levels of processing.

Effective connectivity within and across areas of primate auditory cortex

The third study in the series (Chapter IV) characterized correlations of pairs of neurons within and across areas both under different kinds of stimulation (tones, noise, temporally modulated noise) and under no stimulation (spontaneous). Correlations in

auditory cortex have been best described in the anesthetized cat, where both within and across area correlations have been measured (Dickson and Gerstein, 1974; Frostig et al., 1983; Espinosa and Gerstein, 1988; Eggermont, 1992; Eggermont et al., 1993; Eggermont, 1994; Eggermont and Smith, 1995; Brosch and Schreiner, 1999; Eggermont, 2000; Miller et al., 2001b; Miller et al., 2001a; Valentine and Eggermont, 2001; Tomita and Eggermont, 2005; Eggermont, 2006). In the primate, a few studies have looked at correlation in A1 in either awake or anesthetized states (Vaadia and Abeles, 1987; Ahissar et al., 1992; deCharms and Merzenich, 1996; Ahissar et al., 1998; Bieser, 1998; Brosch et al., 2002; Brosch and Scheich, 2002), but correlation within other areas outside of A1 and between different areas and regions of primate auditory cortex, has been rarely studied (except for one notable, but unfortunately nonquantitative, study examining A1-CM correlations (Brosch and Scheich, 2002)).

We measured correlations in seven areas of auditory cortex in core, belt, and parabelt, and found that correlation measures of pairs within the same area do not differ as a function of area, even between areas at different regional levels, despite known differences in response properties, architecture, and connectivity (Hackett, 2010). We measured correlation in three sets of cross area pairs and find that they were lower than those measured between areas, but were not different from each other. Additionally, correlation strength did not generally change from spontaneous to stimulation conditions, except for tone stimulation. Correlation lags of within area pairs were all zero, as was the core-core cross area pair, and there was only weak evidence for a bias towards nonzero lags in the two sets of core-belt cross-area pairs. These results support the conclusions

based in results from cats (Eggermont, 2000, 2007) that auditory cortex is a weakly yet isotopically effectively connected network.

5.2 Implications for the Primate Model and Future Directions

Evidence for flow along the core-belt-parabelt regional axis

What do these results suggest about flow in the primate model? Along the regional core-belt-parabelt axis, there is evidence from both latency differences and temporal tuning to modulation frequencies that suggest a flow of information across core-belt-parabelt regional level. These results are consistent with other studies comparing latencies across levels (Vaadia et al., 1982; Recanzone, 2000; Crum et al., submitted). Though we saw some evidence of flow with nonzero correlation lags in core-belt, correlation peaks whose lag indicated that core led belt were not consistent across stimuli. However, given the different cortical and thalamic inputs to core and belt, it is perhaps unsurprising that we did not consistently see correlation lags that imply core-belt synchronous firing with core leading. These results supplement cortical connectivity patterns that also suggest the serial nature of processing along regional levels (reviewed in introduction).

The notable exception to this core-belt-parabelt flow appears to be the caudal belt areas CM and CL, where latencies were as fast as or faster than neighboring core area A1. This is similar to studies showing that CM latencies were as fast or faster than A1 latencies (Recanzone, 2000; Kajikawa et al., 2005; Lakatos et al., 2005; Oshurkova et al., 2008). Though temporal tuning was not examined in CM and CL in this study, evidence

from marmosets and squirrel monkeys suggest that CM has temporal tuning similar to A1 (Bieser and Muller-Preuss, 1996; Lakatos et al., 2005; Kajikawa et al., 2008) (but see Oshurkova et al., 2008).

A resolution to this apparent paradox may lay in closer examination of the topography of thalamic inputs. Caudal belt, particularly CM and CL, receive projections from an anterior portion of the MGd, the MGad. This region has not been well characterized in primates, but a possibly corresponding structure in cats (see Hackett, 2010) exhibits fast latencies much like the MGv (Imig and Morel, 1984, 1985a, b). Projections from the MGad to both the medial and lateral belt decrease in strength as one progresses rostrally and are almost absent at the level of RM (de la Mothe et al., 2006a; Hackett et al., 2007), which is then characterized by a dense projection from the MGpd. Thus it is possible that the belt receives some of its inputs serially, but that the fastest latencies in the caudal-most portion may be driven by this extremely fast direct thalamic input from MGad. The connections and response properties of the divisions of the MGC need to be better characterized. We suggest that it is the hypothesized lemniscal nature of the MGad input to caudal belt that makes responses in these areas so similar to core A1.

However, the existence of a fast and possibly tonotopic parallel input to caudal belt is difficult to reconcile with an influential lesion study that showed abolishment of tone responses in CM following ablation of A1 (Rauschecker et al., 1997). It is also difficult to reconcile with the wider spectral tuning seen in this area (Rauschecker et al., 1997; Kajikawa et al., 2005; Lakatos et al., 2005), though this may be a function of convergence of narrowly tuned inputs from the core. Clearly more studies are needed to understand the nature of information flow between A1 and caudal belt CM and CL. Also,

more information is needed about the physiological characteristics (i.e. latency) of the different MGC nuclei, and about the specificity and topography of the projections from neurons in these nuclei to different areas of auditory cortex.

How do these results fit with anatomical predictions made for cortical activation timing? Thalamocortical and corticocortical connectivity predicts core, belt, and parabelt latency differences. We indeed observed the predicted latency differences with regional level. This is consistent with the chemoarchitectural gradients with regional level (e.g. Hackett and de la Mothe, 2009). Cytochrome oxidase expression, a marker of metabolic activity often seen in fast cortices and pathways, is most dense in core and least dense in parabelt.

Thus, these decreases in entrainment rates and vector strengths in belt and parabelt are consistent with both the increased synaptic delays introduced in belt and parabelt as well as the convergence of inputs from cortical (core, belt) and thalamocortical (MGd) sources that belt and parabelt share. Because the degree of convergence would not be expected to differ in the belt and parabelt, just in the number of synaptic delays from core, belt-parabelt differences in entrainment would consequently not be expected to be as large as core-belt differences.

Evidence for flow along the caudal to rostral axis

Another striking pattern in this study is that within the same region, rostral latencies are slower than caudal latencies. These latency differences suggest a second axis of flow, in a caudal to rostral direction. These findings are supported by earlier evidence of latency differences along this axis (Bieser and Muller-Preuss, 1996; Bendor

and Wang, 2008; Kusmierek and Rauschecker, 2009). Despite the striking differences in latencies, we did not see temporal tuning differences along this gradient. Though early studies have shown differences in tuning along this axis in squirrel monkey (Sudakov et al., 1971; Bieser, 1995; Bieser and Muller-Preuss, 1996), the differences seen were slight in a later marmoset studies (Bendor and Wang, 2008). It is possible that there may be a gradient for temporal information, but the effect size in this direction is much smaller than the effect size along the regional axis. Additionally, lags for correlated activity A1-R pairs were consistently centered around zero, a result that is also not consistent with direct driving flow in this direction.

Our results suggest that latency differences along this axis appear to be even larger than latency differences along the regional level axis. This result is not immediately predicted by known thalamocortical connectivity patterns. However, chemoarchitecture of the caudal areas indicates that these areas should be very fast. Caudal areas are marked by high myelin density and cytochrome oxidase density, a marker of metabolic activity often seen in fast cortices and pathways (e.g. Hackett and de la Mothe, 2009). Additionally, corticocortical connectivity of some areas is suggestive of feedforward activity in the rostral direction (connections to layer 4) (Fitzpatrick and Imig, 1980; Galaburda and Pandya, 1983), but his has not been demonstrated conclusively for all areas (see de la Mothe et al., 2006b).

Our finding that the differences between LFP and unit latencies are more pronounced in rostral than caudal areas appear to help resolve some of the apparent discrepancy between the anatomical predictions and physiological timing. In rostral areas neuron latencies are much later (compared to caudal areas) than the corresponding LFP

latency , indicating that the units in these area may have a longer integration time window to generate a response, which will result in longer unit latencies in the rostral areas.

The latency and modulation tuning results appear to provide conflicting evidence for a caudorostral flow, but these results can be resolved by a closer examination of what is driving each measure. Decreases in modulation frequency tuning can be due to increases in variability, which can be due to convergence or variability in input timing (i.e. introduced by synaptic delays). Differences in unit latency can be due to input timing or time constants of integration. Within a region, caudal areas appear to be receiving inputs slower than rostral neighbors, and are also slower to generate a response. However, they do not differ dramatically in the amount of convergence and/or variability in their inputs, so changes in temporal tuning measures in the caudorostral direction are more subtle, if detected at all. Similar convergence from MGC nuclei also explains why measures of temporal tuning do not appear to be markedly different between belt and parabelt. These results supplement cortical connectivity patterns that also suggest a flow of processing in the caudorostral direction (reviewed in chapter II).

Predictions about the nature and basis of the caudorostral flow lead to more questions. How does one explain the difference in unit-LFP 'integration time' along the caudorostral direction? More connectional studies need to be done to determine the extent and specificity of the proposed corticocortical within-region feedforward rostral to caudal connections. Additionally, quantitative studies of thalamocortical connectivity are also lacking. Within a region (i.e. core), do these thalamocortical projections differ in the number of inputs, or the location and efficacy of synapses on neural targets? What is the topographic nature of the thamocortical connections within a region? It is already known

that caudal portions of the MGC project to rostral portions of cortex and vice versa (see: Hackett, 2010); does a latency difference exist within a given nucleus of the MGC? It is presently unclear whether the caudorostral latency gradient is due to the nature and specificity of the thalamic inputs from the MGv, cortical properties (local network properties combined with feedforward cortico-cortical convergence), or both. Current work in our lab is actively trying to characterize the neurochemical signatures of the thalamocortical network in an effort to better characterize this system and answer these outstanding questions (Hackett and de la Mothe, 2009).

Effective connectivity in primate auditory cortex and implications for population coding

Despite known areal differences in neurophysiological responses and sources of their thalamic and cortical inputs (see earlier chapters, also reviewed in Hackett, 2010), correlation measures are similar for all within-area pairs examined here, though weak. Weak correlations have been seen in studies of primate A1 (Vaadia and Abeles, 1987; Ahissar et al., 1992; deCharms and Merzenich, 1996; Ahissar et al., 1998; Bieser, 1998; Brosch et al., 2002; Brosch and Scheich, 2002), and these results extend this finding, suggesting that correlations in the awake primate cortex were similar to what has been found in within-area and across-area pairs of the anesthetized cat (Dickson and Gerstein, 1974; Frostig et al., 1983; Espinosa and Gerstein, 1988; Eggermont, 1992; Eggermont et al., 1993; Eggermont, 1994; Eggermont and Smith, 1995; Brosch and Schreiner, 1999; Eggermont, 2000; Miller et al., 2001b; Miller et al., 2001a; Valentine and Eggermont, 2001; Tomita and Eggermont, 2005; Eggermont, 2006).

Crosscorrelograms have commonly been interpreted as evidence for synaptic coupling if they have a narrow peak, or for common input if they have a broader peak (Perkel et al., 1967a, b; Moore et al., 1970; see also Bryant et al., 1973; reviewed in: Ts'o et al., 1986). There are important caveats to this interpretation. Correlations are biased and are more sensitive to excitatory than inhibitory effects (Aertsen and Gerstein, 1985). Even with corrections (Perkel et al., 1967b; Brody, 1999b; Smith and Kohn, 2008), it is possible to get correlations without synchrony from trial to trial covariations in latency or excitability (Brody, 1999a). Lastly, even with shared connections between a neuron pair, it is possible to get no correlation (Renart et al., 2010). Functional connections based on correlations should be distinguished from anatomical connections, though they are often interpreted as supporting evidence. Instead of assuming that correlations necessarily reflect connectivity, functional connections based on correlation are better thought of as reflecting at least some portion of the dynamic statistical efficacy of neural coupling.

With these caveats in mind, these results suggest that auditory cortex is weakly 'functionally' connected within an area, and even more weakly connected between areas. Converging evidence for this comes from anatomical studies of intrinsic connectivity that also suggest there are more connections within an area than to other areas (Lee and Winer, 2005; de la Mothe et al., 2006b; Lee and Winer, 2008). This study suggests that the functional connectivity aspects of the cat model (such as the similarity to a scale-free network) may be applied to the primate model. Characterizing the spatial scale of correlation should help evaluate hypothetical sources of correlated activity, such as common inputs, since thalamic inputs are supposed to operate on a different spatial scale than cortical inputs (for review see: Eggermont, 2007). More studies examining dual

electrode correlations within an area (beyond A1) are needed to understand how correlations may change with spatial proximity.

This weak but isotopic connectivity is interpreted as being able to create functional assemblies both within and across areas of auditory cortex (Eggermont, 2006) that subserve flexible population coding. The weak synchronization of these assemblies allows for dynamic change in effective connectivity within a network, allowing for flexible stimulus processing using population codes over distinct but overlapping neural assemblies within and across the same areas. Functionally connected networks in auditory cortex can behave differently for different stimuli, as has been suggested by a number of studies (Dickson and Gerstein, 1974; Espinosa and Gerstein, 1988; Ahissar et al., 1992; Eggermont, 1994; Brosch and Schreiner, 1999; Eggermont, 2006), and even behavioral state (Vaadia and Abeles, 1987). Thus, does the architecture of these networks change with stimulus type or behavioral state? Clearly, more task-based studies are needed to fully evaluate this claim. Evidence for functional assemblies also has important clinical relevance, as correlated activity outside of the normal dynamic range is thought to underlie clinical conditions such as tinnitus and even epilepsy (Eggermont and Roberts, 2004; Eggermont, 2007).

Implications for the model of primate auditory cortex

This series of studies adds to a growing body of evidence that suggest that auditory cortex can be thought of as a weakly connected network that receives thalamic input from the MGC in four distinct but overlapping parallel streams. Superimposed on this are two gradients of flow within auditory cortex: one in a roughly medial to lateral

direction between regional levels and the other in a caudorostral direction. Auditory cortex is also characterized by neurochemical gradients (Hackett and de la Mothe, 2009) whose functional significance is an active area of study. However, these gradients seem to correspond to at least some aspects of flow, in both a medial to lateral and caudal to rostral direction. Adjacent areas still appear to process sound in very close timescale to each other, so the highly parallel nature of processing in auditory cortex must also be stressed. In short, the proposed bidirectional flow of information in primate model holds, but in the context of highly parallel processing.

Given this evidence for two axes of processing, a question remains: what is the nature and functional importance of these streams? Though we have focused on latencies and temporal tuning in these studies, Evidence from spectral integration also suggests regional flow. Compared to the core, neurons in the belt respond better to sounds with greater spectral complexity such as noise or FM sweeps (Merzenich and Brugge, 1973; Kosaki et al., 1997; Recanzone, 2000; Poremba et al., 2003; Rauschecker and Tian, 2004; Bendor and Wang, 2005; Kajikawa et al., 2005). This is consistent with increased spectral integration, as neurons in the belt areas are thought to receive inputs from a larger set of frequencies, presumably from the core (Rauschecker and Tian, 2004), although thalamic inputs could also contribute to broad tuning.

To better understand the possible function importance of these bidirectional streams, figure 5.1 shows a schematic of primate auditory cortex (panel A) and summary of sources of information about auditory pathways. Pathways implied by results from response latencies are in panel B, spectral tuning in panel C, and temporal tuning in panel D. The regional flow seem to be marked by spectral and temporal integration, whereas

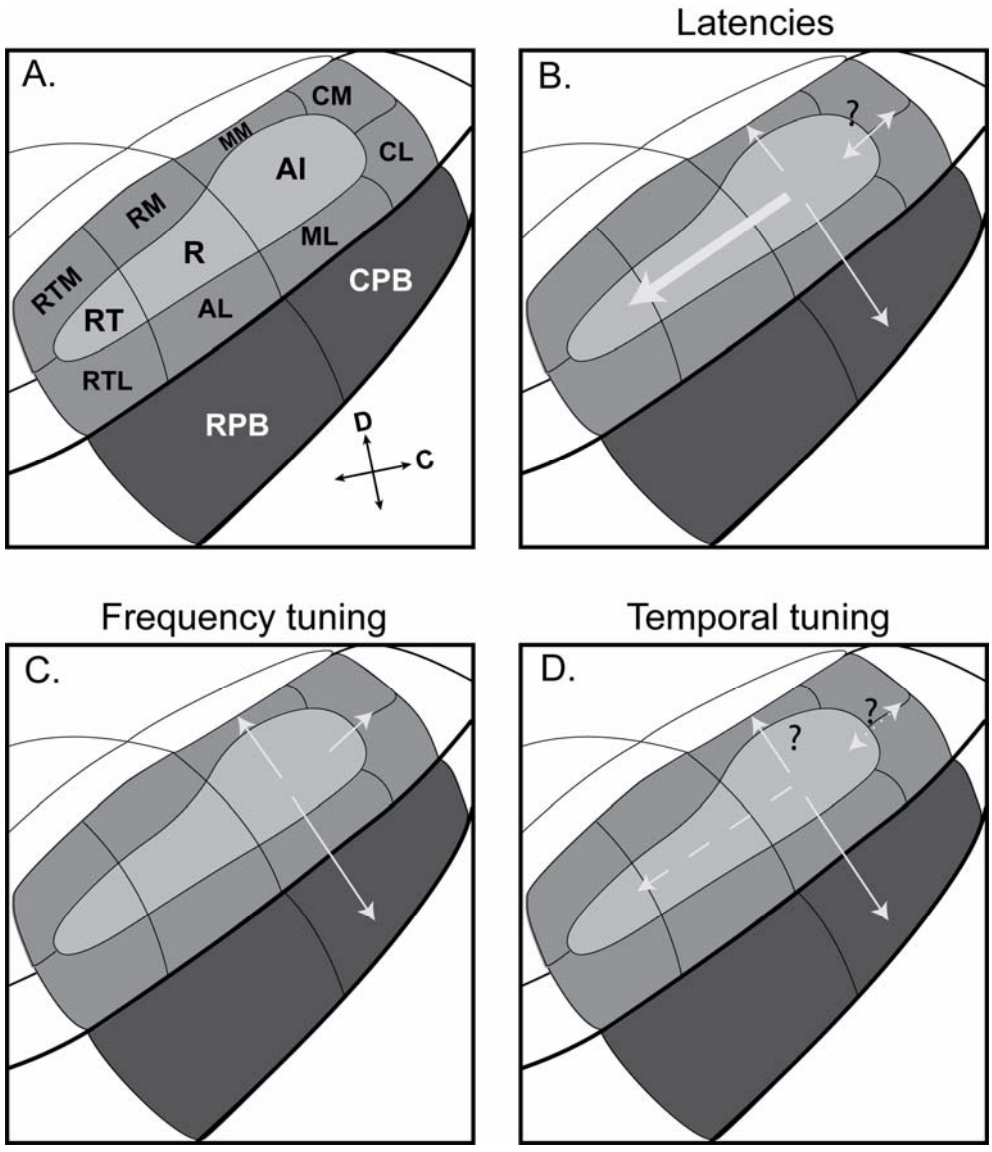

Figure 5.1 Schematic of primate auditory cortex and summary of sources of information about auditory pathways. A. Schematic of auditory cortex. B. Pathways implied by results from response latencies, where arrows with question marks indicate directions where flow is uncertain. Wider arrow indicates the gradient is stronger in this direction. Bidirectional arrows indicates that there is evidence for both directions. C. Pathways implied by results investigating spectral tuning. D. Pathways implied by results investigating temporal tuning. Gradient along the caudorostral axis is denoted as a dotted line to indicate relative weakness/uncertainty.

the caudorostral flow seems to be marked not by feature integration, but by latency differences. This is pure speculation, but perhaps the caudorostral axis has a gradient not in the precision or kind of information that is encoded, but in length of integration window. Perhaps integrating over longer windows allows for the ability to encode not just simple features, but features that change in time such as higher-order envelope shape or dynamic spectral cues. That the auditory system would need to do this seems reasonable given the dynamic time-based nature of sound. Given the speculative nature of this, more comparative studies in coding complex stimuli would help test this hypothesis. Additionally, there are a number of places denoted by question marks where processing flow and integration needs to be better characterized.

Figure 5.2 A shows a recent proposed revision to the model (Bendor and Wang, 2008). This proposal ascribes the bidirectional flow to separate spectral and temporal processing pathways in primate auditory cortex. Here they suggest that temporal processing is along the caudorostral axis and spectral processing is along the mediolateral/regional axis. Additionally, windows of temporal integration increase along the former axis and windows of spectral integration increase along the latter axes. The revisions were based primarily on latency differences seen in the caudal to rostral axis of core, and they note that their predictions that temporal tuning does not change in the medial to lateral direction were untested. This prediction has been tested, both in their lab (Crum et al., submitted) and ours, and it appears that this intriguing model incompletely accounts for response patterns seen in primate auditory cortex. For comparison figure 5.2 B shows an alternative proposal (from above) for the nature of the dual streams of information processing in auditory cortex.

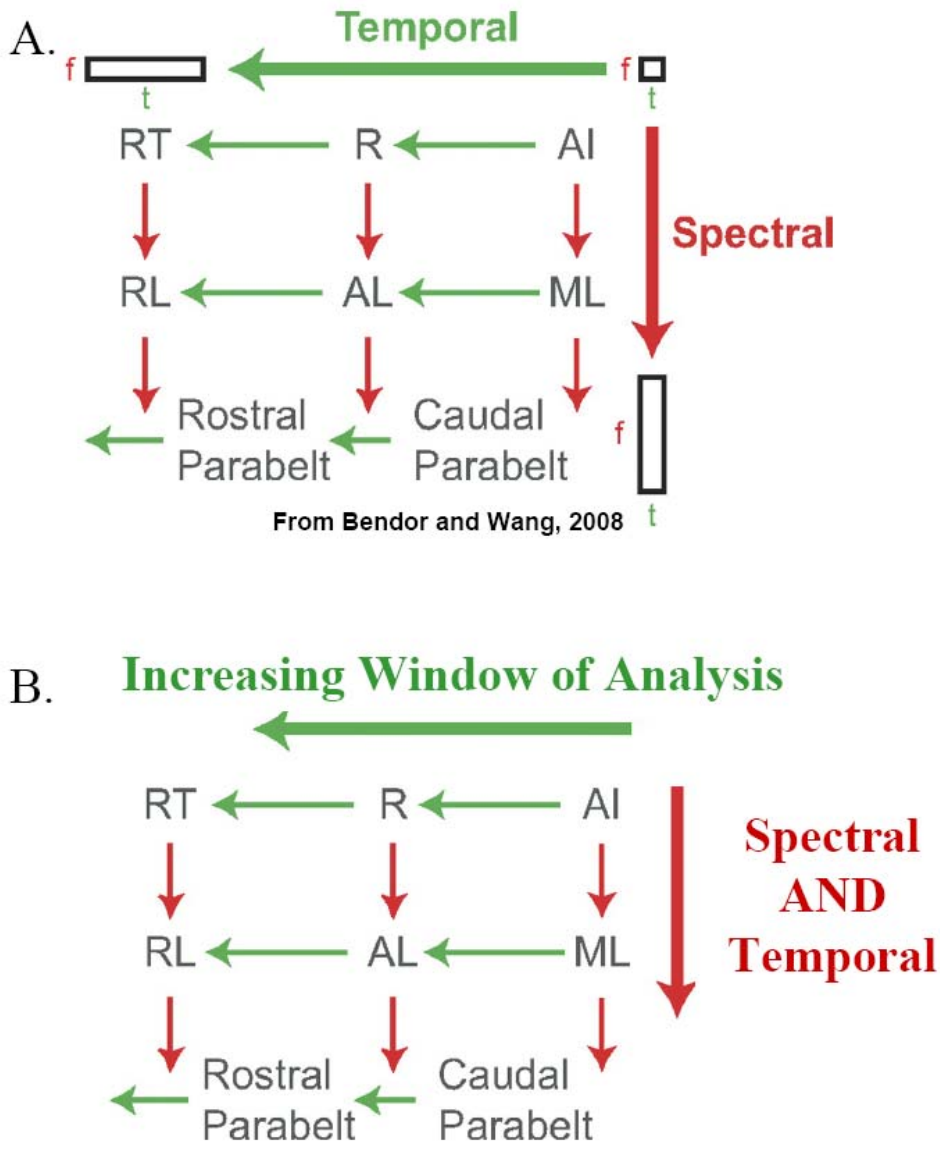

Figure 5.2. A. Bendor and Wang's 2008 proposed model of spectral and temporal processing pathways in primate auditory cortex. Temporal processing is along the caudorostral axis and spectral processing is along the mediolateral/regional axis. In this model, temporal windows of integration increase along the former (denoted by red lines and larger boxes) and spectral window of integration increase along the latter (denoted by green lines and larger boxes) axes. Here, f is frequency and t is time. (Figure and description from 2008 paper) B. For comparison, the figure from that paper has been altered to reflect an alternate view of the nature of the dual streams consistent with current data. Here, both spectral and temporal integration occur in the regional direction and the temporal window of analysis changes in the rostrocaudal direction.

Processing streams in auditory cortex are dominated by parallel processing

Almost 20 years ago, known connections were used to make predictions about the processing hierarchy of another sensory system, the visual system (Felleman and Van Essen, 1991). This work identified levels of hierarchy and divided processing into dorsal/ventral streams. Based on known connectivity at the time (primarily Galaburda and Pandya, 1983), it also attempted to extend reasoning to the auditory system. They noted suggestions of a hierarchy between core and belt, as well as a caudal to rostral flow, but noted that root (medial belt) connectivity did not fit into an 'internally consistent hierarchy'. In the intervening decades, work from many labs is filling in these gaps, indicating that there is flow from core to belt to parabelt (Vaadia et al., 1982; Bieser and Muller-Preuss, 1996; Recanzone, 2000; Crum et al., submitted), as well as a caudorostral flow (Bieser and Muller-Preuss, 1996; Bendor and Wang, 2008; Kusmierek and Rauschecker, 2009).

Is this flow serial? Studies based in the cortical visual system concluded that serial across-areal transfer time should be approximately 10 ms (reviewed in Nowak and Bullier, 1997). In the auditory cortex, latency differences between regions do not appear to be of such magnitude. However, neural onset latencies in the belt and parabelt are in response to a mix of inputs from separate cortical but overlapping thalamic sources. Given the numerous parallel pathways from the MGC, the lack of evidence for strict serial processing and the more parallel timing of processing in cortex is perhaps unsurprising.

What is perhaps most striking is that though there are clear regional and caudorostral trends in the flow of information, there is enormous overlap in the latency

distributions. This is no doubt indicative of the massively parallel inputs coming in from the subdivisions of the primary thalamic nuclei. Because of the ongoing nature of sound, auditory stimuli must be processed very rapidly. A system that is wired to process information in many streams at once is best suited for fast processing. The auditory cortical system processes in serial, probably in a graded manner, but its stunning feature is massively parallel processing.

Implications of flow for sound processing: 'what' versus 'where' streams hypothesis

In the broader context of cortical processing of sound, what are the implications of the primate model? Based on the topography of prefrontal cortical projections from auditory cortex, it has been suggested that there is functional correspondence between the dorsal/ventral streams of the visual system and proposed caudal/rostral streams in the auditory system (e.g. Romanski et al., 1999; Rauschecker and Tian, 2000). Dorsal prefrontal areas are targets of the caudal auditory areas and ventral prefrontal areas are targets of more rostral areas, which has commonly been interpreted as evidence for the 'where' and 'what' streams (reviewed in introduction).

Our data indicate that there is a caudal advantage in latencies. Because caudal areas are faster, dorsal 'where' prefrontal targets also presumably receive information faster than the ventral prefrontal targets. A similar dorsal temporal advantage in latencies for the 'where' stream has also been observed in the visual system (see: Schroeder et al., 1998), so this topography in latency differences may be a common crossmodal processing schema of the primate brain. As discussed in the introduction, processing of auditory object location and identity rely on an overlapping set of spectral and temporal

cues, so the lack of low-level differences that we see in tuning along the rostrocaudal gradient is perfectly consistent with the what/where streams. However, functional correspondence between the streams of the visual system and the auditory system remains to be determined, and studies contained in this paper do not evaluate the what/where stream hypothesis in auditory cortex.

Implications of common primate schema for encoding of temporally modulated sound

Perception of temporal modulation appears to be dependent on an intact auditory cortex (Whitfield, 1980; Heffner and Heffner, 1986; Zatorre, 1988; Phillips and Farmer, 1990; Kelly et al., 1996; Griffiths, 1999). Recall from the introduction that the propagation of amplitude modulated sound is dependent on the environment (reviewed in: Wiley and Richards, 1978; Brown and Handford, 2000). However, despite differences in evolutionary history and ecological niche, results from this study and others suggest that temporal modulation frequency tuning in auditory cortex appears to be quite similar across both Old and New World primate species, (Sudakov et al., 1971; Bieser, 1995; Bieser and Muller-Preuss, 1996; Liang et al., 2002; Malone et al., 2007; Bendor and Wang, 2008; Oshurkova et al., 2008; Crum et al., submitted).

This may suggest that temporal modulation frequency tuning is less driven by ethological niche, and more by the constraints put on it by flow in a common primate organization. Additionally, there may be a slight overrepresentation of lower modulation frequencies less than 20 Hz with the temporal and rate codes. This may be epiphenomenal, but it is striking that these are also the frequencies common to communication sounds in Old and New World primates (macaque < 20 Hz

(Hammerschmidt and Todt, 1995; Hammerschmidt and Fischer, 1998; Hauser et al., 1998; Rendall et al., 1998), squirrel monkey 6-46 Hz (Schott, 1975) , marmoset 7-15 Hz (Epple, 1968)).

The analysis of the LFP is important to connect results across methods and species

Lastly, a note is needed to motivate the collection and analysis of the LFP that we used here. LFPs are an estimate of the summed transmembrane currents in a local cortical area as discrete as 250 μm (Katzner et al., 2009). Especially for the initial volley of activity (the "evoked" component) the poststimulus deflection of the LFP is indicative of the initial current flow into a local area and is an estimate of the timing of incoming activity. Even for sustained stimuli, the LFP has amplitude dependent and time locked components useful for interpreting stimulus processing (e.g. Steinschneider et al., 1998; Brosch et al., 2002; Norena and Eggermont, 2002). We agree that the interpretation of this signal can be complicated, since the LFP is a mesotopic signal that can't be tied to the activity of a single unit (Logothetis et al., 2001), but they (and their derivative the current source density (CSD)) can be used to infer laminar processing through identification of local membrane sources and sinks (e.g. Steinschneider et al., 1998). Additionally, the LFP is considered to be a better marker of the population activity that underlies EEG or the BOLD signal in fMRI. This latter method has enjoyed increasing popularity for studying the organization of macaque auditory cortex at high fields (i.e. Petkov et al., 2006). Additionally noninvasive measures such as fMRI and EEG are among the few measures available for studying stimulus processing in human auditory cortex in nonclincial populations. If we are to meaningfully connect results across species

(including humans) that are derived from heterogeneous measures, consideration of the LFP is a necessary step.

5.3 In Closing

As we refine the primate model using a multiplicity of approaches, there are still many fundamental questions left to be answered on the nature of auditory processing within the primate auditory cortex, and how it applies to processing in the human brain. In the course of primate evolution, the brain underwent dramatic expansion, and the auditory cortices are no exception (Hackett et al., 2001). Comparing evidence from different primates such as squirrel monkeys, marmosets, macaques, and humans inspires a search for similarities and differences between species. Any differences seen may be due to evolutionary selection pressures in their specific ecological niche, or due to common constraints to minimize the metabolic cost and connection length of a larger brain, such as lateralization of function (reviewed in: Kaas, 2000). Clearly, more studies are needed for a more complete understanding of the anatomical and physiological underpinnings of cortical processing of sound, especially in close human relatives.

This is indeed an exciting time to be studying the auditory system (despite, or perhaps because of, the inefficiencies of working in a developing field, such as needing to establish and refine analyses appropriate for auditory stimuli, as in Chapter III or the Appendix). Advances in methods allow for better characterization of multiple areas at once, as well as a more precise understanding of the chemical and structural aspects of the neural networks that give rise to activity. We are in the privileged position of being

able to draw from previous advances in the visual system to inform hypotheses (King and Nelken, 2009), and ultimately, any differences that we see between systems are informative about the specialized nature of the systems that evolved to process our auditory environment.

5.4 References

Aertsen AM, Gerstein GL (1985) Evaluation of neuronal connectivity: sensitivity of cross-correlation. Brain Res 340:341-354.

Ahissar E, Abeles M, Ahissar M, Haidarliu S, Vaadia E (1998) Hebbian-like functional plasticity in the auditory cortex of the behaving monkey. Neuropharmacology 37:633-655.

Ahissar M, Ahissar E, Bergman H, Vaadia E (1992) Encoding of sound-source location and movement: activity of single neurons and interactions between adjacent neurons in the monkey auditory cortex. J Neurophysiol 67:203-215.

Bendor D, Wang X (2005) The neuronal representation of pitch in primate auditory cortex. Nature 436:1161-1165.

Bendor D, Wang X (2008) Neural response properties of primary, rostral, and rostrotemporal core fields in the auditory cortex of marmoset monkeys. J Neurophysiol 100:888-906.

Bieser A (1995) Amplitude envelope encoding as a feature for temporal information processing in the auditory cortex of squirrel monkeys. In: Primate Vocal Communication (Zimmerman E, ed), pp 221-232. New York, NY: Plenum Press.

Bieser A (1998) Processing of twitter-call fundamental frequencies in insula and auditory cortex of squirrel monkeys. Exp Brain Res 122:139-148.

Bieser A, Muller-Preuss P (1996) Auditory responsive cortex in the squirrel monkey: neural responses to amplitude-modulated sounds. Exp Brain Res 108:273-284.

Brody CD (1999a) Correlations without synchrony. Neural Comput 11:1537-1551.

Brody CD (1999b) Disambiguating different covariation types. Neural Comput 11:1527-1535.

Brosch M, Schreiner CE (1999) Correlations between neural discharges are related to receptive field properties in cat primary auditory cortex. Eur J Neurosci 11:3517-3530.

Brosch M, Scheich H (2002) Neural representation of sound patterns in the auditory cortex of monkeys. In: Primate Audition: Ethology and Neurobiology (Ghazanfar A, ed), pp 151-176. London: CRC Press.

Brosch M, Budinger E, Scheich H (2002) Stimulus-related gamma oscillations in primate auditory cortex. J Neurophysiol 87:2715-2725.

Brown TJ, Handford P (2000) Sound design for vocalizations: Quality in the woods, consistency in the fields. Condor 102:81-92.

Bryant HL, Jr., Marcos AR, Segundo JP (1973) Correlations of neuronal spike discharges produced by monosynaptic connections and by common inputs. J Neurophysiol 36:205-225.

Cheung SW, Bedenbaugh PH, Nagarajan SS, Schreiner CE (2001) Functional organization of squirrel monkey primary auditory cortex: responses to pure tones. J Neurophysiol 85:1732-1749.

Crum P, Issa E, Hackett T, Wang X (submitted) Hierarchical processing in awake primate auditory cortex.

de la Mothe LA, Blumell S, Kajikawa Y, Hackett TA (2006a) Thalamic connections of the auditory cortex in marmoset monkeys: core and medial belt regions. J Comp Neurol 496:72-96.

de la Mothe LA, Blumell S, Kajikawa Y, Hackett TA (2006b) Cortical connections of the auditory cortex in marmoset monkeys: core and medial belt regions. J Comp Neurol 496:27-71.

deCharms RC, Merzenich MM (1996) Primary cortical representation of sounds by the coordination of action-potential timing. Nature 381:610-613.

Dickson JW, Gerstein GL (1974) Interactions between neurons in auditory cortex of the cat. J Neurophysiol 37:1239-1261.

Eggermont JJ (1992) Neural interaction in cat primary auditory cortex. Dependence on recording depth, electrode separation, and age. J Neurophysiol 68:1216-1228.

Eggermont JJ (1994) Neural interaction in cat primary auditory cortex II. Effects of sound stimulation. J Neurophysiol 71:246-270.

Eggermont JJ (2000) Sound-induced synchronization of neural activity between and within three auditory cortical areas. J Neurophysiol 83:2708-2722.

Eggermont JJ (2006) Properties of correlated neural activity clusters in cat auditory cortex resemble those of neural assemblies. J Neurophysiol 96:746-764.

Eggermont JJ (2007) Correlated neural activity as the driving force for functional changes in auditory cortex. Hear Res 229:69-80.

Eggermont JJ, Smith GM (1995) Separating local from global effects in neural pair correlograms. Neuroreport 6:2121-2124.

Eggermont JJ, Roberts LE (2004) The neuroscience of tinnitus. Trends Neurosci 27:676-682.

Eggermont JJ, Smith GM, Bowman D (1993) Spontaneous burst firing in cat primary auditory cortex: age and depth dependence and its effect on neural interaction measures. J Neurophysiol 69:1292-1313.

Epple G (1968) Comparative studies on vocalization in marmoset monkeys (Hapalidae). Folia Primatol (Basel) 8:1-40.

Espinosa IE, Gerstein GL (1988) Cortical auditory neuron interactions during presentation of 3-tone sequences: effective connectivity. Brain Res 450:39-50.

Felleman DJ, Van Essen DC (1991) Distributed hierarchical processing in the primate cerebral cortex. Cereb Cortex 1:1-47.

Fitzpatrick KA, Imig TJ (1980) Auditory cortico-cortical connections in the owl monkey. J Comp Neurol 192:589-610.

Frostig RD, Gottlieb Y, Vaadia E, Abeles M (1983) The effects of stimuli on the activity and functional connectivity of local neuronal groups in the cat auditory cortex. Brain Res 272:211-221.

Galaburda AM, Pandya DN (1983) The intrinsic architectonic and connectional organization of the superior temporal region of the rhesus monkey. J Comp Neurol 221:169-184.

Griffiths TD (1999) Human complex sound analysis. Clin Sci (Lond) 96:231-234.

Hackett TA (2010) Information flow in the auditory cortical network. Hear Res.

Hackett TA, de la Mothe LA (2009) Regional and laminar distribution of the vesicular glutamate transporter, VGluT2, in the macaque monkey auditory cortex. J Chem Neuroanat 38:106-116.

Hackett TA, Preuss TM, Kaas JH (2001) Architectonic identification of the core region in auditory cortex of macaques, chimpanzees, and humans. J Comp Neurol 441:197-222.

Hackett TA, De La Mothe LA, Ulbert I, Karmos G, Smiley J, Schroeder CE (2007) Multisensory convergence in auditory cortex, II. Thalamocortical connections of the caudal superior temporal plane. J Comp Neurol 502:924-952.

Hammerschmidt K, Todt D (1995) Individual-differences in vocalizations of young barbary macaques (macaca sylvanus) - a multi-parametric analysis to identify critical cues in acoustic signaling. Behaviour 132:381-399.

Hammerschmidt K, Fischer J (1998) The vocal repertoire of Barbary macaques: a quantitative analysis of a graded vocalizazation signal system. Ethology 104:203-216.

Hauser M, Agnetta B, Perez C (1998) Orienting asymmetries in rhesus monkeys: the effect of time-domain changes on acoustic perception. Anim Behav 56:41-47.

Heffner HE, Heffner RS (1986) Hearing loss in Japanese macaques following bilateral auditory cortex lesions. J Neurophysiol 55:256-271.

Imig TJ, Morel A (1984) Topographic and cytoarchitectonic organization of thalamic neurons related to their targets in low-, middle-, and high-frequency representations in cat auditory cortex. J Comp Neurol 227:511-539.

Imig TJ, Morel A (1985a) Tonotopic organization in lateral part of posterior group of thalamic nuclei in the cat. J Neurophysiol 53:836-851.

Imig TJ, Morel A (1985b) Tonotopic organization in ventral nucleus of medial geniculate body in the cat. J Neurophysiol 53:309-340.

Joris PX, Schreiner CE, Rees A (2004) Neural processing of amplitude-modulated sounds. Physiol Rev 84:541-577.

Kaas J (2000) Why is brain size so important: design problems and solutions as neocortex gets bigger or smaller. Brain and Mind 1:7-23.

Kajikawa Y, de La Mothe L, Blumell S, Hackett TA (2005) A comparison of neuron response properties in areas A1 and CM of the marmoset monkey auditory cortex: tones and broadband noise. J Neurophysiol 93:22-34.

Kajikawa Y, de la Mothe LA, Blumell S, Sterbing-D'Angelo SJ, D'Angelo W, Camalier CR, Hackett TA (2008) Coding of FM sweep trains and twitter calls in area CM of marmoset auditory cortex. Hear Res 239:107-125.

Katzner S, Nauhaus I, Benucci A, Bonin V, Ringach DL, Carandini M (2009) Local origin of field potentials in visual cortex. Neuron 61:35-41.

Kelly JB, Rooney BJ, Phillips DP (1996) Effects of bilateral auditory cortical lesions on gap-detection thresholds in the ferret (Mustela putorius). Behav Neurosci 110:542-550.

King AJ, Nelken I (2009) Unraveling the principles of auditory cortical processing: can we learn from the visual system? Nat Neurosci 12:698-701.

Kosaki H, Hashikawa T, He J, Jones EG (1997) Tonotopic organization of auditory cortical fields delineated by parvalbumin immunoreactivity in macaque monkeys. J Comp Neurol 386:304-316.

Kusmierek P, Rauschecker JP (2009) Functional specialization of medial auditory belt cortex in the alert rhesus monkey. J Neurophysiol.

Lakatos P, Pincze Z, Fu KM, Javitt DC, Karmos G, Schroeder CE (2005) Timing of pure tone and noise-evoked responses in macaque auditory cortex. Neuroreport 16:933-937.

Lee CC, Winer JA (2005) Principles governing auditory cortex connections. Cereb Cortex 15:1804-1814.

Lee CC, Winer JA (2008) Connections of cat auditory cortex: III. Corticocortical system. J Comp Neurol 507:1920-1943.

Liang L, Lu T, Wang X (2002) Neural representations of sinusoidal amplitude and frequency modulations in the primary auditory cortex of awake primates. J Neurophysiol 87:2237-2261.

Logothetis NK, Pauls J, Augath M, Trinath T, Oeltermann A (2001) Neurophysiological investigation of the basis of the fMRI signal. Nature 412:150-157.

Malone BJ, Scott BH, Semple MN (2007) Dynamic amplitude coding in the auditory cortex of awake rhesus macaques. J Neurophysiol 98:1451-1474.

Merzenich MM, Brugge JF (1973) Representation of the cochlear partition of the superior temporal plane of the macaque monkey. Brain Res 50:275-296.

Miller LM, Escabi MA, Schreiner CE (2001a) Feature selectivity and interneuronal cooperation in the thalamocortical system. J Neurosci 21:8136-8144.

Miller LM, Escabi MA, Read HL, Schreiner CE (2001b) Functional convergence of response properties in the auditory thalamocortical system. Neuron 32:151-160.

Moore GP, Segundo JP, Perkel DH, Levitan H (1970) Statistical signs of synaptic interaction in neurons. Biophys J 10:876-900.

Norena A, Eggermont JJ (2002) Comparison between local field potentials and unit cluster activity in primary auditory cortex and anterior auditory field in the cat. Hear Res 166:202-213.

Nowak L, Bullier J (1997) The timing of information transfer in the visual system. In: Cerebral Cortex (Rockand K, Jones EG, Peters A, Kaas JH, eds), pp 205-241. New York: Plenum Press.

Oshurkova E, Scheich H, Brosch M (2008) Click train encoding in primary and non-primary auditory cortex of anesthetized macaque monkeys. Neuroscience 153:1289-1299.

Perkel DH, Gerstein GL, Moore GP (1967a) Neuronal spike trains and stochastic point processes. II. Simultaneous spike trains. Biophys J 7:419-440.

Perkel DH, Gerstein GL, Moore GP (1967b) Neuronal spike trains and stochastic point processes. I. The single spike train. Biophys J 7:391-418.

Petkov CI, Kayser C, Augath M, Logothetis NK (2006) Functional imaging reveals numerous fields in the monkey auditory cortex. PLoS Biol 4:e215.

Philibert B, Beitel RE, Nagarajan SS, Bonham BH, Schreiner CE, Cheung SW (2005) Functional organization and hemispheric comparison of primary auditory cortex in the common marmoset (Callithrix jacchus). J Comp Neurol 487:391-406.

Phillips DP, Farmer ME (1990) Acquired word deafness, and the temporal grain of sound representation in the primary auditory cortex. Behav Brain Res 40:85-94.

Poremba A, Saunders RC, Crane AM, Cook M, Sokoloff L, Mishkin M (2003) Functional mapping of the primate auditory system. Science 299:568-572.

Rauschecker JP, Tian B (2000) Mechanisms and streams for processing of "what" and "where" in auditory cortex. Proc Natl Acad Sci U S A 97:11800-11806.

Rauschecker JP, Tian B (2004) Processing of band-passed noise in the lateral auditory belt cortex of the rhesus monkey. J Neurophysiol 91:2578-2589.

Rauschecker JP, Tian B, Pons T, Mishkin M (1997) Serial and parallel processing in rhesus monkey auditory cortex. J Comp Neurol 382:89-103.

Recanzone GH (2000) Response profiles of auditory cortical neurons to tones and noise in behaving macaque monkeys. Hear Res 150:104-118.

Renart A, de la Rocha J, Bartho P, Hollender L, Parga N, Reyes A, Harris KD (2010) The asynchronous state in cortical circuits. Science 327:587-590.

Rendall D, Owren MJ, Rodman PS (1998) The role of vocal tract filtering in identity cueing in rhesus monkey (Macaca mulatta) vocalizations. Journal of the Acoustical Society of America 103:602-614.

Romanski LM, Tian B, Fritz J, Mishkin M, Goldman-Rakic PS, Rauschecker JP (1999) Dual streams of auditory afferents target multiple domains in the primate prefrontal cortex. Nat Neurosci 2:1131-1136.

Schott D (1975) Quantitative analysis of the vocal repertoire of squirrel monkeys (Saimiri sciureus). Zeitschrift für Tierpsychologie 38:225-250.

Schroeder CE, Mehta AD, Givre SJ (1998) A spatiotemporal profile of visual system activation revealed by current source density analysis in the awake macaque. Cereb Cortex 8:575-592.

Smith MA, Kohn A (2008) Spatial and temporal scales of neuronal correlation in primary visual cortex. J Neurosci 28:12591-12603.

Steinschneider M, Reser DH, Fishman YI, Schroeder CE, Arezzo JC (1998) Click train encoding in primary auditory cortex of the awake monkey: evidence for two mechanisms subserving pitch perception. J Acoust Soc Am 104:2935-2955.

Sudakov K, MacLean PD, Reeves A, Marino R (1971) Unit study of exteroceptive inputs to claustrocortex in awake, sitting, squirrel monkey. Brain Res 28:19-34.

Tomita M, Eggermont JJ (2005) Cross-correlation and joint spectro-temporal receptive field properties in auditory cortex. J Neurophysiol 93:378-392.

Ts'o DY, Gilbert CD, Wiesel TN (1986) Relationships between horizontal interactions and functional architecture in cat striate cortex as revealed by cross-correlation analysis. J Neurosci 6:1160-1170.

Vaadia E, Abeles M (1987) Temporal firing patterns of single units, pairs and triplets of units in the auditory cortex. Isr J Med Sci 23:75-83.

Vaadia E, Gottlieb Y, Abeles M (1982) Single-unit activity related to sensorimotor association in auditory cortex of a monkey. J Neurophysiol 48:1201-1213.

Valentine PA, Eggermont JJ (2001) Spontaneous burst-firing in three auditory cortical fields: its relation to local field potentials and its effect on inter-area cross-correlations. Hear Res 154:146-157.

Whitfield IC (1980) Auditory cortex and the pitch of complex tones. J Acoust Soc Am 67:644-647.

Wiley RH, Richards DG (1978) Physical constraints on acoustic communication in atmosphere - implications for evolution of animal vocalizations. Behavioral Ecology and Sociobiology 3:69-94.

Zatorre RJ (1988) Pitch perception of complex tones and human temporal-lobe function. J Acoust Soc Am 84:566-572.

APPENDIX

ESTIMATION OF NEURAL RESPONSE LATENCY IN THE AUDITORY CORTEX OF AWAKE PRIMATES: A COMPARISON OF COMMON METHODS

This chapter has been submitted for publication as: Camalier, C.R. and T.A. Hackett. The estimation of neural response latency in awake primate auditory cortex: a comparison of common methods. Other than format changes necessary for the dissertation, the content has not been altered.

A.1 Abstract

Latency is an important parameter of neural responses, but selecting the most appropriate method to express latency is an enduring issue. Often, the sensitivity of a given latency method is somewhat dependent on the dynamics of the neural response, and given the increasing popularity of the awake preparation to understand cortical responses, it is increasingly important to examine latency methods in the context of a conscious animal. In this study we compared five established methods for determining the onset latency of neural responses in the auditory cortex of the alert macaque. The comparison of methods on the same dataset allows us to systematically examine latency and hit/miss differences between methods to identify a method that is maximally reliable. The five methods included are Gaussian Standard Deviation, Poisson Standard Deviation, Poisson Fit, Poisson Surprise Index, and Beginning of Activation. Our results indicate that the Gaussian Standard Deviation method outperforms the other methods both in reliability and realistic latencies. Given the differences between the results from the methods

examined here, care should be taken both in choosing a method for a specific study, as well as when deriving conclusions from latencies derived from different methods.

A.2 Introduction

The onset latency of a neural response is a measure of when incoming information (e.g. a stimulus) first affects a neuron's firing. The order and time frame of these onset latencies between and across regions of the brain is often used to predict functional connectivity (e.g. Schmolesky et al., 1998; Schroeder et al., 1998). Since the advent of computational approaches to study neural activity, numerous methods have been used to determine the onset of neural activity. In this study, we are interested in determining a robust and reliable measure of latencies in awake primate auditory cortex. Certain methods, such as first spike latency, have been useful and popular in the anesthetized preparation (e.g. Cheung et al., 2001; Philibert et al., 2005), where cells show low spontaneous firing, with a preference toward phasic onset response responses (see Wang et al., 2005). However the awake brain is often characterized by high levels of spontaneous activity. Under these conditions it cannot be assumed that the first action potential after stimulus onset is a stimulus driven spike, so first spike analysis may be unreliable.

The question of what algorithm is most sensitive for estimating onset latency has been addressed previously, but often these studies are of limited applicability because they use simulated data or data for which the latency is visually obvious (e.g. Friedman and Priebe, 1998; Berenyi et al., 2007). The sensitivity of a given latency method is

somewhat dependent on the data it is applied on. For example, a previous study comparing latency methods to determine latency across different areas of frontal cortex shows almost no differences between the methods (Pouget et al., 2005), even though modeling results would predict differences (Friedman and Priebe, 1998). We are interested in response latency as an index of signal flow through auditory cortex. Thus, it seems important to evaluate latency methods specifically in the context of real neural responses in the cortex of awake animals, in particular for awake auditory cortex.

Here, we choose five established methods for determining neural onset latency to compare results derived from the same dataset. These are not an exhaustive selection of methods, but include the primary ones used in previous studies of awake primate auditory cortex (Recanzone et al., 2000; Bendor and Wang, 2008; Kusmierek and Rauschecker, 2009), as well as some that are not currently applied to auditory cortex, but are commonly used in other fields (see methods Legendy and Salcman, 1985; Maunsell and Gibson, 1992; Hanes et al., 1995; Azzopardi et al., 2003). These particular methods were chosen to guide our own choice of latency analyses, as well as to directly illustrate how differences in choice of methods can influence estimates of latency reported in the literature. If systematic differences are found even when the same dataset is used, this understanding will aid in the interpretation and comparison of results derived with different methods.

In addition to estimating the onset time of a response, we are also interested in how well a latency measure reliably predicts a response. We also investigated the degree to which these measures were correlated with a significant elevation of firing rate over spontaneous activity. This study uses these comparisons to identify a latency method for

awake auditory cortex that both describes a large percentage of the data and produces latencies that are realistic and coincide with what seems reasonable based on visual inspection of the data. We find that, though no method tested is infallible, the Gaussian Standard Deviation method is overall most reliable and produces realistic latencies.

A.3 Materials and Methods

Animal subjects

Two adult macaque monkeys SP and DY were used for neural recordings (SP male bonnet macaque (*Macaca radiata*) 10.0 kg; and DY female rhesus macaque (*Macaca mulatta*) 7.0 kg). Animals were housed in an AAALAC-accredited facility under supervision of laboratory and veterinary staff. All animal care and experimental procedures were in accordance with the U.S. National Institutes of Health *Guide for the care and use of laboratory animals*, under a protocol approved by the Vanderbilt Institutional Animal Care and Use Committee.

Surgical procedure

After completing training to enter a primate chair and initial acclimatization, a headpost (in-house design) was implanted under aseptic conditions. The monkey was initially tranquilized with Ketamine (10-30 mg/kg IM) and Robinul (0.015 mg/kg IM) for intubation, catheterization and scrubbing, and premedicated with Cefazolin (2.2 mg/kg IM). Through the duration of the procedure, anesthesia was maintained with inhalation Isofluorane in O_2 (2-4%). Respiration was maintained with a mechanical ventilator and

body temperature was maintained at 37°C. Heart rate, blood pressure, expiratory CO_2, and peripheral oxygen levels were monitored as well. After 4-8 weeks of acclimatization of the monkey to the headpost, and training to sit tranquilly in a primate chair with insert earphones, a second surgery was performed. In this surgery (details above) we implanted a recording chamber (22 mm wide; Crist Instruments, Hagerstown MD), oriented vertically over the left caudal auditory cortex (sterotaxic coordinates of the center of the chamber were approximately A7: L23 mm from earbar zero). A craniotomy slightly smaller than the chamber was also made at this time.

Stimulus generation and neurophysiological acquisition

Stimulus generation and delivery**.** Recording sessions were conducted in a double walled chamber (Industrial Acoustics Corp, NY) that attenuated sounds, particularly at the mid to high frequencies. Acoustic stimuli were generated by Tucker-Davis technologies (TDT, Gainesville, FL) System II hardware and software (SigGen), controlled by a custom software interface between the stimulus generation and acquisition setups. Stimuli were delivered using Beyer DT911 insert earphones (range 0.10-25 kHz), coupled to custom earmolds in both ears. These earmolds were made individually for each monkey by constructing a silicon mold of the concha and first few millimeters of the ear canal of each ear to completely seal the ear canal. A stainless steel tube (inner diameter ~1 mm) passed through the ear mold to protrude 2-3 mm into the ear canal. The transducer tube interfaced to the mold tube to form a sealed system. Stimuli were calibrated for intensity using a ¼ inch microphone (Model 7017; ACO Pacific, CA), pistonphone (Bruel and Kjaer type 4220) and custom software (TDT, SigCal). Amplitude

corrections are saved in a data file and applied to each stimulus to pre-equalize the response of each earphone independently. All stimuli were delivered diotically 30 times, randomly interleaved with other stimuli (e.g. tones, clicks, noise) with a jittered inter-onset interval between 700-1100 ms, sufficient time for cortical activity to return to baseline.

Stimuli. We used two different kinds of wideband stimuli for these investigations: biphasic 0.25 ms clicks and 250 ms Gaussian frozen white noise with a 5 ms $\cos^2$ onset and offset ramp, both calibrated to 60 dB SPL. Both stimuli reliably evoked responses from many neurons. The stimuli also have different onset shapes and durations, and can evoke different dynamics of responses, from quick and phasic to sustained in the awake animal. The inclusion of two different stimulus shapes was to ensure that the results from this study could generalize to broader stimulus batteries.

Electrophysiological recording. Electrode penetrations were made through a recording grid 15 mm wide with 1 mm spacing which fit over the implanted chamber (Crist Instruments, Hagerstown MD). This ensured a roughly perpendicular trajectory through most parts of the superior temporal plane corresponding to the caudal two-thirds of auditory cortex. After a local anesthetic (0.13% bupivicaine and 0.5% lidocaine in sterile saline) was topically applied and then removed, a sharpened stainless steel guide tube was inserted to puncture the dura. The use of a guide tube also ensured that the penetration ran parallel to the recording chamber. One to two tungsten microelectrodes (2-4 MOhm, FHC, Bowdoin, MA) aligned mediolaterally were advanced through the guide tube to somatosensory cortices and into auditory cortex using manual microdrives (Narishige, Tokyo, Japan).

From the first auditory-responsive hash until the end of auditory-responsive cortex, all isolated neurons, irrespective of responsiveness, were tested with all or most of the stimulus battery to avoid biasing the sample. In between isolations the microdrives were moved at least 200 μm to avoid resampling units. For most runs, we recorded through all layers until the white matter was reached. We assigned a relative cortical depth to each penetration by normalizing the recording depth with respect to the first auditory responses, presumably from the first layer or two of auditory cortex. While unequivocal laminar depths cannot be established, it is likely that the majority of recorded neurons are coming from the middle and upper layers, consistent with the cytoarchitecture of auditory cortex (see Hackett, 2010). During recording sessions the monkey sat quietly alert and was visually monitored via closed-circuit television.

Multichannel spike recordings were acquired with a 64 channel system that controls amplification, filtering and related parameters (Many Neuron Acquisition Processor, Plexon Inc, Dallas, TX). Both signals were referenced to ground. Spike signals were amplified (100x), filtered (150-8800 Hz), and digitized at 40 kHz. The signal was further DC-offset corrected with a low-cut filter (0.7 Hz). Spikes were sorted online for all channels using real-time window discrimination. Digitized waveforms and timestamps of stimulus events were also saved for final offline analysis and sorting (Plexon offline sorter), and graded according to isolation quality (single or multi units). Since we were interested in finding a method that worked for both single and multi units, we present results combined across unit types. We also analyzed them separately, but since results for each method were the same regardless of isolation, we combined across single and multi units. To ensure timing precision, the Plexon acquisition software interfaced with

the stimulus delivery system (Tucker Davis Technologies) and both systems were controlled by custom software (SGPlay, TDT).

Histology and identification of cortical areas

At the end of the electrophysiological recording, lesions were made in representative grid sites to facilitate reconstruction. Additionally, best-frequency matched sites were identified and 2-3 tracer injections were placed for a parallel anatomical study of auditory cortex. After a 12-14 day tracer transport period, the monkey was initially tranquilized with Ketamine and a lethal dose of Euthasol (120mg/kg) was administered. Just after cardiac arrest, the monkey was perfused with 4ºC 0.1M phosphate buffered saline containing heparin (10 units/ml) , followed by 4ºC paraformaldehyde (4%) dissolved in 0.1M phosphate buffer (pH 7.4). Immediately after perfusion, the head was placed in a sterotaxic apparatus to for precise measurement of chamber placement and electrode angles. The brain was removed from the skull and photographed. The cerebral hemispheres were separated from the thalamus and brainstem, blocked, and placed in 30% sucrose for 1-3 days. To facilitate reconstruction, the left hemisphere was cut at a stereotaxic vertical angle (angle of the electrode) in 40 μm sections. Alternating series of sections were stained for Nissl substance with thionin, cytochrome oxidase (Wong-Riley, 1979), acetylcholinesterase (Geneser-Jensen and Blackstad, 1971), myelinated fibers (Gallyas, 1979), and the stains appropriate for the neuronal tracers (not shown here). Using information from the lesions, electrode tracks, and histological reconstruction of areas, areal locations of electrodes were determined and confirmed by electrophysiological properties. Neurons came from multiple areas from the caudal two-

thirds of auditory cortex, identified by architectonic criteria established in previous studies (Hackett et al., 1998; Hackett et al., 2001; Hackett and de la Mothe, 2009). Since we were interested in identifying a method that generalizes across auditory cortex, neurons from all areas were included in this analysis.

Data analysis

For the click stimulus, we analyzed responses from a total of 1364 single and multi units from the caudal portion of auditory cortex of two alert macaque monkeys (622 from monkey S and 742 from monkey D). For the noise stimulus, we analyzed responses from a total of 1295 units, (452 from monkey S and 813 from monkey D). No systematic differences were seen between monkeys, so the results were amalgamated.

Five different excitatory latency analysis methods were chosen. The Poisson Surprise analysis (Legendy and Salcman, 1985; Hanes et al., 1995) and related Beginning of Activation (Hanes et al., 1995) methods have not been extensively used in primate auditory cortex, but have been applied usefully in other sensory systems. In particular, the Poisson Surprise analysis was used in two studies comparing latencies from different areas of the visual system (Schmolesky et al., 1998; Pouget et al., 2005), and one study of latency measures concludes that the Poisson Surprise method is the most frequently used method (Berenyi et al., 2007). The Poisson Fit method (Maunsell and Gibson, 1992), is also popular in analyzing visual system latencies. We also included Gaussian Standard Deviation, used in the auditory system of awake primates (Recanzone et al., 2000; Bendor and Wang, 2008; Kusmierek and Rauschecker, 2009), and Poisson Standard Deviation (Azzopardi et al., 2003). All analyses were coded using in-house Matlab

scripts (MathWorks, Natick, MA). Spike times were binned at 1 ms to preserve precision in the response. Certain methods, such as Poisson Surprise and Beginning of Activation are performed on spike times of a single trial, thus smoothing is irrelevant. For the rest of the analyses, no smoothing was used to maintain precision of timing. The five methods used are described in detail below:

1. GAUSSIAN STANDARD DEVIATION (GAUSSIAN SD) (e.g. Recanzone et al., 2000; Bendor and Wang, 2008; Kusmierek and Rauschecker, 2009). This algorithm is based on the averaged neural response in the form of a peristimulus time histogram (PSTH). The neural latency was the first bin after stimulus presentation to cross a response threshold and remain there for a minimum number of bins (here, 3 bins). The algorithm defined a response threshold as 3 Gaussian standard deviations of the spontaneous rate above the mean spontaneous firing rate.

2. POISSON STANDARD DEVIATION (POISSON SD) (Azzopardi et al., 2003). This algorithm is similar to the Gaussian Standard Deviation method, but this variant is sometimes used since it is commonly assumed that firing rate is approximately Poisson distributed. Thus, a Poisson-based standard deviation may be a better descriptor of variability in the PSTH. As above, the neural latency was defined as the first bin after stimulus presentation to cross a response threshold and remain there for 3 bins. The algorithm defined a response threshold as 3 Poisson standard deviations of the spontaneous rate above the mean spontaneous firing rate.

3. POISSON FIT (Maunsell and Gibson, 1992). This algorithm defines latency as the first of three bins containing a number of spikes more than what would be expected from a Poisson process. The mean of the Poisson process is defined as the spontaneous rate and

the α threshold must be at the level of $p < 0.01$ for the first and $p < 0.05$ for the second and third bins.

4. POISSON SPIKE TRAIN ANALYSIS (POISSON SURPRISE) (Legendy and Salcman, 1985; Hanes et al., 1995). This algorithm is derived from a method to search for bursts of spikes in continuous spike trains (Legendy and Salcman, 1985). On a single trial basis, the method detected post-stimulus intervals where there is a burst, defined as an interval where the number of spikes exceeds the number (at the $p < 0.05$ level) that would be expected from a Poisson process whose mean is defined as the firing rate of the entire trial period. The surprise index quantified the amount by which the observed number of spikes exceeds the number that would be expected. Overall latency was the median of all the single trial values. Since it is generated on a trial by trial basis, this method had the added advantage that it also generates a measure of latency variability.

5. BEGINNING OF ACTIVATION (BOA) (Hanes et al., 1995). This method is a variant of the Poisson surprise. It was developed for cells whose beginning of activation may not be defined by a burst (Hanes et al., 1995). It followed all the steps described above to detect bursts. After the beginning and end of the first burst was determined (see above), spikes from the original train were added to the beginning of the burst and the surprise index was calculated each time. The point at which the surprise index fell below the desired significance level ($p < 0.05$) is defined as the beginning of activation.

For each unit, each method was used to determine latency. Parameters for each of these methods were preserved from the original presentation in the literature as much as possible. Thus, for these data, spontaneous activity for Gaussian SD, Poisson SD, and Poisson Fit was defined as the first 200 ms immediately preceding stimulus onset,

consistent with previous uses of these methods (see above). For Poisson Surprise and Beginning of Activation, the mean spike rate was derived from the entire trial, consistent with previous definitions of these methods (see above).

As an independent measure of response, we performed a one-tailed paired t-test (α threshold at $p < 0.05$) comparing the firing rates of spontaneous firing 200 ms immediately preceding stimulus onset to the evoked activity within 100 ms after stimulus onset on individual trials. A small window was used for evoked activity to increase the chance that brief phasic responses were properly categorized. If the firing rates were significantly elevated, it was classified to have a significant response.

A.4 Results

Latency estimates as a measure of significant response

An exemplar raster and PSTH for a click response is shown in figure A-1. For this unit, the evoked activity met the criterion for a significant response, and each latency method generated a value, though the exact latency value varied by method. On these plots, the level of spontaneous is shown as the dashed line, and thresholds for Gaussian and Poisson SD are shown as black and gray solid lines, respectively. Note that the Poisson SD threshold was lower than the Gaussian SD threshold; this is generally true of all cells. From visual inspection of a cell like that shown in figure A-1, it is clear why the first spike method is not universally appropriate for cells with high level of spontaneous (e.g. awake cortex). On a given trial, the first spike after the stimulus is ambiguous and often fell earlier than the actual response onset.

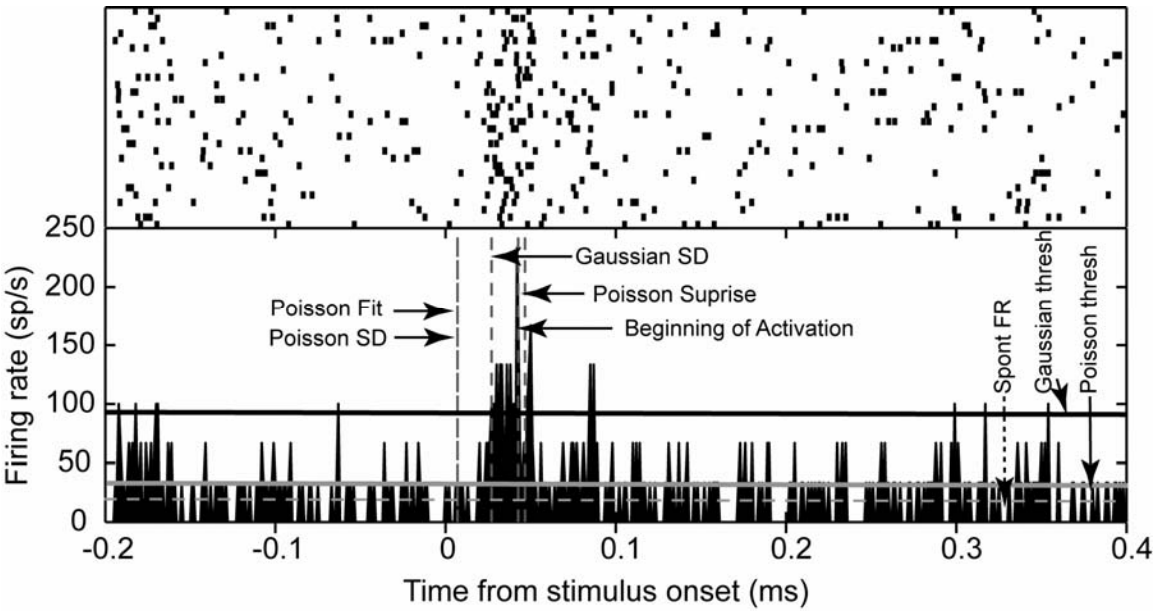

Figure A-1. Exemplar raster, PSTH, and latency values from each method for a click response. Raster, top panel, where each trial is a row. Bottom panel, PSTH with time on the x axis and firing rate on the y axis. Horizontal gray dashed line is spontaneous firing rate, solid gray and black lines are thresholds for Poisson and Gaussian SD methods, respectively (labeled). Latencies for each method are shown in dotted vertical lines, labeled for each method. Here the latencies estimated by the Poisson SD and Poisson Fit methods are the same, and are earlier then that estimated by the Gaussian SD. Also, shows Poisson Surprise and Beginning of Activation measures falling later than Gaussian SD measure.

Our first aim was to determine how well-correlated a given latency measure is with an independent measure of response. For a given unit, a latency was classified as a "correct hit" if the latency was measured and it also had a significant response, or if no latency was measured and it did not have a significant response (also termed "correct rejection"). For all methods, the latency in figure A-1 would be classified as a correct hit. A cell was classified as a "false hit" if the method determined a latency but it did not have a significant response, and as a "false rejection" if the method did not determine a

latency though the response was significant. Figure A-2 shows the classification percentage of responses for each estimation method. Regardless of whether the response was from a click or noise stimulus, the Gaussian SD method outperformed the other methods in correct classification by at least 10%. It had slightly more false hits (1-5%) than the Poisson Surprise or Beginning of Activation methods (especially for the noise stimulus), but much less than the Poisson SD or Poisson Fit measures. The Gaussian SD method had slightly more false rejections (2-5%) than the Poisson SD or Poisson Fit, but much less than the Poisson Surprise and Beginning of Activation methods.

Due to the algorithmic similarities underlying the Poisson Surprise and Beginning of Activation methods, the numbers of hits, false hits, and false rejections are quite similar for these measures. The same is true for the results from the Poisson Fit and Poisson SD measures.

Reliability of latency estimates

Our second aim was to establish the reliability of these latency estimates. Specifically, we were interested both in how similar estimates were to each other, as well as whether these estimates provide physiologically realistic latencies for cortex. Figure A-3A shows the distributions of latencies in response to clicks from all of the estimates, regardless of whether the response was classified as significant.

For the click stimulus, latencies derived from each method followed the following pattern: estimates from the Poisson Fit were the earliest, followed by those derived from Poisson SD, Gaussian SD, Beginning of Activation, and Poisson Surprise was the latest. This pattern can also be seen at the unit level in figure A-1. All differences

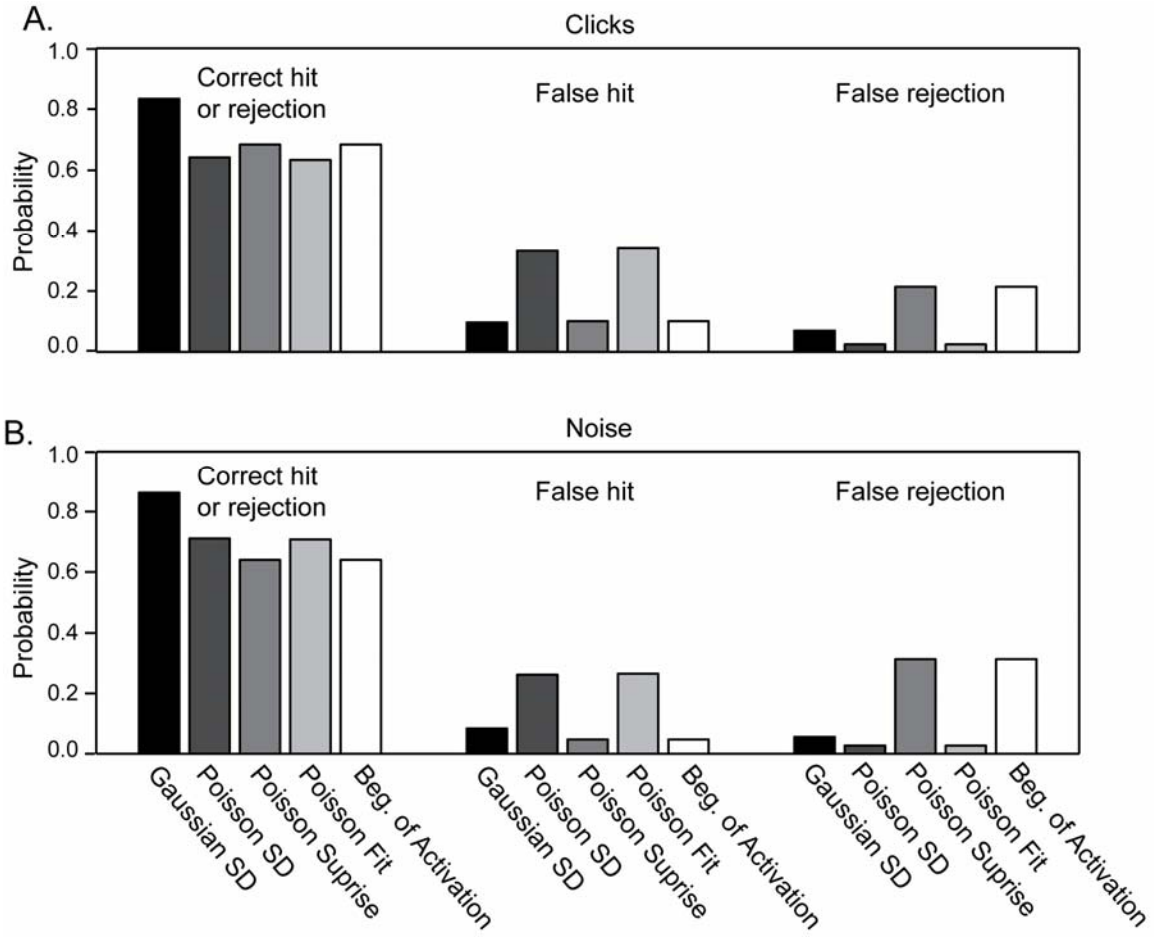

Figure A-2. Response classification percentage for each latency method. Percentage of hits (i.e. correct classification or rejection), false hits, or false rejections for each method. Click responses are shown in panel A and noise responses are shown in panel B.

except between latencies derived from the Poisson Surprise and Beginning of Activation are statistically significant (two-tailed t-test, $p < 0.05$, Bonferonni corrected for multiple comparisons).

Latency estimates in response to the noise stimulus are in figure A-3B. The noise latencies show the same pattern as the click stimulus, however, they are generally longer than to the click, probably due to the slower onset ramp. Again, all differences except for

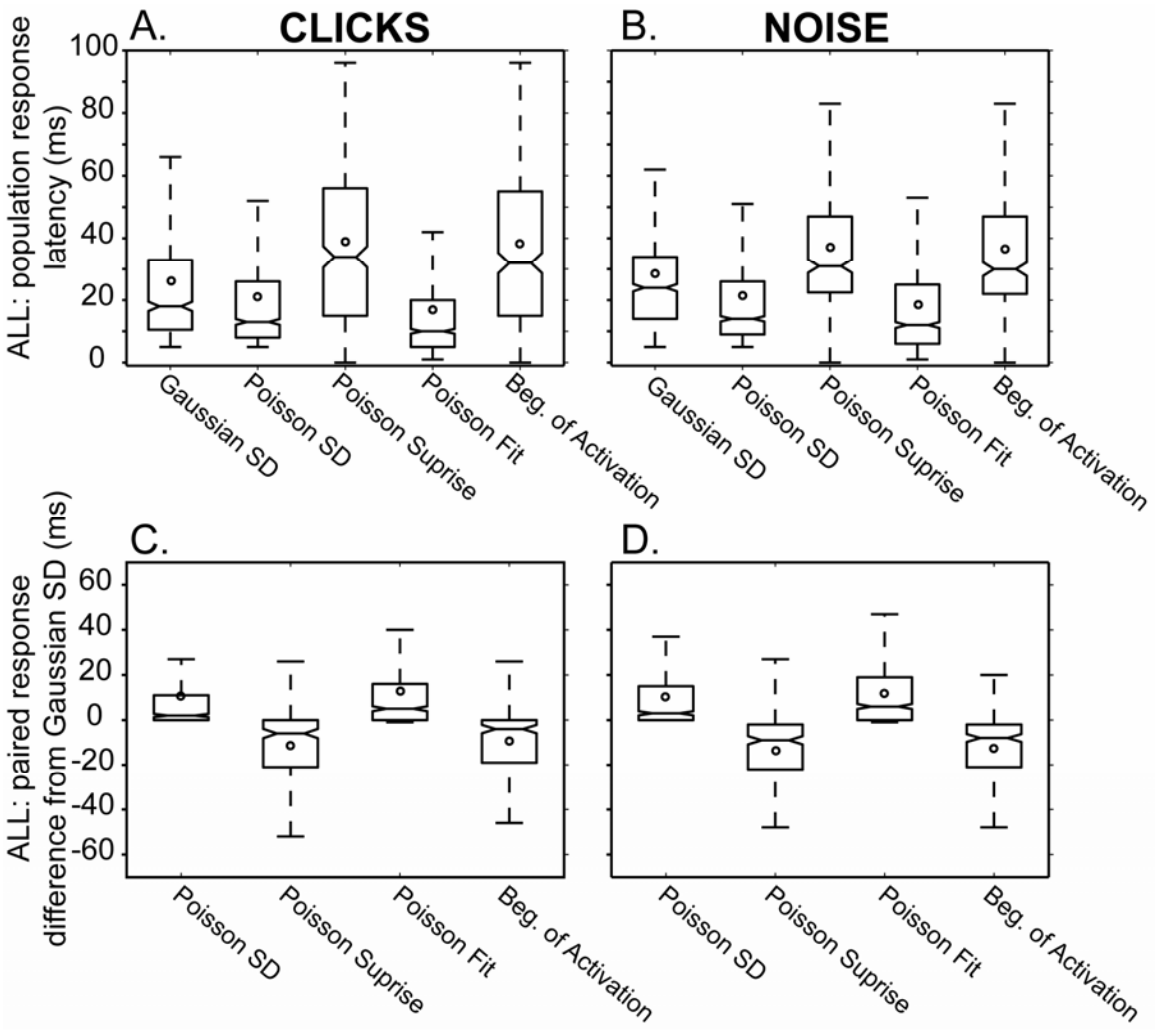

Figure A-3. Distribution of latency estimates: all latencies. A and B. Boxplots of latency estimates for each stimulus type (click and noise) and each latency method. C and D. Differences from Gaussian SD measure for other estimates calculated on a per neuron basis. The box denotes the upper quartile, median, and lower quartile of the distribution. Whiskers denote the extent of the rest of the data. Notches indicate an estimate of the uncertainty about the median. (If notches do not overlap, the medians differ at the level of $p < 0.05$).

the Poisson Surprise and Beginning of Activation are statistically significant (two-tailed t-test, $p < 0.05$, Bonferonni corrected for multiple comparisons).

Note that these plots (figure A-3A and A-B) show population measures. A more precise comparison is to directly compare the latencies derived from different methods on

the same unit (assuming a latency from both methods exist for that unit). Since the Gaussian SD method tended to correctly classify a higher percentage of units (figure A-2), for comparison we subtracted each latency from the latency derived from the Gaussian SD. These differences are shown in parts C and D of figure A-3. Similar to the population measures, the Poisson Fit method tends to generate the earliest latencies compared to the estimate from the Gaussian SD by about 15 ms. The Poisson SD also generally underestimates latencies relative to the Gaussian SD by about 10 ms (although it is very often close to the Gaussian SD). The Poisson Surprise and Beginning of Activation latencies are both later than the Gaussian SD by about 10 ms. For latencies taken from the same unit, all measures are significantly different from each other (paired two-tailed t-test, $p< 0.05$, Bonferonni corrected for multiple comparisons).

Because some of the latencies are from responses that are not classified as a significant and may not measure a true response, we performed the same analysis restricted to statistically significant responses. The overall pattern of latency measures is almost the same. The population results are shown in figure A-4A and B for clicks and noise, respectively. In this case, no statistically significant difference can be found between the Poisson Surprise and Beginning of Activation, or between the Poisson Fit and Poisson SD methods. On an individual unit level, differences relative to Gaussian SD are again shown in parts C and D of figure A-4. Here, all measures are significantly different from each other (paired two-tailed t-test, $p< 0.05$, Bonferonni corrected for multiple comparisons).

A comparison of figure A-3 and figure A-4 shows that, regardless of the latency method and stimulus type, means are slightly earlier and distributions slightly less

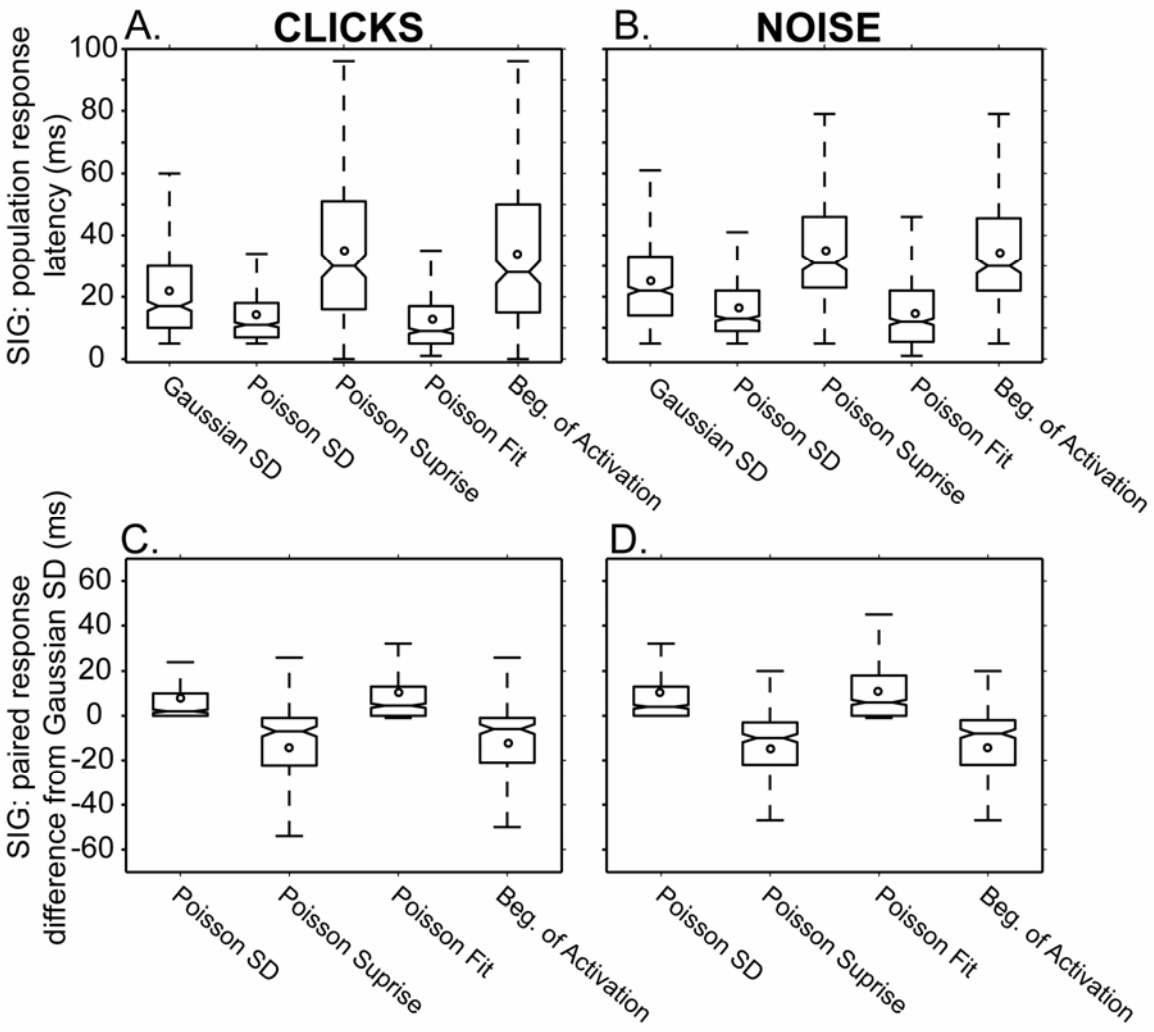

Figure A-4. Distribution of latency estimates: significant responses only. Conventions as in figure A-2. A and B. Boxplots of latency estimates for each stimulus type and each latency method. C and D. Differences from Gaussian SD measure for other estimates calculated on a per neuron basis.

variable when one only considers significant responses. We can conclude that latency values classified as false hits tend to be later than values in the middle of the distribution. However, the trends seen between methods are completely consistent between figures A-3 and 4.

Certain methods produce a high percentage of latencies that are 5 ms or less in this dataset. For this dataset in cortex, it is probably unrealistic to have many latencies this short. These very short latencies are produced more from the Poisson Fit method (about 24% of the time) and to a lesser extent the Poisson SD method (7-8% of the time). The incidence of very fast latencies is lowest using the Gaussian SD method (0.7%). Incidence of short latencies in both the Poisson Surprise and Beginning of Activation measures is about 2%, even though these methods tend to estimate longer latencies than the Gaussian SD.

As a last analysis there are few neurons whose responses are clear and are significant, but so sparse and phasic that none of the methods generate a latency. As an example of one of these false rejections, see figure A-5. If one was to visually estimate latency from the PSTH (a trivial process, though time consuming) and add these missing latencies, would the latency estimates change significantly from the estimates derived for a purely automatic method, such as Gaussian SD? Overall, about 10% of the missed responses changed to have a latency, but the population-level change is very small. The population including visually-corrected click latencies is on average 2.4 ms slower than the original latencies. Corrected noise latencies are 0.5 ms faster than the original latencies. If we only consider significant responses, then the differences are even smaller. Corrected click latencies are on average 0.01 ms faster than the automatic latencies. Hand-corrected noise latencies are 1.8 ms slower than the automatically derived latency. While it is useful to visually inspect latency estimates to confirm results, these analyses suggest that correction for "missed" latencies may not have a major effect on the estimates of population level responses.

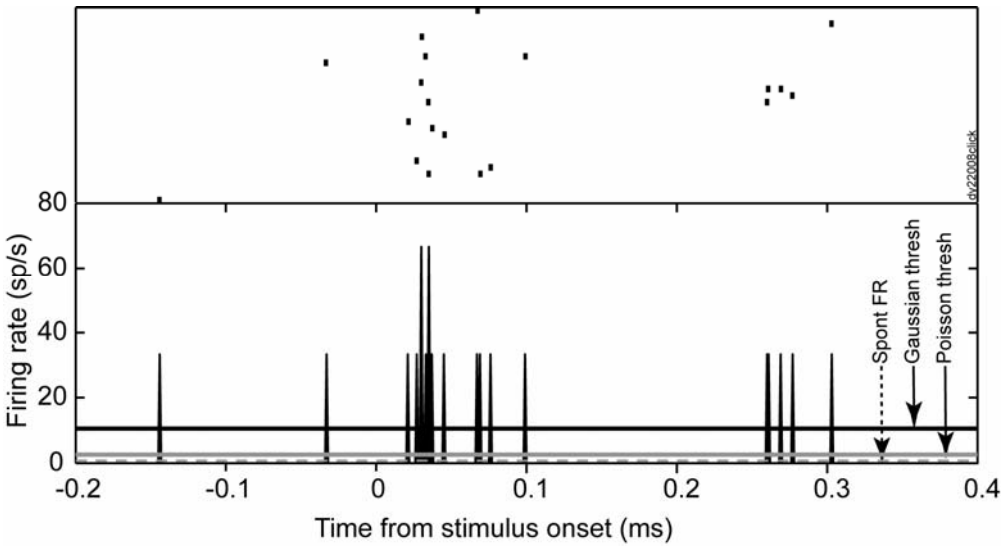

Figure A-5. Example of a click response where the response is significant and visually obvious, but sparse. Conventions are the same for figure A-1. No method examined here is able to estimate this latency.

A.5 Discussion

In this study, we used five different methods to derive latency from the same dataset collected across caudal areas of auditory cortex in the awake macaque. Even though the stimuli we chose had different onset shapes and sound envelopes, which could generate different kinds of responses, results from the different methods generalized across stimuli. This analysis is designed to look at these latency methods using real data in auditory cortex of awake animals. An objective measure of true latency is unavailable for this and all high background datasets - - thus a comparison to the 'true' latency is irrelevant. Instead, we looked for a measure that described a large percentage of the data and produced latencies that are realistic and coincide with what seems reasonable based on visual inspection of the data. We found that the Gaussian SD method was most likely

to give a latency when a response was actually present (i.e. significant), and also gave latency estimates that were more physiologically realistic than the other methods tested. Other methods, such as Poisson SD and Poisson Fit, were more likely to falsely generate latencies when there was not a significant response. They also tended to generate latencies that were too short to be realistic (i.e., 5 ms or less). The other two methods tested here, the Poisson Surprise and related Beginning of Activation, were less likely to generate a response onset latency even if the response was significant, and also reported many latencies that were too short.

In terms of the actual latency values, noise latencies tended to be about 10 ms later than click latencies. This difference can be at least partially attributed to the 5 ms onset ramp of the noise. Regardless, a consistent trend was seen across stimuli. Population latencies derived from the Poisson Fit and Poisson SD tended to be the earliest, latencies from the Gaussian SD method were later, and latencies from the Poisson Surprise and Beginning of Activation tended to be the latest. This was true both at a population and single-neuron level.

What is the basis of the differences seen between methods? Both the Poisson SD and Poisson Fit tended to report many early false positive latencies. On visual inspection of the dataset, these methods tended to be oversensitive to post-stimulus fluctuations in baseline that were not part of the response. The thresholds of the Poisson SD were much lower than those of Gaussian SD. These thresholds are based on standard deviation of the baseline rate. We can explain this trend because the standard deviation of a Poisson process is approximated by the square root of the mean, and is thus limited to never more than the mean, unlike the Gaussian standard deviation which can be greater than the

mean. Though not formally examined here, note that the first spike latency method is the most extreme example of a low-threshold method, as any post-stimulus action potential is counted as a response. Thus, it would also be expected to have many false positive early latencies.

Conversely, the Poisson Surprise and Beginning of Activation methods tended to have many false negatives (significant responses with no latency) and the latencies they reported tended to be later. For many of the very phasic or weak responses, an individual spike train rarely reached criteria for a burst. It could be argued that the Poisson Surprise and Beginning of Activation methods are later than others because the expected firing rate for these measures is defined as the mean rate over the whole train, not just a pre-stimulus baseline. Using this reasoning, a robust response will increase the "spontaneous" mean rate, leading to an increase in the threshold criteria for response, resulting in generally later responses. However, this is unlikely to completely account for the false negatives and late responses since it is obvious that phasic responses add very little to the average firing rate and criteria would not be changed significantly. Therefore, the Gaussian SD method appears to be sufficiently sensitive to catch weak responses that may not be robust on every trial, but not so sensitive that post-stimulus fluctuations create false positives.

Based on the high percentage of hits, the Gaussian SD measure described more of the significant responses in this dataset. The Gaussian SD measure also tends to report more latencies that are within a physiologically relevant range. Lastly, visual inspection of each cell in the dataset confirms that the Gaussian SD measure consistently corresponds to a subjective estimate of the onset of the neural response.

The question of what makes an appropriate latency estimator has been addressed previously, but these studies often necessarily use simulated data or restrict neural responses only to where a latency is visually obvious (e.g. Friedman and Priebe, 1998; Berenyi et al., 2007). In previous studies of latencies the Poisson Surprise method was found to be a biased estimator and tended to overestimate responses (Berenyi et al., 2007). This is similar to what we found. Another study found that in simulated data, the Poisson Fit method was biased and tended to overestimate latencies, particularly when initial responses are weak (Friedman and Priebe, 1998). They also reported a high proportion of false rejections. We saw the opposite effect, perhaps because our PSTHs were noisier than simulated data. Additionally, they analyze this method on responses from two neurons in awake macaque V1 and report that Poisson Fit falsely rejects both responses. We also saw an elevated false rejection rate in the Poisson Fit, but since the sample size was so small, it is difficult to draw a comparison.

When applied to real data, the sensitivity of the latency method seems dependent on the dynamics of the response. For example, a previous study comparing latency methods to determine latency in three areas of frontal cortex shows almost no differences between the Poisson SD, Poisson Fit, and Poisson Surprise methods (Pouget et al., 2005). We did see a difference between methods. This may be due in part that activity from those areas was during a decision task and is characterized by a relatively slow rise to activation. Sensory responses such as these data tend to be more discrete. We do not conclude that results that are inappropriate for the awake auditory cortex are universally inappropriate for all other areas of cortex and all other tasks. Instead, it is clear that the method used must be chosen with care. Bear in mind that no method has been shown to

be completely robust across all areas of cortex and all response types - visual corroboration of the latency with the raster and PSTH is critical.

Latency is an important indicator of timing in the brain, and is often used to test hypotheses about flow and hierarchy. Given the latency and sensitivity differences due to method that we report here, these results have important implications for interpreting latencies across studies. When one aims to compare latencies clearly it is best to use the same method. When that is not available (as in when comparing reported latencies between studies), these results can be used to estimate a correction factor. Since the trends seen in these data hold up across different wideband stimulus types used here, it is likely general trends will be preserved across more than just these stimuli. To determine a correction factor between papers using different methods, parts A and B of figures A-3 and 4 are most useful (parts C and D only included units that had latencies from both methods and does not account for population-level changes). Thus, means derived from Gaussian SD will be ~5-10 ms later than those from Poisson SD and Poisson Fit. Means derived from Gaussian SD will be ~15 ms earlier than those derived from Poisson Surprise and Beginning of Activation methods.

Turning to awake auditory cortex, an overview of the current literature reveals differences in latency estimates even from a single area (Recanzone et al., 2000; Bendor and Wang, 2008; Kusmierek and Rauschecker, 2009; Crum et al., submitted). What are calculation factors that affect the differences in latency measures? Clearly one factor is choice of onset latency calculation method. The majority of the studies use Gaussian SD based measures, so the methods are comparable. Some papers additionally report the latency of the peak response, which generally falls ~ 20 ms after minimum latency, but

individual values vary with response dynamics (Recanzone et al., 2000; Bendor and Wang, 2008). A second factor is choice of stimuli, as noticed in this dataset; the onset latency of clicks is faster than noise. Stimulus choice is complicated by the fact that areas may respond differently to tones versus wideband stimuli depending on cortical region (Rauschecker and Tian, 2004; Kusmierek and Rauschecker, 2009). Thus, tone and noise latencies often cannot be directly compared if taken from different regions. A third factor is the composition of the PSTH, as averaging responses across both optimal and suboptimal stimuli will lower the maximum of the PSTH, likely lengthening latencies. A fourth factor is choice of bin size and smoothing function, which will also increase or decrease latencies slightly. A fifth factor particular to the auditory domain is choice of free-field versus headphone sound delivery. Free-field stimuli necessarily have nontrivial travel time because of the relative slowness of the speed of sound (~340 m/s) that should be considered. For example, placing speakers 1.7 m away from the monkey creates a transport delay of 5ms (Kusmierek and Rauschecker, 2009), which was accounted for by subtracting that value from the response. Due to these numerous factors affecting latency reported, care should be taken when comparing latencies between studies.

In summary, we find that the Gaussian SD measure is a robust estimator of neural latencies, especially if it is also coupled with an additional criterion of response significance to eliminate longer latency false hits. Of the five methods considered, it is the most likely to give a latency when there actually is a significant response, and is most likely to provide latencies that are both physiologically realistic and consistent with what seems visually appropriate. While certain methods may be more appropriate for auditory cortex (i.e. Gaussian SD), no method is completely foolproof. Care must be taken when

comparing across studies since not only the differences in method described here, but also differences in stimuli, PSTH composition, smoothing, and sound delivery method will also affect reported latency values. To really address current questions of information flow in the auditory cortex, it would be best to have latencies from multiple areas taken from the same animal under the same conditions and using the same methods.

A.6 References

Azzopardi P, Fallah M, Gross CG, Rodman HR (2003) Response latencies of neurons in visual areas MT and MST of monkeys with striate cortex lesions. Neuropsychologia 41:1738-1756.

Bendor D, Wang X (2008) Neural response properties of primary, rostral, and rostrotemporal core fields in the auditory cortex of marmoset monkeys. J Neurophysiol 100:888-906.

Berenyi A, Benedek G, Nagy A (2007) Double sliding-window technique: a new method to calculate the neuronal response onset latency. Brain Res 1178:141-148.

Cheung SW, Bedenbaugh PH, Nagarajan SS, Schreiner CE (2001) Functional organization of squirrel monkey primary auditory cortex: responses to pure tones. J Neurophysiol 85:1732-1749.

Crum P, Issa E, Hackett T, Wang X (submitted) Hierarchical processing in awake primate auditory cortex.

Friedman HS, Priebe CE (1998) Estimating stimulus response latency. J Neurosci Methods 83:185-194.

Gallyas F (1979) Silver staining of myelin by means of physical development. Neurol Res 1:203-209.

Geneser-Jensen FA, Blackstad TW (1971) Distribution of acetyl cholinesterase in the hippocampal region of the guinea pig. I. Entorhinal area, parasubiculum, and presubiculum. Z Zellforsch Mikrosk Anat 114:460-481.

Hackett TA (2010) Information flow in the auditory cortical network. Hear Res.

Hackett TA, de la Mothe LA (2009) Regional and laminar distribution of the vesicular glutamate transporter, VGluT2, in the macaque monkey auditory cortex. J Chem Neuroanat 38:106-116.

Hackett TA, Stepniewska I, Kaas JH (1998) Subdivisions of auditory cortex and ipsilateral cortical connections of the parabelt auditory cortex in macaque monkeys. J Comp Neurol 394:475-495.

Hackett TA, Preuss TM, Kaas JH (2001) Architectonic identification of the core region in auditory cortex of macaques, chimpanzees, and humans. J Comp Neurol 441:197-222.

Hanes DP, Thompson KG, Schall JD (1995) Relationship of presaccadic activity in frontal eye field and supplementary eye field to saccade initiation in macaque: Poisson spike train analysis. Exp Brain Res 103:85-96.

Kusmierek P, Rauschecker JP (2009) Functional specialization of medial auditory belt cortex in the alert rhesus monkey. J Neurophysiol.

Legendy CR, Salcman M (1985) Bursts and recurrences of bursts in the spike trains of spontaneously active striate cortex neurons. J Neurophysiol 53:926-939.

Maunsell JH, Gibson JR (1992) Visual response latencies in striate cortex of the macaque monkey. J Neurophysiol 68:1332-1344.

Philibert B, Beitel RE, Nagarajan SS, Bonham BH, Schreiner CE, Cheung SW (2005) Functional organization and hemispheric comparison of primary auditory cortex in the common marmoset (Callithrix jacchus). J Comp Neurol 487:391-406.

Pouget P, Emeric EE, Stuphorn V, Reis K, Schall JD (2005) Chronometry of visual responses in frontal eye field, supplementary eye field, and anterior cingulate cortex. J Neurophysiol 94:2086-2092.

Rauschecker JP, Tian B (2004) Processing of band-passed noise in the lateral auditory belt cortex of the rhesus monkey. J Neurophysiol 91:2578-2589.

Recanzone GH, Guard DC, Phan ML (2000) Frequency and intensity response properties of single neurons in the auditory cortex of the behaving macaque monkey. J Neurophysiol 83:2315-2331.

Schmolesky MT, Wang Y, Hanes DP, Thompson KG, Leutgeb S, Schall JD, Leventhal AG (1998) Signal timing across the macaque visual system. J Neurophysiol 79:3272-3278.

Schroeder CE, Mehta AD, Givre SJ (1998) A spatiotemporal profile of visual system activation revealed by current source density analysis in the awake macaque. Cereb Cortex 8:575-592.

Wang X, Lu T, Snider RK, Liang L (2005) Sustained firing in auditory cortex evoked by preferred stimuli. Nature 435:341-346.

Wong-Riley M (1979) Changes in the visual system of monocularly sutured or enucleated cats demonstrable with cytochrome oxidase histochemistry. Brain Res 171:11-28.